1971

Fluorescence Lifetimes And Quantum Efficiencies Of Some 1,10-Phenanthrolines

Paul John Tabakian
University of the Pacific

FLUORESCENCE LIFETIMES AND QUANTUM EFFICIENCIES OF SOME 1,10-PHENANTHROLINES

A Dissertation

Presented to

The Faculty of the Graduate School

University of the Pacific

In Partial Fulfillment

of the Requirement for the Degree

Doctor of Philosophy

---

by

Paul John Tabakian

May 1971

FLUORESCENCE LIFETIMES AND QUANTUM

EFFICIENCIES OF SOME 1,10-PHENANTHROLINES

Abstract of Dissertation

Fluorescence properties of fourteen substituted 1,10-Phenanthrolines were determined using two different solvent systems. Four different sets of experiments were performed in order to measure fluorescence lifetimes, quantum efficiencies, absorption and corrected fluorescence spectra, oscillator strengths, and Stoke's shifts. Two of the phenanthrolines, the 5-Nitro-1,10-Phenanthroline and the 1,10-Phenanthroline-5,6-Dione, did not fluoresce.

A new equation was developed in order to extract the true fluorescence lifetimes τ from the observed fluorescence output f(t), and the lamp decay function I(t). This equation was

$$\tau = \frac{A_I I(t) - A_f f(t)}{A_f (df(t)/dt)}$$

where "A" was the weight factor or the normalization constant for the appropriate functions. A test of this equation on compounds with known lifetimes gave excellent results.

The experimental results indicated that there was a close relationship between the fluorescence parameters and the effect of different substituents on the different π-electron density positions of the ring. These parameters were also found to increase with an increase of solvent polarity thus indicating a (π,π^*) singlet transition in the polar solvents.

ACKNOWLEDGMENT

The author wishes to thank Dr. Richard P. Dodge, the Chairman of the Dissertation Committee, for his supervision and support of this project.

The author further thanks Dr. Herschel G. Frye for the unquestioned use of his laboratory equipment; Dr. C. Roscoe for the generous use of his spectrofluorometer; and Dr. Carl E. Wulfman and the Physics Department for the use of their equipment and facilities.

TABLE OF CONTENTS

LIST OF TABLES

LIST OF FIGURES

CHAPTER I

INTRODUCTION

The 1,10-phenanthrolines are an important class of compounds in chemical analysis and in various chemical industries. These compounds and their metal complexes have also produced much interest with their biological and physiological activities (1).

The phenanthrolines are organic bases with a condensed ring aromatic structure of phenanthrene but having two nitrogen atoms in the ring and having a planar structure. The 1,10-phenanthrolines,

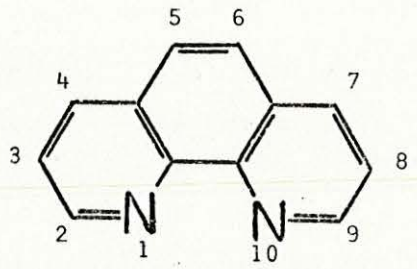

as compared to the other phenanthrolines, have the two nitrogen atoms at a distance of 2.5 A° from each other. This makes these molecules unique for the fact that they act strictly as a bidentate ligand to form a five-membered chelate ring with a metal or hydrogen ion. A monodentate behavior of these compounds has never been reported.

Some very interesting experimental observations have resulted from this bidentate behavior. pK studies have shown that at high concentrations of 1,10-phenanthrolines, and at different pH, and even with concentrated sulfuric and perchloric acids, poly-phenanthroline

molecules exist having different phenanthroline to acid ratios (2) (3).

Interest was developed in the 1,10-phenanthrolines when this compound was used as a colorimetric reagent in chemical actinometers (4). An extensive search of the literature revealed that only a limited amount of research had been done with regards to its luminescence properties. This was surprising since many other nitrogen containing aromatic compounds, such as acridine and bi-pyridine, had been thoroughly studied.

The fluorescence studies of the 1,10-phenanthrolines have mainly involved the chelates. The recent increase of papers dealing with the fluorescence of rare earth complexes of the 1,10-phenanthrolines indicate the importance of these compounds as fluorescimetric reagents. The reason for this is because they involve only sub-microgram quantities of the metals. Only a few workers have attempted luminescence studies of the phenanthrolines in solution. Langmuir (2) studied the ground - and excited - state pK values of some of the 1,10-phenanthrolines, and tried to determine the excited state electron densities from the change in protonation equilibria when the molecule undergoes a transition to the excited state. Unfortunately her fluorescence spectra are uncorrected. Jones (3) carried out similar studies, while Perkampus, et al. (5) published fluorescence spectra of the unsubstituted parent phenanthrolines. Some phosphorescence work has also been carried out (6), but only on the parent 1,10-phenanthroline.

CHAPTER II

THEORY OF FLUORESCENCE

Introduction

Absorption of ultraviolet or visible radiation by molecules involves electronic transitions in which these molecules are raised to some electronic excited states. The ground state electronic configuration would be a singlet following Pauli's principle, but the excited states would involve a large number of configurations. Fortunately, organic photoluminescence processes involve only the low lying singlet and triplet states in which lone paired and delocalized π electron systems of the ground states take part. These are the (π, π^*) and the (n, π^*) states. The σ electronic systems, that is the (σ, σ^*) and the (n, σ^*) require high electromagnetic energies of the far ultraviolet, and are therefore outside the scope of this work. The energies involved in the different electronic transitions can be summarized by the sequence $(\sigma, \sigma^*) > (n, \sigma^*) > (\pi, \pi^*) > (n, \pi^*)$.

At room temperature it is assumed that the molecules are at their lowest vibrational level of their electronic ground state singlet. Excitation will lead to all the vibrational levels of the excited state, and, according to the Franck-Condon principle, there will be no initial change in nuclear configuration during this process. Selection rules forbid transitions between states of different multiplicities so that the ground state singlet, on absorption of radiation, would be raised to only an excited state singlet; the excited triplet state, which has an energy lower than the excited singlet, might then become populated. The absorption spectra of

these molecules in solution will therefore represent electronic transitions showing vibrational levels as maximum peaks, and containing the closely spaced rotational levels.

When the excited molecule returns to the ground state it would do so by one or more paths and are as follows (Figure 1).

(a) It will immediately undergo a process of internal conversion (vibrational relaxation) whereby the molecule, due to collision with solvent molecules, passes from one of the higher vibrational levels of an excited singlet to the lowest vibrational level of the first excited singlet state.

(b) The spontaneous transition of the molecule from the lowest vibrational level of the excited singlet to a vibrationally excited ground state singlet and the emission of radiation or fluorescence.

(c) It may undergo a process of intersystem crossing from the excited state singlet to one of the vibrational levels of the excited state triplet.

(d) If the molecule is in one of the higher vibrational levels of an excited state triplet, it may undergo an internal conversion to the lowest vibrational level of the first excited state triplet.

(e) From process (d) the molecule may return to the ground state by the emission of radiation known as phosphorescence.

(f) When the molecule is in the lowest vibrational level of the excited singlet or triplet state it may return to the ground state without the emission of radiation. This process occurs when the excited molecules collide with solvent molecules, or with themselves, or other foreign molecules or quenchers, and the excess energy is given off to the surroundings as heat. This is the reason why phosphorescence is not usually observed in solution at room temperature.

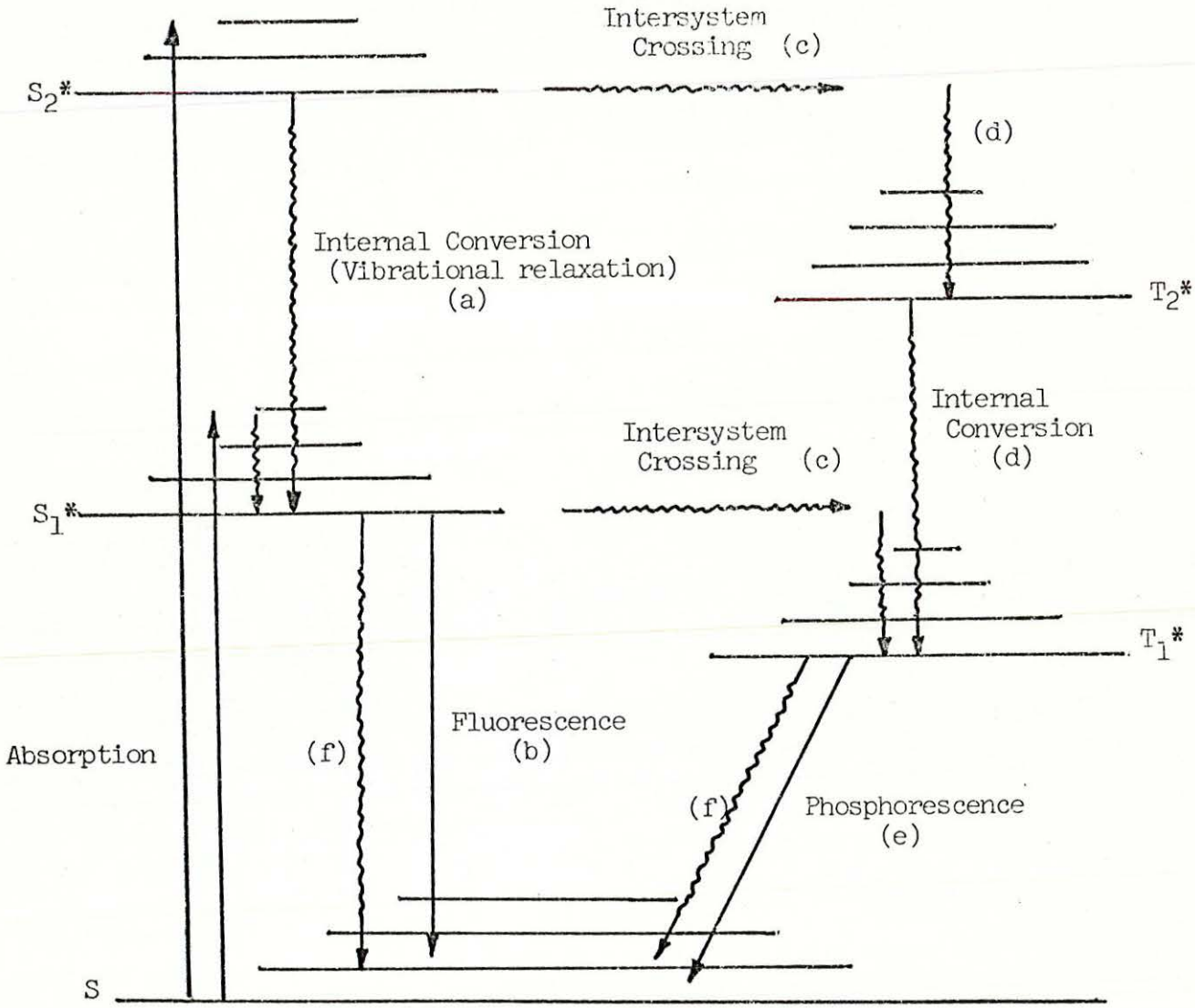

Figure 1: Schematic State Energy Level Diagram

The paths (a), (c), (d), and (f) are sometimes referred to as radiationless transitions. Other minor paths not considered in this work are E and P type delayed fluorescence which occur when molecules in the triplet excited state are thermally excited to an excited singlet from which emission of radiation occurs.

Kinetic Mechanism

Assuming that there is no phosphorescence emission in dilute solution and at room temperature, and also in the absence of a chemical reaction, a simplified kinetic mechanism could be set up for the energy scheme discussed previously (13).

$$S_o \longrightarrow S^* \qquad \text{rate} = P_A \qquad (2\text{-}1)$$

$$S^* \longrightarrow S_o + h\nu \qquad -\frac{dN}{df} = k_f N \qquad (2\text{-}2)$$

$$S^* \longrightarrow S_o + \text{heat} \qquad = k_n N \qquad (2\text{-}3)$$

$$S^* + Q \longrightarrow S_o + Q \qquad = k_Q N[Q] \qquad (2\text{-}4)$$

Here N is the concentration of the excited molecules at any time t; P_A is the rate of radiation absorption; k_f is the rate constant of fluorescence emission; k_n is the rate constant for all monomolecular radiationless transitions including all internal conversions and intersystem crossings; k_Q is the bimolecular rate constant for quenching by foreign molecules and, or the molecule itself. The self quenching process becomes negligible if very dilute solutions are employed.

Fluorescence Lifetimes and Quantum Efficiencies

Equations (2-2) to (2-4) show that when exciting radiation is withdrawn, the rate of disappearance of N would be

$$-\frac{dN}{dt} = N(k_f + k_n + k_Q [Q]) \qquad (2\text{-}5)$$

and a steady state consideration for all the processes represented by equations (2-1) to (2-4) would give the following relationship

$$P_A = N(k_f + k_n + k_Q[Q]) \tag{2-6}$$

The integration of (2-5) gives

$$N = N_o \exp\left(-\frac{t}{\tau'}\right) \tag{2-7}$$

where τ', the observed fluorescence lifetime when a quencher is present, is defined as the time required for the fluorescence intensity to fall to 1/e of its initial value, and is equal to the reciprocal of all the rate constants, that is

$$\tau' = \frac{1}{k_f + k_n + k_Q[Q]} \tag{2-8}$$

In the absence of a quencher, (2-7) is written as

$$N = N_o \exp\left(-\frac{t}{\tau}\right) \tag{2-9}$$

where τ, the observed fluorescence lifetime when a quencher is absent, is given as

$$\tau = \frac{1}{k_f + k_n} \tag{2-10}$$

When the only processes in the kinetic mechanism are equations (2-1) and (2-2), then (2-7) becomes

$$N = N_o \exp\left(-\frac{t}{\tau_o}\right) \tag{2-11}$$

where $\tau_o = 1/k_f$ and is usually called the natural lifetime (the average or mean radiative lifetime), and is defined as the time required for

the fluorescence intensity to fall to 1/e of its initial value in the absence of all other processes.

The quantum efficiency of fluorescence ϕ_f is defined as the ratio of the rate of emission over the rate of absorption of radiation, that is

$$\phi_f = \frac{F}{P_A} \tag{2-12}$$

Therefore from equations (2-2), (2-6), (2-10), and (2-12)

$$\phi_f' = \frac{k_f}{k_f + k_n + k_Q[Q]} \tag{2-13}$$

and,

$$\phi_f' = \frac{\tau'}{\tau_o} \tag{2-14}$$

In the absence of a quencher, equation (2-13) reduces to

$$\phi_f = \frac{k_f}{k_f + k_n} \tag{2-15}$$

From equations (2-10), (2-13), and (2-15), the following is obtained

$$\frac{\phi_f}{\phi_{f'}} = 1 + k_Q\tau\,[Q] \tag{2-16}$$

Equation (2-16) is the Stern-Volmer equation where τ is the observed lifetime in the absence of a quencher.

Relationship between Radiation Absorption and Emission

Equation (2-12) could be written as

$$F = (P_o - P_T)\ \phi_f \qquad (2\text{-}17)$$

where P_o and P_T are the radiant power of incident and transmitted beams respectively after passing through a sample. Substituting for P_T from Beer-Lambert's law, (2-17) could be written as

$$F = P_o[1 - \exp(-\varepsilon bc)]\ \phi_f \qquad (2\text{-}18)$$

For very small values of (εbc), that is in very dilute solutions, the expansion of the exponential term will approximate to ($1 - \varepsilon bc$), so that (2-18) becomes

$$F = P_o(\varepsilon bc)\ \phi_f \qquad (2\text{-}19)$$

Equation (2-19) shows that for very dilute solutions F is directly proportional to the concentration if P_o, ε, b, and ϕ_f are held constant. For higher concentrations, the error introduced in F is termed inner filter effect (self-quenching).

Equations (2-18) and (2-19) are very important relationships specially when quantum efficiencies and fluorescence spectra are being determined. Large inner filter effects will distort the lower wavelength end of the fluorescence emission spectum.

Radiative Lifetimes from Absorption Spectra

Four different equations have been given for the calculation of the mean radiative lifetime τ_o from the absorption spectra (7) (8). The latest, and the one which is commonly used these days, is the one devised by Birks and Dyson

$$\frac{1}{\tau_o} = 2.88 \times 10^3\ \frac{g_l}{g_u}\ \frac{n_f^3}{n_a}\ \left\langle \bar{\nu}_f^{-3} \right\rangle_{av}^{-1}\ \int \frac{\varepsilon(\bar{\nu})d\bar{\nu}}{\bar{\nu}} \qquad (2\text{-}20)$$

Where $\bar{\nu}$ is expressed in μm^{-1}, τ_o is in seconds, n_a and n_f are the mean refractive indices of the solvent over the absorption and fluorescence bands, and g_l and g_u are the multiplicities of the ground and excited states and are equal to unity in the case of fluorescence. The quantity

$$\left\langle \bar{\nu}_f^{-3} \right\rangle_{av}^{-1} = \frac{\int F(\bar{\nu})d\bar{\nu}}{\int \bar{\nu}^{-3} F(\bar{\nu})d\bar{\nu}} \qquad (2\text{-}21)$$

The authors report that for compounds for which the difference between nuclear configurations in the ground and excited states is small, the τ_o calculated from equation (2-20) agrees with the experimentally determined values.

If it is assured that $n_f = n_a = n$ where n is the mean refractive index of the medium over the fluorescence and absorption bands, then (2-20) reduces to the form derived by Strickler and Berg (8). If mirror symmetry between the fluorescence and absorption spectra is also assumed then (2-20) reduces to Forster's equation (7) which is

$$\frac{1}{\tau_o} = 2.88 \times 10^3 n^2 \int \frac{(2\bar{\nu}_o - \nu)^3}{\bar{\nu}} \varepsilon(\bar{\nu})d\bar{\nu} \qquad (2\text{-}22)$$

where $\bar{\nu}_o$ is the wave number of the mirror symmetry point between the fluorescence and absorption bands.

Stokes' Shift

This is defined as the difference between the wave number of the longest wavelength absorption maximum $\bar{\nu}_A$ and the wave number of the shortest wavelength fluorescence maximum $\bar{\nu}_F$ (10), that is

$$\text{Stokes Shift} = \bar{\nu}_A - \bar{\nu}_F \qquad (2\text{-}23)$$

Leeman et al. (11) consider (2-23) as a parameter which is closely connected with chemical structures.

Oscillator Strength

This deals with the probability of electronic transitions which give rise to a particular absorption or emission band, and is defined as the ratio of the observed integrated absorption coefficient to the theoretical transition moments for an ideal molecule (12)(13a). The oscillator strength f is therefore expressed as follows:

$$f = 4.33 \times 10^{-5} \int \varepsilon d\bar{\nu} \qquad (2\text{-}24)$$

The determination of f is useful when forbidden transitions are being considered.

Outline of Method

It was found desirable to carry out four different sets of experiments in order to evaluate the fluorescence lifetimes, the fluorescence quantum efficiencies, and the absorption and the corrected fluorescence spectra of the 1,10-phenanthrolines in two different solvent systems.

The observed lifetimes were measured directly using the existing pulse fluoremeter (the fluorescence lifetime apparatus). It was found necessary to make improvements on this instrument so that reliable data could be obtained, and literature values could be duplicated.

The determination of quantum efficiencies required the measurement of corrected fluorescence spectra and the use of equation (2-19).

The natural lifetime, the oscillator strength and Stokes' Shift required the measurement of the absorption and the fluorescence spectra in order to evaluate the variables in equations (2-20), (2-21), (2-23), and (2-24).

In the course of these studies it became possible to correlate the experimentally determined fluorescence parameters with the polarity of the solvent and the effect of substituents and electron densities on the 1,10-phenanthroline ring.

CHAPTER III

EXPERIMENTAL

Chemicals

The 1,10-phenanthrolines used in this work were obtained from J.T. Baker of Philipsburg, New Jersey. The following were of Baker Analytical Reagent grade purity; the parent compound 1,10-phenanthroline, the 1,10-phenanthronine-4,7-diolmonohydrochloride, the 2,9-dimethyl-1,10-phenanthroline, the 4,7-diphenyl-1,10-phenanthroline, and the 2,9-dimethyl-4,7-diphenyl-1,10-phenanthroline. The following were of Baker grade purity only; the 5,6-dimethyl-1,10-phenanthroline, the 4,7-dimethyl-1,10-phenanthroline, the 5-methyl-1,10-phenanthroline, the 5-phenyl-1,10-phenanthroline, the 3,5,6,8-tetramethyl-1,10-phenanthroline, the 3,4,7,8-tetramethyl-1,10-phenanthroline, the 5-nitro-1,10-phenanthroline, and the 5-chloro-1,10-phenanthroline. The 1,10-phenanthroline-5,6-dione was obtained from the K and K Laboratories, and was of an unknown purity grade.

In fluorescence work the melting point of a compound cannot be taken as the only criterium of purity. Tiny amounts of impurities may alter the fluorescence spectrum by quenching and energy transfer. It was therefore necessary to further check the purity of the compounds under consideration even if these were rated as "Analytical Reagent Grade", and to recrystallize them several times. Of course care was taken not to introduce other impurities during the recrystallization.

The 1,10-phenanthrolines were recrystallized from methanol or methanol-water systems, and their purity was tested according to the criteria of purity given by Parker (13b). Thus for every phenanthroline examined, the fluorescence emission spectrum was independent

of the wavelength of excitation, and the fluorescence emission band maximum was at a longer wavelength than the long wavelength absorption band. In addition to this, the photomultiplier response to the fluorescence emission signal of the compound before the crystallization was compared with that of the recrystallized compound at the same wavelength and for the same optical density (that is the same concentration). Out of a total of fourteen phenanthrolines, only the 5-phenyl-1,10-phenanthroline showed any difference. The fluorescence signal for the recrystallized versus the original sample was 5.7% greater in the methanol solution and 16.6% greater in the acid solution. This meant that the 5-phenyl-1,10-phenanthroline, as received from the manufacturer, contained an impurity which quenched its fluorescence, while all the other phenanthrolines could have been used without recrystallization.

As a final check, the purity of the recrystallized 1,10-phenanthrolines were tested by paper chromatography using an eluting solvent system of butanol: acetic acid: water in a 4:1:1 volume ratio (2) and the spots were located by means of their fluorescence under UV light (a blank was first run on the paper to check for any fluorescing spots). When only one spot was found the compound was considered pure enough for the fluorescence measurements. To further identify the spots, a tenth molar solution of ferrous ammonium sulfate in 0.1N H_2SO_4 was also sprayed on the paper. The ferrous ions form pink to dark red colored complexes with the phenanthrolines. There was only one colored spot found in every case.

The standard compounds, quinine sulfate and 2-aminopyridine, were obtained from J.T. Baker, and were of Baker grade purity. The

former was recrystallized several times from one normal sulfuric acid, and the latter from cyclohexane.

The following compounds were used without recrystallization: fluorescein A.R. from Baker, 9,10-diphenylanthracene from K and K Laboratories, anthracene (blue-violet fluorescence grade) from Eastman, eosin Y, and acridine orange.

Solvents

Methanol and dilute sulfuric acid were the two primary solvent systems used in this work.

High purity methanol of J.T. Baker GC-Spectrophotometric quality was used. A fluorescence spectrum was taken to further check its purity because even the best quality solvents sometimes contain traces of fluorescing impurities. The spectrum was run with the highest photomultiplier sensitivity setting and a large slit opening, and it was found that this grade of methanol was fluorescence free. The dilute sulfuric acid solution was made with distilled water and was analyzed in a similar fashion, and was also found to be fluorescence free. Deionized water was found to be unsuitable since it gave some indications of containing fluorescing impurities.

The cyclohexane used in some cases was of GC-Spectrophotometric quality, and was found to be fluorescence free.

The only recorder response detected in the above fluorescence analysis was that of a small Raman emission at the expected wavelengths, and some scattering signals around the excitation wavelengths.

Cleaning of glassware and sample cuvettes

Extra precautions were taken when cleaning glassware and sample

cuvettes so that trace impurities would not interfere with the fluorescence measurement.

The glassware was first washed with detergent, then soaked in hot chromic acid mixture, and then rinsed thoroughly first with tap then with distilled water. Finally it was dried in an oven.

The sample cuvettes used were made from fluorescence free quartz and were cleaned according to Burch's method (14). They were first rinsed with a polar or nonpolar solvent, depending which one was used in a previous experiment, then dried, and then they were boiled in a half-concentrated nitric acid solution, then rinsed with distilled water, and finally with the pure solvent used for the particular measurement.

Preparation of Stock Solution

Because of the errors introduced due to inner filter effects as described in Chapter two, it was found desirable to use concentrations small enough so that a linear relationship would exist between fluorescence intensities and concentration (equation 2-18). It was found that the limiting concentration for the phenanthrolines was about 10^{-4}M below which the fluorescence intensity was linear with concentration. A phenanthroline concentration of 10^{-5}M was chosen which met this criteria for equation (2-18) and at the same time was concentrated enough to give a good absorption spectrum.

All phenanthroline solutions were prepared from one stock solution in the following manner: The stock solution was prepared by weighing 10^{-4} moles of the compound and dissolving it in 100 ml of methanol thus giving a 10^{-3}M solution. Aliquots of this methanolic solution were then diluted down with either methanol or 0.1N sulfuric acid

to give the desired 10^{-5}M concentration.

Concentrations of 10^{-5}M were also used for the standards quinine sulfate and 2-aminopyridine. The stock solution of these compounds were 10^{-3}M in 0.1N sulfuric acid.

Recording the Absorption Spectra

The absorption spectra were measured on a Perkin-Elmer Model 202 UV-VIS Spectrophotometer. Since this instrument recorded absorbance versus wavelength, the phenanthroline spectra were replotted on coordinates having the molar absorptivity ε as the ordinate, and the wave number $\bar{\nu}$, in units of μm^{-1}, as the abscissa.

In the determination of the fluorescence quantum efficiencies, Absorbances of the samples and the standard were compared and adjusted on a modified Beckman DU Spectrophotometer. The modification of this instrument is a Gilford attachment which presents Absorbances in a digital form.

Recording the Fluorescence Spectra

The uncorrected fluorescence emission spectra were measured on a Coleman Hitachi EPS-3T Spectrophotometer with a Hitachi Model G-3 Spectral Fluorescence attachment. This fluorescence attachment consisted of an excitation monochromator, a 150 watt xenon lamp light source, a 90° sample compartment, and a power source for the xenon lamp (15).

Alignment of Monochromators

Two methods were used for the wavelength alignment of the emission monochromator. In the first method the EPS-3T was used as a spectrophotometer, and the spectrum of a holmium oxide glass as measured

with the instrument was compared with the one given by the manufacturer.

In the second method, the EPS-3T was used with its fluorescence attachment, and the wavelength alignment of the monochromator was carried out by comparing the maximum detector signal at different settings of the monochromator with the known lines of a mercury arc. The low pressure mercury arc lamp in the Bausch and Lomb Precision Spectrophotometer lamp housing was used for this purpose. A freshly prepared suspension of 1 g of glycogen per liter of water (a light scattering solution) was placed in a cuvette and this in turn was placed in the fluorescence sample compartment. The lamp housing was then placed on top of this, and the focusing mirrors adjusted so that the radiation from the mercury lamp was focused into the cuvette. The emission monochromator was then turned manually until a maximum signal was obtained around one of the known mercury lines.

Table I shows the results of this calibration.

TABLE I

SPECTROFLUOROMETER WAVELENGTH CALIBRATION

Spectral Region	Known Hg lines(mμ)	Monochromator Setting(mμ)	Deviation(mμ)
210-360 mμ	253.7	253.5	0.2
	313.2	313.0	0.2
340-700 mμ	404.7	402.5	2.2
	435.8	433.5	2.3

As shown, the correction in the ultra violet region was negligible, but a correction of 2mμ was applied for the visible region.

The excitation monochromator was calibrated using the calibrated

emission monochromator (16). The mercury lamp was removed, and, by using the same glycogen suspension, the excitation wavelength was checked against the calibrated emission wavelength over the entire ultraviolet-visible range. A maximum detector signal was taken as the wavelength when both the emission and excitation monochromator settings were the same. The wavelength settings of the two monochromators were found to be less than 0.5 mμ.

Test for Linearity of Photomultiplier Response

For accurate measurement of fluorescence spectra and quantum efficiencies a test was carried out to check the linearity of the photomultiplier response.

A series of quinine sulfate in 0.1N H_2SO_4 solutions were prepared ranging in concentration from 10^{-6}M to 5 x 10^{-5}M (the limiting concentration was about 10^{-4}M). The fluorescence readings of these solutions were then recorded at different photomultiplier sensitivity settings and at constant slit widths. It was found that for each sensitivity setting the detector response was linear within about 0.5% of the full scale.

It also became necessary to compare the detector response between the different photomultipliers sensitivity settings. Using the above solutions or varying amounts of light scattering suspensions the detector response for different sensitivities was recorded. Table II gives the conversion factors necessary for converting a detector reading to any desirable photomultiplier sensitivity.

TABLE II

CONVERSION FACTORS FOR P.M. SENSITIVITIES

Sens. 1	Sens. 2	Sens. 3	Sens. 4	Sens. 5	Sens. 6
				3.2	1
			3.4	1	
			11.5		1
		4.3	1		
		15.4		1	
		49.6			1
	5.8	1			
	24.7		1		
	88.3			1	
	285.1				1
9.6	1				
55.2		1			
237.4			1		
847.4				1	
2737.0					1

Operating Procedure for the Measurement of Fluorescence Spectra

The manufacturer's recommended operating procedure for the Spectrofluorometer was modified. The modified procedure was as follows:

1. The EPS-3T Spectrophotometer was set in the mode of "energy measurement", similar to single beam operations in absorption spectrophotometry.
2. The power supplies for the instruments were turned on, and about thirty minutes warm up time was allowed.
3. The xenon lamp was lighted as recommended, and the current was adjusted to 7 amps. It took from thirty to sixty minutes for the lamp to reach its optimum operational condition. During this time the power supply was manually readjusted

to keep the current output at 7 amps. The equilibrium conditions for the xenon arc were assumed to be reached when the current output remained constant.

4. The fluorescence free quartz cells containing the samples were placed in the cell holder, and this in turn was placed in the sample compartment, and the fluorescence signal was measured at 90° to the excitation radiation as recommended for dilute solutions (13).

5. An excitation wavelength which gave a strong fluorescence signal was chosen from the known absorption spectrum of the sample. This was not necessarily the maximum of an absorption band since the intensity of the xenon lamp could be weaker at that wavelength, but care was taken to check whether there was a fluorescence emission band shift with the excitation wavelengths (17). In the absence of this band shift, the emission monochromator was set at a certain wavelength of the fluorescence spectrum, and the excitation monochromator was slowly varied over the wavelength range of the absorption spectrum of most interest until a strong fluorescent signal was obtained. This wavelength was then considered to be the excitation wavelength. The method just described gave the best signal-to-noise ratio. For the phenanthrolines, the wavelength region between 275 to 285 mμ gave the strongest fluorescence signal, but 285 mμ was chosen for all the samples because the quantum efficiency of the standard, with which they were compared, was determined at that wavelength.

6. Certain precautions were taken when setting the excitation

monochromator slit. Although a wide open slit gave a high intensity of exciting radiation and thus a good signal-to-noise ratio, scattered and second order radiation from the excitation monochromator became a problem. In order to overcome this difficulty, a narrower slit opening was used at the expense of the signal-to-noise ratio. Another point kept in mind was photodecomposition, and, whenever this was suspected, the slit was kept as small as possible and the spectrum of the sample was recorded at a faster rate.

7. The slit on the emission monochromator was set as small as possible in order to have a good resolution, and this required a high photomultiplier sensitivity for weakly fluorescing samples. At this sensitivity the signal-to-noise ratio again became a problem, and so the slit was adjusted in such a way as to have a good balance between resolution and signal-to-noise ratio.
8. To check for variations in the intensity of the source, a Bausch and Lomb Spectronic 20 was modified in such a way as to continuously monitor the light source. It was found that once the xenon lamp obtained its equilibrium conditions, and once the current output remained constant at 7 amps, then the intensity variations of the light source was less than 1%.
9. When all the above procedures were carried out, a blank was run in order to obtain a base line, and to determine the extent of scatter and Raman emission of the solvent. The slit openings and the photomultiplier sensitivities for

the blank and for the fluorescing sample were the same.

Light Source Calibration

Melhuish's method (18) was used for calibrating the light source-emission monochromator system of the spectrofluorometer. Chen's (16) procedure was adopted in a slightly modified form, and which was as follows: A solution of 3 grams per liter of Rhodamine B in ethylene glycol (Baker A.R.) was used as a fluorescence quantum counter. It is assumed that the Rhodamine B solution has such a high absorbancy at wavelengths up to about 600 mμ that all the excitation energy is absorbed in a thin layer at the surface, that the quantum yield is independent of excitation wavelength, and that the fluorescence intensity is therefore proportional only to the number of quanta incident on the counter. The cuvette containing the Rhodamine B solution was placed in the sample holder of the spectrofluorometer which is constructed in such a way that it could be rotated around a central axis so that one of the surfaces of the cuvette could be exposed to both the exciting radiation and the entrance slit of the main instrument. Therefore the cuvette was placed at about 30° to the incident beam, and the fluorescence was observed from this angle. The emission monochromator was then set at 615 mμ, the excitation monochromator scanned manually, and the fluorescence intensities recorded. Table III gives the spectral distribution of the xenon lamp in relative units. These values usually change with the age of the lamp.

Detector System Calibration

The fluorescence spectrum obtained from the spectrofluorometer

was not the true emission spectrum. To determine the true spectrum the uncorrected curve was corrected for wavelength sensitive factors, and these were the response of the photomultiplier, the monochromator and slit optics, the geometry of the sample compartment, and the differing light losses in the system (13c)(20)(21). It was thus necessary to determine a correction factor $S\lambda$ which included corrections for all the above wavelength dependent factors. Thus if $R\lambda$ was the photomultiplier response recorded as a function of wavelength, and $(dQ/d\lambda)_{std}$ was the light intensity of some standard lamp then

$$\left(\frac{dQ}{d\lambda}\right)_{std} = R\lambda/S\lambda \qquad (3\text{-}1)$$

where Q represents total number of quanta of all wavelengths per unit time.

It thus became necessary to determine the response of the photomultiplier-monochromator system as compared to a standard lamp output. $(dQ/d\lambda)_{std}$ could have been obtained by utilizing a U.S. National Bureau of Standard lamp, and since this was not available, Melhuish's method (18) was again used. This method employed the previously calibrated xenon lamp as follows: A piece of aluminum foil was coated with magnesium oxide by holding it over some burning magnesium. This magnesium oxide screen was then placed at 45° to the incident radiation, and at a constant slit width and photomultiplier sensitivity, the excitation monochromator was adjusted manually to give the maximum reading at each step (16) (each of these readings were multiplied by the reflectivity of the MgO). This was repeated for several slit

TABLE III

SPECTRAL SENSITIVITY FACTOR Sλ

Wavelength λ	Relative Intensity of Xenon Lamp $(dQ/d\lambda)_{std}$	Relative Response of P.M. and Optics Rλ	$S\lambda = R\lambda/(dQ/d\lambda)_{std}$ (Relative values)	
			Xenon lamp	Quinine sulfate
240	0.12	0.01	0.08	
260	0.22	0.02	0.14	
280	0.35	0.05	0.20	
300	0.47	0.09	0.26	
310	0.53	0.12	0.30	
320	0.58	0.15	0.36	
330	0.63	0.19	0.42	
340	0.67	0.23	0.48	
350	0.70	0.28	0.54	
360	0.73	0.33	0.61	
370	0.76	0.38	0.68	
380	0.77	0.43	0.74	
390	0.81	0.47	0.85	0.74
400	0.83	0.54	0.90	0.90
410	0.82	0.55	0.96	0.97
420	0.80	0.58	0.98	1.00
430	0.81	0.59	1.00	1.00
440	0.86	0.64	1.00	1.00
450	0.93	0.68	1.00	0.99
460	0.99			0.97
465				0.96
470				0.94
480	0.98	0.66	0.92	0.92
490	0.92	0.60	0.90	0.90
500	0.87	0.55	0.86	0.85
520	0.80	0.46	0.76	0.76
540	0.77	0.36	0.62	0.61
560	0.74	0.26	0.46	0.44
580	0.66	0.16	0.31	0.27
600	0.46	0.07	0.18	
620	(0.22)	(0.02)	(0.13)	

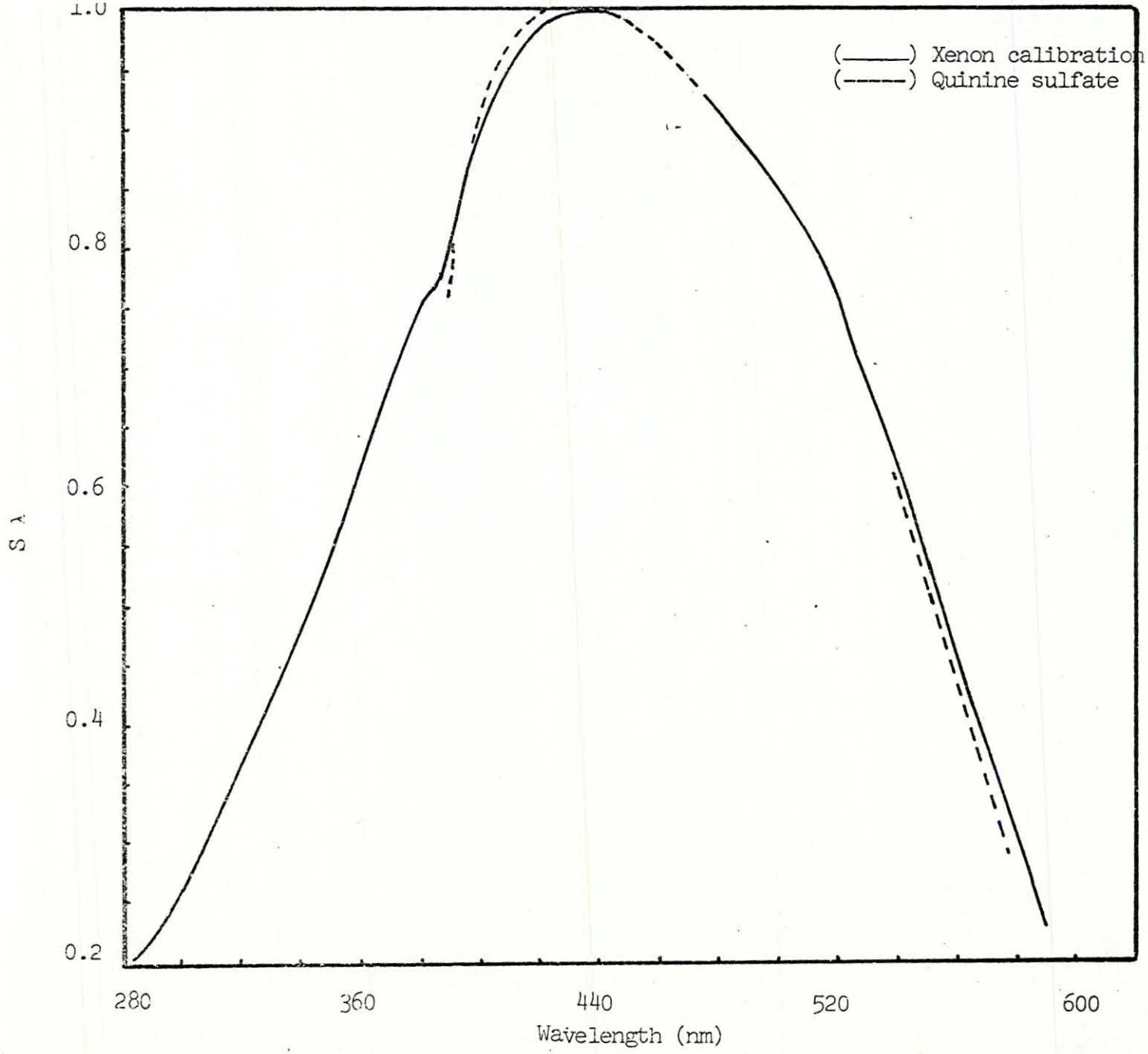

Figure 2: Spectral Sensitivity Factor versus Wavelength

widths, care being taken to have the same excitation and emission slit widths, thus the same band widths. The relative response of the photomultiplier to the xenon lamp is listed in Table III.

Table III also lists the spectral sensitivity factor S_λ which is obtained by dividing the relative response of the photomultiplier by the relative intensity distribution of the xenon lamp and normalizing the result to one. The blank spots between 460 mμ and 470 mμ are in a region where very sharp and intense lines of the xenon spectrum exist.

Another method for the determination of S_λ was also used in order to check the accuracy of the above method. In this method the known corrected emission spectrum of a standard compound is compared with that of the uncorrected emission spectrum run on the spectrofluorometer. From (3-1), the $(dQ/d\lambda)_{std}$ now represented the known spectral distribution of the standard, and R_λ were the values from the uncorrected spectrum (13d). Quinine Sulfate in 0.1N H_2SO_4 was used as the standard compound, and Melhuish's (19) values were used for $(dQ/d\lambda)_{std}$. Table III lists S_λ from this comparison method, and are in excellent agreement with the standard lamp method for the 400 mμ to 560 mμ wavelength region.

The S_λ versus wavelength values were also plotted and are shown in figure 2.

Instrumentation for the Measurement of Fluorescence Lifetimes

Fluorescence lifetimes were measured using a Bennett type pulse fluorometer (22)(23) in which the fluorescence was excited by a light pulse of nanosecond duration and the fluorescence decay was observed directly during the intervals between the excitation pulses. Use was made of a delay line which delayed the activation of the detector system with respect to the triggering of the light pulse; and so if

the pulsed light source was cut off in a time shorter than the fluorescence lifetime of the sample, if the intensity of each pulse was constant during the time the light was on, if the detector system had a fast time response, and if this was repeated synchronously for several times a second, then a whole electronically integrated curve was obtained which was actually a time stretched recording of the actual fluorescence decay.

The electronic circuit details of the pulse fluorometer are described elsewhere by Petz (22), and a block diagram is shown in figure 3. The existing instrument did not function as expected so that many of the electronic sub-circuits were rewired and new and better components and control meters were installed without changing the basic electronic design.

The existing optical system was found to be inadequate, and was therefore discarded. A new system was designed and constructed, and a schematic diagram of the optics is shown in figure 4. The fluorescence emission was viewed at 90° to the exciting radiation, similar to a 90° design of standard spectofluorometers. Quartz lenses were used for focusing both the excitation and the emission radiation, with the excitation lens being of high quality and fluorescence free quartz. Adequate light filter compartments were provided, the excitation end having liquid light filter (for a 40mm quartz cell) and glass filter plate holders. An old Beckman DU phototube housing was used as the photomultiplier housing, and this contained a 1P28 photomultiplier tube used as the main detector, and a phototube, with leads to a Spectronic 20, for focusing purposes. Enclosed in the lamp housing were some components of the lamp pulsing circuit such as the 7191 A

thyratron tube which needed to have a very short connection with one of the lamp electrodes. The sample compartment was thermostated and was similar in design as the one used by Petz.

The details of the lamp design are described elsewhere (22)(24)(25)(26). It had a flat quartz optical window and was attached to a pyrex glass envelope with high melting black apiezan wax. The electrodes were of platinum or tungsten and were set to about 0.3 to 1.0 mm apart. If the lamp was operated with hydrogen gas then it was more desirable to use the smaller gap distances, and if it was operated with dry air or nitrogen gas then gap distances between 0.5 to 1.0 suited better. It was found that for air or nitrogen the desirable gas pressure was about 200 to 300 mm Hg pressure for electrode gaps of around 0.5 mm. For the larger sized gaps, gas pressure of up to 700 mm Hg were required. Hydrogen gas required lower pressures of about 100 mm Hg.

The primary requirement for a normal operation of the lamp was to obtain a very short lifetime. There were no set conditions for this (25), and thus a trial and error method was used to find the optimum condition for the lamp in this particular instrument. A good indication to this effect was to check the full width at half maximum of the lamp decay curve. The smaller this value was the smaller was the lifetime. The minimum full width at half maximum for the system under study was found to be 4 nsec, and such conditions as the electrode gaps, the pressure of the gas, and the operating voltage of the lamp were always checked and adjusted in order to keep this value the same, and the lamp was replaced whenever this condition was not met.

The lamp was centered with respect to the sample cuvette by putting a small mirror in the cell, and, by placing a small light source

over the sample compartment, viewing the light source through the lens with a cathetometer. The position of the lamp was sdjusted in such a way as to have the reflection of the light source centered in the middle between the two electrodes as viewed with the cathetometer. This procedure could also be carried out visually.

Petz's method (22) of determining the time scale of the time coordinate was not used because it was found to be in error. In her method she had assumed a calibrated delay line, and, by considering the speed with which this variable delay line was turning and equating it with the recorder chart speed, she had come up with a certain time scale. In our method the time scale was calibrated by using the known fluorescence lifetime of a compound.

Quinine sulfate in 0.1N H_2SO_4 was chosen as a standard because reliable lifetime values were found in the literature, and because it had a relatively long lifetime of 19.4 nsec. (27)(28)(10). Thus for a certain delay line and recorder chart speed, the lifetime of the standard was calculated in terms of the recorder chart units $\tau_{\text{rec. units}}$ and this was compared with the actual lifetime of the compound τ_{ref} in nsecs, thus

$$\tau_{\text{ref.}} = S_\tau \ \tau_{\text{rec. units}} \qquad (3\text{-}2)$$

and, in terms of 19.4 nsec

$$S_\tau = \frac{19.4}{\tau_{\text{rec. units}}} \qquad (3\text{-}3)$$

where S_τ was the time base calibration factor for the particular delay line and recorder speed.

Operating Procedure for the Measurement of Fluorescence Lifetimes

1. The heaters in the electronic tubes were turned on and about

ten minutes were allowed for the warm up. The switch for the 67 V battery of the 5687 tube bias control of the photomultiplier circuit was also engaged.

2. The four power supplies were then turned on and their voltages adjusted in the following order: 300V, 600V, 1000V, and 800V. It was important that this order was kept and, specially, that the 800V supply was turned on last.
3. The plate current of the 5687 tube (Step 1, above) was adjusted to a value of 2.5ma to 3ma.
4. While about 30 minutes were given to the electronic system to attain its operational conditions, the lamp was readied by evacuating and refilling it several times with the appropriate gas, and, in the final filling, by adjusting the pressure to the appropriate value determined previously.
5. The light filters were then inserted (figure 5), and the sample cell was placed in the cuvette holder.
6. The lamp was turned on by turning on the lamp power supply (4KV to 7KV), and about ten minutes were given for it to reach thermal equilibrium.
7. The motor for the variable delay line and recorder was then started and the decay curve obtained.
8. A decay curve for the lamp was first run by having a light scattering suspension (1 g of glycogen per liter of water) as the sample,(for this step the light filters were removed).
9. A decay curve for the fluorescing sample was then obtained.
10. With the filters in place a blank was finally run on the solvent in order to check the extent of scatter.

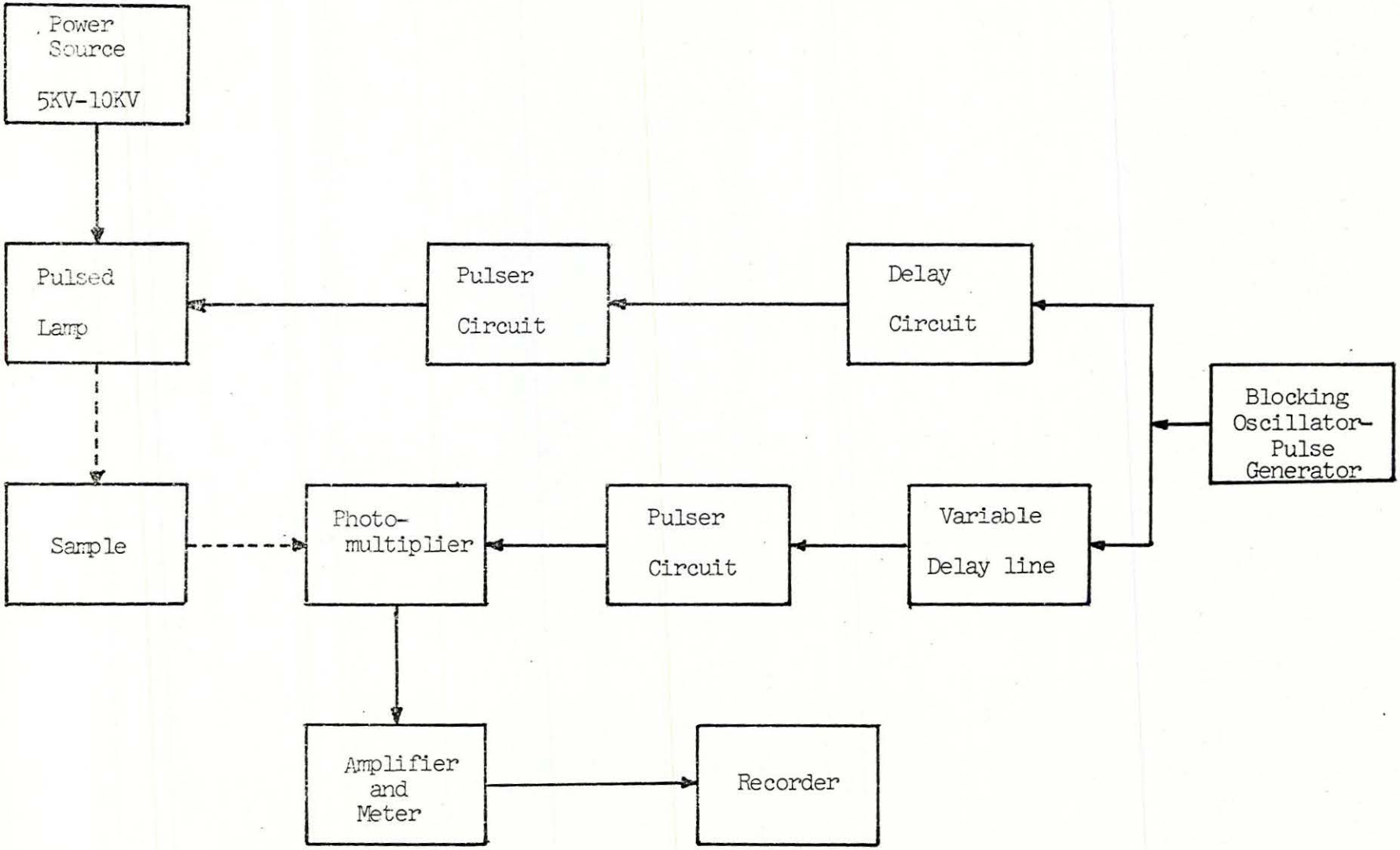

Figure 3: Block Diagram for the Pulse Fluorometer

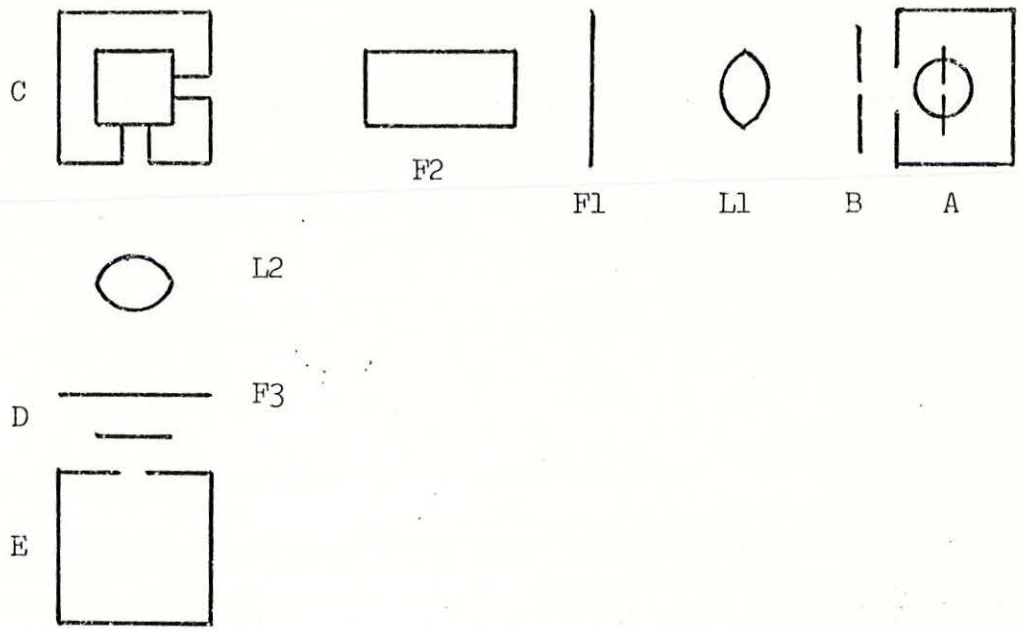

A	Lamp housing	L1	Focusing Lens
B	Iris Diaphragm	L2	Focusing Lens
C	Sample Compartment	F1	Light Filter (glass)
D	Shutter	F2	Light Filter (liquid)
E	P.M. housing	F3	Light Filter (glass)

Figure 4: Schematic Diagram of the Optical System of the Pulse Fluorometer

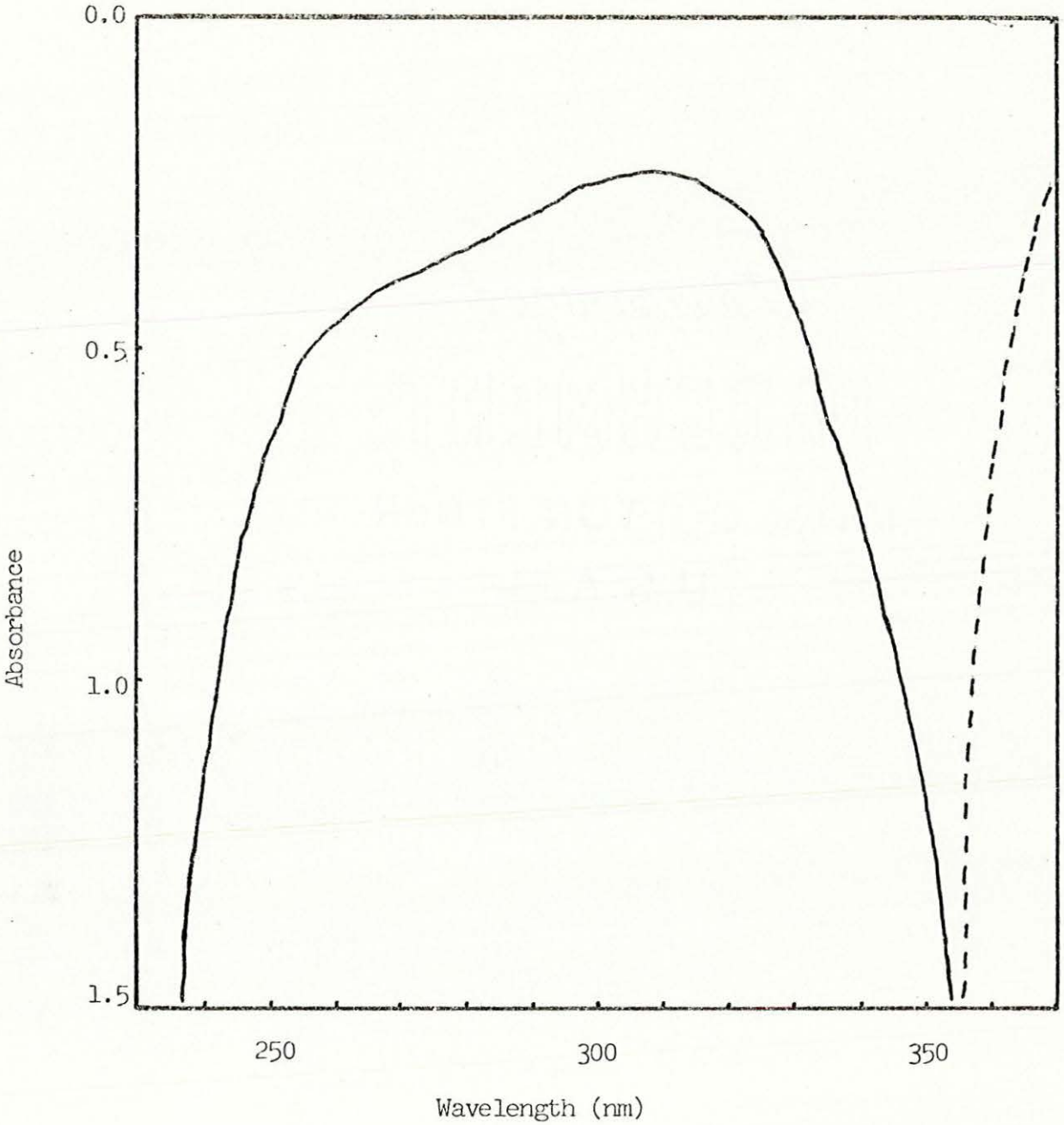

Excitation Filter (——): 150 g/lt $NiSO_4 \cdot 5H_2O$ + Corning 9863
Emission Filter (------): Kodak Haze

Figure 5: Absorbance Curves of the Filter System

CHAPTER IV

TREATMENT OF DATA

PART I: Fluorescence Lifetimes

Figures 6 through 17 show the decay curves of the phenanthrolines obtained with the pulse fluorometer. Each figure contains three decay curves which represent the ones for the phenanthrolines in methanol and 0.1N H_2SO_4, and the one for the lamp. These are reproductions from the actual curves drawn by the instrument recorder and represent the average value of many runs. The ordinate of the graph represents fluorescence intensities in relative units.

In terms of fluorescence intensities, F equation (2-9) could be written in the form

$$2.303 \log \frac{F}{F^o} = - \frac{t}{\tau} \qquad (4-1)$$

There is an assumption made when using (4-1). It is assumed that the fluorescence emission decays exponentially (23). This assumption is justified when a semilogarithmic plot of F/Fo versus the t gives a straight line. Sometimes nonexponential decay is also observed, and this might be due to impurities so that the semilogarithmic plot would indicate two or more straight lines with two different slopes; or it might be due to excimer formation, and, in this case, other straight lines could be observed usually in the long tail-end side of the decay curve.

Instrumental Response Time Correction of Fluorescence Lifetimes

Equation (4-1) will give true τ values only if the lifetime of

the fluorescing sample is much greater than the decay time of the lamp, otherwise an instrument time correction should be carried out. Brody (29), Birks, et al. (7), and others (30) studied this subject thoroughly and presented different methods of correction. A recent article by Demas and Crosby (31) summarizes many of the methods. It should be realized that an analog or a digital computer is necessary in every case.

We have developed a new method for correcting fluorescence lifetimes. It is based on Tanesescu's work (32)(33) which dealt with pulse shapes in scintillation counters. Our method is as follows:

The true fluorescence output F(t) is generated in response to the excitation by the lamp (called a δ-function excitation (7)). But the observed lamp decay curve I(t) is not the true shape of the excitation source because it depends on such factors as the actual shape of the flash, the spread of transit time of the electrons in the photomultiplier, and the time response of the cables and all the other electronic components to the flash. Therefore the observed fluorescence output f(t) is the true fluorescence F(t) distorted by the instrumental response function I(t).

The true fluorescence output F(t) could be extracted from f(t) and I(t) by using the superposition principle (7) (also known as the convolution theorem or "Faltung"), that is

$$f(t) = \int_0^t F(t')\, I\,(t-t')dt' \qquad (4\text{-}2)$$

Equation (4-2) is the starting point of our method as well as all the other methods. In the other methods F(t) is assumed to be exponential, and, by computer trial and error, several exponential functions are

synthesized to match f(t) for given I(t) values (32).

If F(t) is assumed to be exponential then equation (4-1) could be written in a differntial form as follows:

$$F(t) = \frac{1}{\tau} \exp(-t/\tau) \qquad (4\text{-}3)$$

Substitution of (4-3) into (4-2) gives

$$f(t) = \int_{t'=o}^{t'=t} \frac{1}{\tau} \exp(-t'/\tau)\, I\,(t-t')dt' \qquad (4\text{-}4)$$

Let y=t-t' and t'=t-y, therefore dy=-dt', then

$$f(t) = \int_{y=t}^{y=o} \frac{1}{\tau} \exp[(-(t-y)/\tau]I(y)(-dy) \qquad (4\text{-}5)$$

$$f(t) = \frac{\exp(-t/\tau)}{\tau} \int_{y=o}^{y=t} \exp(y/\tau)I(y)dy \qquad (4\text{-}6)$$

and this rearranges to

$$\tau \exp(t/\tau)f(t) = \int_{y=o}^{y=t} \exp(y/\tau)I(y)dy \qquad (4\text{-}7)$$

Differentiation of (4-7) with respect to t gives

$$\frac{d}{dt} [\tau\exp(t/\tau)\ f(t)] = \exp(t/\tau)\ I(t) \qquad (4\text{-}8)$$

$$\tau \left[\frac{\exp(t/\tau)f(t)}{\tau} + \exp(t/\tau)f'(t)\right] = \exp\ (t/\tau)\ I(t) \qquad (4\text{-}9)$$

where f'(t) is the differential form of f(t), and so by rearranging (4-9) we obtain the final equation which is

$$\tau = \frac{I(t) - f(t)}{f'(t)} \qquad (4\text{-}10)$$

The experimentally obtained values of I(t) and f(t) must be multiplied by a weight factor (34) or a normalization constant, since the convolution integral actually represents a weighted average over the past of f(t). Thus, the weight factors are

$$A_I = \int_o^\infty I(t)dt \qquad (4\text{-}11)$$

$$A_f = \int_o^\infty f(t)dt \qquad (4\text{-}12)$$

that is the areas under I(t) and f(t) curves. Equation (4-10) then becomes

$$\tau = \frac{A_I I(t) - A_f f(t)}{A_f f'(t)} \qquad (4\text{-}13)$$

The best way of determining f'(t) is from the semilog plot of the exponential decay side of the f(t) curve, and is as follows:

$$f'(t) = \frac{df(t)}{dt} = -ae^{-at} = -af(t) \qquad (4\text{-}14)$$

where "a" is the slope of the semilog plot; and, in terms of logarithm to the base 10, (4-14) becomes

$$f'(t) = 2.303 \frac{\log \frac{f(t)_2}{f(t)_1}}{t_2 - t_1} \cdot f(t) \qquad (4\text{-}15)$$

Equation (4-13) thus reduces to equation (4-1) if

$$A_f f(t) \gg A\ I(t)$$

In order to test the validity of (4-13) several compounds with known τ values were tested and the results are given in Table IV. As could be seen, there is excellent agreement between our values and those of the literature.

Table V gives the lifetimes of the phenanthrolines in methanol and 0.1N H_2SO_4 at 25° C.

TABLE IV

COMPARISON OF CORRECTED AND UNCORRECTED

τ VALUES OF SOME COMPOUNDS

Compound	τ nsec uncorrected	τ nsec corrected	τ nsec literature	Reference
Fluorescein in 0.1N NaOH	5.30	4.50	4.5	(28)
9,10-diphenylanthracene in cyclohexane*	9.38	9.35	9.35	(10)
Anthracene in cyclohexane*	5.42	4.87	4.9	(10)
Eosin Y in 0.1N NaOH	3.26	1.55	1.7	(28)
Acridine Orange in H_2O	3.7	2.05	2.0	(28)

*deaerated

TABLE V

UNCORRECTED AND CORRECTED FLUORESCENCE
LIFETIMES OF THE 1,10-PHENANTHROLINES AT 25° C*

COMPOUND	τ uncorrected (nsec)		τ corrected (nsec)	
	Methanol	0.1N H_2SO_4	Methanol	0.1N H_2SO_4
Quinine Sulfate **				19.4
1,10-phenanthroline	4.12	3.26	2.04 ± 0.04	1.56 ± 0.05
5-methyl-	5.52	10.2	4.74 ± 0.03	9.77 ± 0.07
5-phenyl-	3.68	24.8	2.29 ± 0.06	24.8 ± 0.4
5-chloro-	4.69	3.27	2.68 ± 0.05	2.03 ± 0.03
5,6-dimethyl-	5.45	12.3	4.62 ± 0.02	12.0 ± 0.2
2,9-dimethyl-	4.25	5.96	2.14 ± 0.04	5.22 ± 0.02
4,7-dimethyl-	3.89	3.65	2.74 ± 0.03	2.49 ± 0.05
4,7-diphenyl-	3.94	6.60	2.04 ± 0.04	5.87 ± 0.05
2,9-dimethyl -4,7-diphenyl-	3.73	8.07	2.00 ± 0.05	7.54 ± 0.04
3,5,6,8-tetramethyl-	5.06	11.4	4.30 ± 0.02	11.0 ± 0.1
3,4,7,8-tetramethyl-	4.39	4.12	3.59 ± 0.06	3.07 ± 0.05
-4,7-diol · HCl	4.84	3.34	3.70 ± 0.05	1.12 ± 0.05
5-nitro-	***	***	***	***
-5,6-dione	***	***	***	***

* Deaeration of samples did not change the τ values, thus O_2 quenching is negligible
** Time base calibration standard
*** Fluorescence is too weak or is nonexistent

CHAPTER V

TREATMENT OF DATA

Part II: Corrected Spectra and Quantum Efficiencies

Corrected Fluorescence Spectra

Fluorescence intensities are usually expressed in relative units, that is, all intensities are expressed relative to the maximum of the fluorescence band. In this work, for the sake of convenience, the maximum was chosen to be unity.

Following Parker's method (13d) the fluorescence spectra of the phenanthrolines are presented in relative quanta per unit wavenumber (μm^{-1}) plotted versus wavenumber. These are given in figures 18 through 29. The spectrofluorometer automatically records the uncorrected spectra in terms of intensity versus wavelength with the wavelength scale being linear. The intensity scale, after correction, is therefore proportional to the relative quanta per unit wavelength interval, that is to $dQ/d\lambda$, where Q is the total number of quanta per unit time. These $dQ/d\lambda$ values were obtained by dividing the photomultiplier response values by the spectral sensitivity factor $S\lambda$(equation 3-1).

The conversion from relative quanta per unit wavelength to per unit wavenumber was done according to the Parker and Rees's procedure (35), and is as follows:

$$\frac{dQ}{d\lambda} = \frac{dQ}{d\bar{\nu}} \cdot \frac{d\bar{\nu}}{d\lambda} \qquad (5\text{-}1)$$

Since $\lambda = 1/\bar{\nu}$, where $\bar{\nu}$ is the wavenumber, then

$$\frac{d\lambda}{d\bar{\nu}} = -\frac{1}{\bar{\nu}^2} = -\lambda^2 \qquad (5\text{-}2)$$

Substitution of (5-2) into (5-1) gives

$$\frac{dQ}{d\bar{\nu}} = -\frac{1}{\bar{\nu}^2}\frac{dQ}{d\lambda}$$

$$= -\lambda^2 \frac{dQ}{d\lambda} \qquad (5\text{-}3)$$

that is, in the replotting of the corrected spectra, the $dQ/d\lambda$ values were multiplied by λ^2, and the spectrum height was normalized to unity (the negative sign in 5-3 is immaterial since intensity values are in relative units only).

The Corrected Fluorescence Spectrum of 2-Aminopyridine

During our work with correction of fluorescence spectra and the determination of spectral sensitivity factors (Chapter III), we tried to find a standard compound, in addition to quinine sulfate, in order to check the $S\lambda$ values obtained by the calibrated xenon lamp method. 2-aminopyridine, as suggested by Rusakowicz and Testra (36)(37), was chosen, but the $S\lambda$ values determined using this compound were completely different from the $S\lambda$ values determined by using the xenon lamp and the quinine sulfate methods. We therefore concluded that the spectrum presented by these authors was in error. Their spectrum as well as ours are shown in figure 30.

Since 2-aminopyridine was also used as a standard in the determination of quantum efficiencies, their value of 0.60 ± 0.05 was also checked using their procedure (36), and by comparing it against quinine sulfate. This value was found to be correct within their given uncertainty range.

Fluorescence Quantum Efficiencies

Fluorescence quantum efficiencies were determined using the method of relative fluorescence measurement, and the parker and Rees procedure was adopted (35). In this method, the total fluorescence emission of the sample was compared with the total fluorescence emission of a standard compound with a known quantum efficiency. This comparison was carried out using the same optical geometry, the same sample cell, and the same intensity of exciting radiation. Thus for dilute solutions, and from equation (2-19)

$$\frac{F_1}{F_2} = \frac{(\varepsilon bc)_1 \, \phi_{f1}}{(\varepsilon bc)_2 \, \phi_{f2}} \qquad (5\text{-}4)$$

where subscript 1 and 2 refer to the two compounds under consideration. In terms of total number of quanta per unit time, (5-4) is written as

$$\frac{Q_1}{Q_2} = \frac{A_1}{A_2} \cdot \frac{R_1}{R_2} = \frac{(\varepsilon bc)_1 \, \phi_{f1}}{(\varepsilon bc)_2 \, \phi_f{}^2} \qquad (5\text{-}5)$$

where A_1/A_2 is the ratio of the two corrected fluorescence areas of the compounds expressed in the same recorder chart units and R_1/R_2 is the ratio of the detector responses at their respective peak height maximum (each divided by $S\lambda$ if the peak heights are at different wavelengths).

The best way to use equation (5-5) is to adjust the concentration of the standard compound in such a way as to have $(\varepsilon bc)_1 = (\varepsilon bc)_2$ (it is suggested that absorbances should be kept below 0.4 (13c). Thus (5-5) reduces to

$$\phi_{f1} = \frac{A_1}{A_2} \cdot \frac{R_1}{R_2} \cdot \phi_f \qquad (5\text{-}6)$$

Table VI gives the fluorescence quantum efficiencies of the 1,10-phenanthrolines as compared to the fluorescence quantum efficiency of 2-aminopyridine at 25° C.

TABLE VI

FLUORESCENCE QUANTUM EFFICIENCIES
OF THE 1,10-PHENANTHROLINES AT 25° C

COMPOUND	A(sample)/A(std.)		R(sample)/R(std.)		ϕ_f	
	Methanol	0.1N H_2SO_4	Methanol	0.1N H_2SO_4	Methanol	0.1N H_2SO_4
2-aminopyridine *	-	-	-	-	-	0.6 ± 0.05
1,10-phenanthroline	0.746	1.42	0.010	0.007	0.004 ± 0.002	0.006 ± 0.001
5-methyl-	0.768	1.67	0.040	0.038	0.018 ± 0.005	0.038 ± 0.003
5-phenyl-	0.958	1.70	0.092	0.990	0.053 ± 0.003	1.00 ± 0.05
5-chloro-	0.612	1.64	0.004	0.006	0.002 ± 0.001	0.006 ± 0.001
5,6-dimethyl-	0.883	1.70	0.032	0.069	0.017 ± 0.005	0.07 ± 0.005
2,9-dimethyl-	0.644	1.50	0.004	0.027	0.002 ± 0.001	0.024 ± 0.003
4,7-dimethyl-	0.679	1.31	0.064	0.068	0.026 ± 0.004	0.054 ± 0.002
4,7-diphenyl-	0.818	1.56	0.132	0.185	0.064 ± 0.004	0.17 ± 0.01
2,9-dimethyl -4,7-diphenyl-	0.874	1.62	0.039	0.224	0.020 ± 0.005	0.22 ± 0.01
3,5,6,8-tetramethyl-	0.861	1.71	0.026	0.081	0.013 ± 0.002	0.082 ± 0.005
3,4,7,8-tetraethyl-	0.568	1.35	0.070	0.041	0.024 ± 0.002	0.033 ± 0.002
-4,7-diol · HCl	0.805	1.41	0.011	0.007	0.005 ± 0.001	0.006 ± 0.001
5-nitro-	-	-			**	**
-5,6-dione	-	-			**	**

* Standard Compound (36)
** Fluorescence is too weak or is nonexistent.

CHAPTER VI

TREATMENT OF DATA

Part III: Radiative Lifetimes, Oscillator Strength, Stokes Shift

Absorption and corrected fluorescence emission spectra were required for the evaluation of the radiative lifetimes, the oscillator strengths, and the Stokes shifts. It was therefore necessary to have the spectra expressed in terms of wavenumbers (μm^{-1}) rather than the usual wavelength scale.

Evaluation of some of the terms in equation (2-20) required the plotting of $F(\bar{\nu})/\bar{\nu}^3$ and $\varepsilon(\bar{\nu})/\bar{\nu}$ versus $\bar{\nu}$ so that the areas under the $\int F(\bar{\nu})/\bar{\nu}^3 \, d\bar{\nu}$ and $\int \varepsilon(\bar{\nu})/\bar{\nu} \, d\bar{\nu}$ curves could be obtained. The integration for $\int \varepsilon(\bar{\nu})/\bar{\nu} \, d\bar{\nu}$ is supposed to be carried out over the modified first absorption band. Unfortunately the phenanthroline spectra (figures 31 through 42) contain high order absorption bands which overlap the first absorption band. The high wavenumber end of the spectrum was therefore extrapolated and was made to fall to zero (13a).

The oscillator strength required the determination of the integral $\int \varepsilon(\bar{\nu}) d\bar{\nu}$, that is the area under the absorption curve. Here, again, the above mentioned extrapolation had to be carried out.

Leeman's method for the determination of Stokes shift is only an approximation (equation 2-23). A better method (10) is to find the center of gravity of the absorption and the fluorescence bands, and then to take the difference between the wavenumbers at these two points. Half the value of this difference is termed Stokes loss. This method could not be applied to the phenanthrolines because of the spectral band overlap described above.

Table VII summarizes the calculations necessary to evaluate these three parameters.

TABLE VII

EVALUATION OF RADIATIVE LIFETIMES, OSCILLATOR STRENGTH, AND STOKE S SHIFT

COMPOUND	$10^{-4}\int\varepsilon(\bar{\nu})\,d\bar{\nu}$		$10^{-3}\int\varepsilon(\bar{\nu})/\bar{\nu}\,d\bar{\nu}$		$\bar{\nu}^{-3}$ av.		$\bar{\nu}_A$ max (μm^{-1})		$\bar{\nu}_F$ max (μm^{-1})	
	Methanol	H_2SO_4 0.1N	Methanol	H_2SO_4 0.1N	Methanol	H_2SO_4 0.1N	Methanol	H_2SO_4 0.1N	Methanol	H_2SO_4 0.1N
1,10-phenanthroline	1.32	1.68	3.47	4.56	0.92	0.92	3.80	3.69	2.72	2.33
5-methyl-	1.47	1.64	3.92	4.54	0.90	0.94	3.74	3.60	2.69	2.13
5-phenyl-	3.57	3.53	8.99	9.37	0.89	0.95	3.98	3.80	2.67	2.06
5-chloro-	1.56	1.59	4.16	4.39	0.95	0.94	3.76	3.62	2.72	2.17
5,6-dimethyl-	1.72	1.70	4.67	4.84	0.84	0.94	3.69	3.51	2.60	2.06
2,9-dimethyl-	1.80	1.76	4.86	4.96	0.92	0.92	3.58	3.54	2.72	2.30
4,7-dimethyl-	1.39	1.85	3.68	5.08	0.94	0.90	3.79	3.65	2.75	2.41
4,7-diphenyl-	2.98	2.45	8.13	7.00	0.89	0.91	3.66	3.50	2.63	2.15
2,9-dimethyl -4,7-diphenyl-	2.02	2.53	5.62	7.38	0.86	0.91	3.60	3.43	2.60	2.13
3,5,6,8-tetramethyl-	1.58	1.97	4.40	5.75	0.83	0.92	3.60	3.43	2.63	2.06
3,4,7,8-tetramethyl-	1.82	1.92	4.40	5.38	0.88	0.90	4.13	3.56	2.76	2.41
-5,6-diol · HCl	2.12	2.12	5.57	5.76	0.92	0.93	3.80	3.69	2.76	2.31

For methanol and 0.1N H_2SO_4 $n_a \sim n_f \sim 1.34$ (8)(9)

TABLE VIII

FLUORESCENCE PARAMETERS OF 1,10-PHENANTHROLINES
IN METHANOL AND IN 0.1N H_2SO_4 AT 25°C

COMPOUND	f		$\bar{\nu}_A - \bar{\nu}_F$ (μm^{-1})		ϕ_f		τ (nsec)		τ_o (nsec) Calculated		$\tau_o = \tau/\phi_f$ (nsec)	
	Methanol	H_2SO_4 0.1N	Methanol	H_2SO_4 0.1N	Methanol	H_2SO_4 0.1N	Methanol	H_2SO_4 0.1N	Methanol	H_2SO_4 0.1N	Methanol	H_2SO_4 0.1N
1,10-phenanthroline	0.15	0.20	1.08	1.36	0.004	0.006	2.04	1.56	64	49	510	260
5-methyl-	0.17	0.20	1.05	1.48	0.018	0.038	4.74	9.77	58	48	263	257
5-phenyl-	0.39	0.40	1.31	1.73	0.053	1.00	2.29	24.8	25.7	23.1	43	25
5-chloro-	0.18	0.19	1.04	1.44	0.002	0.006	2.68	2.03	52	50	1340	338
5,6-dimethyl-	0.20	0.21	1.09	1.45	0.017	0.07	4.62	12.0	52	45	272	171
2,9-dimethyl-	0.21	0.21	0.87	1.24	0.002	0.024	2.14	5.22	46	45	1070	217
4,7-dimethyl-	0.16	0.22	1.04	1.24	0.026	0.054	2.74	2.49	59	45	105	46
4,7-diphenyl-	0.35	0.30	1.03	1.35	0.064	0.17	2.04	5.87	28.5	32	32	34.5
2,9-dimethyl -4,7-diphenyl	0.24	0.32	0.99	1.30	0.020	0.22	2.00	7.54	42.5	31	100	34
3,5,6,8-tetramethyl	0.19	0.25	0.96	1.37	0.013	0.082	4.30	11.0	56	39	331	134
3,4,7,8-tetramethyl	0.19	0.23	1.38	1.16	0.024	0.033	3.59	3.07	53	42	150	93
-5,6-Diol · HCl	0.24	0.25	1.04	1.38	0.005	0.006	3.70	1.12	40	38	740	187

For methanol and 0.1N H_2SO_4 $n_a \sim n_f \sim 1.34$ (8)(9)

CHAPTER VII

DISCUSSIONS AND CONCLUSIONS

Outline of Results

The observed lifetime τ, the quantum efficiency ϕ_f, the radiative lifetime τ_o, the oscillator strength f, and the Stokes shift $(\bar{\nu}_A - \bar{\nu}_F)$ of the 1,10-phenanthrolines in methanol and in 0.1N H_2SO_4 have been collected in Table VIII. The τ values were listed in units of nanoseconds (nsec), and the frequencies $\bar{\nu}$ in units of micrometers (μm^{-1}).

It was very difficult to determine the overall magnitude of the errors involved in the measurement of the fluorescence parameters. The following is an attempt to estimate the errors associated with each of these parameters.

1. Observed lifetime τ: The uncertainties for τ have been listed in Table V. These represent errors associated with the linearity of the semilog plots (F/F_o values being taken between 0.15 and 0.85) for several runs of the same sample, and the reproducibility of values of the lifetime from sample to sample (for at least two samples) (39). For weak fluorescence signals (very low quantum efficiencies), there were large errors associated with the instrument response and with the signal-to-noise ratios, so that an additional 10% error in the measurement of τ values is possible.
2. Molar absorbtivity ε: Values of ε_{max} are accurate to within 5% as determined by comparison with reported values (2)(40).
3. $\bar{\nu}_A - \bar{\nu}_F$: An estimated uncertainty of $\pm$ 0.04 $m\mu^{-1}$ is possible.
4. Quantum efficiencies ϕ_f: The uncertainties for ϕ_f have been

listed in Table VI. These represent variations for within the same experiment, and for the reproducibility of the results from sample to sample (for two samples). A serious source of error occurs in the determination of quantum efficiencies of weakly fluorescing compounds. Since the efficiencies of these compounds were found by comparing against a standard, usually a relatively strong fluorescing compound, small variations of concentrations, temperature, and instrument calibration produced large changes in the quantum efficiencies of these weakly emitting compounds. This is the reason why ϕ_f values in the literature are rarely given a definite number if they are smaller than 0.01. The only solution to this dilemma is to use a low quantum yield standard, but none is available at present. The one with low enough value that could possibly have been used was d,l-Tryptophan in water (ϕ_f = 0.13), but even this ϕ_f would have been too high for the very small quantum yields of less than 0.01. This source of error could possibly account for some of the discrepancies observed between the calculated τ_o and the τ_o determined from τ and ϕ_f (Table VIII). For most of the compounds having efficiences of 0.02 or higher, the τ_o values determined by the two methods compared favorably within the listed uncertainty limits.

The Fluorescence Spectrum of 2-Aminopyridine

The source of error made by Rusakowicz and Testa (figure 30) in the measurement of the corrected fluorescence spectrum of 2-aminopyridine could have been due to one of the following reasons: (a) They

corrected their spectrum by using a secondary standard lamp instead of a National Bureau of Standard Lamp, and thus the calibration of their lamp could have been off; or (b) calibration data for standard lamps are provided in the form of watts per unit wavelength interval so that they might have made a mistake when converting this unit to relative quanta per unit frequency interval. The conversion should have been carried out by multiplying the watts per unit wavelength interval by λ^3 (13d).

Substituent Effects

The 1,10-phenanthrolines studied contained the following functional groups: methyl, phenyl, chloro, hydroxyl, nitro, and carbonyl. Of these the carbonyl and the nitro substituted phenanthrolines did not exhibit any fluorescence. Of the remaining groups, the quantum efficiencies tended to decrease in the approximate order of phenyl, methyl, hydroxyl, and chloro. The efficiency of the parent compound was about the same order of magnitude as the chloro group.

Longuet-Higgens and Coulson (38) have calculated the ground state π-electron densities at the different external positions of the unsubstituted 1,10-phenanthrolines, and these are listed in the following table

TABLE IX

RELATIVE π-ELECTRON DENSITIES

Ring Positions	π-electron Densities
1-, 10-	-0.377
2-, 9-	0.138
3-, 8-	0.019
4-, 7-	0.120
5-, 6-	0.015

It had been found that there was a close correlation between the π-electron densities and the chemical behavior in substitution reactions (1). Nucleophilic substitutions occured at the 2-, 4-, 7-, and 9- positions, and electrophilic substitutions occured at the 5- and 6- positions. From pK studies it had been found that methyl substituents in (2-,9-), (4-,7-) and (3-,8-,5-,6-) positions decreased the basicity of the 1,10-phenanthroline in the listed order. It had also been found from the same studies that the electron densities on the ring nitrogens (i) decreased when a phenyl group was in the (2-,4-) positions and increased when in the (3-,5-) positions, and (ii) decreased with halogen substituents.

The four fluorescence parameters listed in Table VIII showed a similar trend. Substitution of similar groups in the higher π-electron density positions increased the values for the Stokes shift, the quantum efficiencies and the observed lifetimes. Substitution of different groups in the same position paralleled the trend shown by the pK studies. There were insufficient data for the 3-,8- positions, but, most probably, it would have followed the same pattern.

Solvent Effects

There was a large change in all the fluorescence parameters as the solvent was changed from methanol to an acidic solution. This change was more pronounced for substituents in the 5-,6- positions.

Table VII indicates that changing the solvent system to a more polar one produced a red shift in both the absorption and the fluorescence maxima. The reason for this could be attributed to the formation of the mono-protonated 1,10-phenanthroline in which the lone paired electrons on the nitrogen are bound. Langmuir (2) reported

that the di-protonated 1,10-phenanthroline had a stronger fluorescence intensity than the mono-protonated specie. She also reported that in nonpolar solvents (cyclohexane) 1,10-phenanthroline did not fluoresce. It is therefore predicted that in nonpolar solvents all the 1,10-phenanthrolines would be nonfluorescing similar to many other nitrogen heterocyclic compounds.

Conclusions

Based on the experimental observations it became important to know the types of electronic transitions, and to be able to classify the excited states from which fluorescence was occuring.

The assignment of transitions in the 1,10-phenanthrolines were carried out using Kasha's rules (41)(42)(43) and these were as follows:

1. The ε_{max} (as well as the oscillator strength) increased in more polar solvents to ε_{max} values of between 10^4 and 10^5. This was a good indication for a (π, π^*) transition.
2. The red shift in an acid media was a sign of a (π,π^*) transition.
3. The increase of quantum efficiency in polar solvents indicated that the lone paired electrons were bound, and that a (π, π^*) transition was occuring.
4. Smaller radiative lifetimes in polar solvents were also an indication of a (π, π^*) transition.

The following conclusions can therefore be reached. In polar solvents the lowest excited singlet state would be a (π, π^*), and thus fluorescence would be observed. In nonpolar solvents the lowest excited singlet state would be a (n, π^*), and intersystem crossing to the triplet state would occur with ease, thus the compounds would

be nonfluorescing or very weakly fluorescing. This means that as the solvent polarity is increased there would come a time when the low lying (n, π^*) state would interchange its level with that of the (π, π^*) state.

For a detailed study of all the excited state properties of the compounds the phosphorescence spectra and other phosphorescence parameters should also be determined. No such studies were carried out in the present work due to the lack of suitable instrumentation.

BIBLIOGRAPHY

BIBLIOGRAPHY

1. Schilt, A.A., "Analytical applications of 1,10-Phenanthroline and related compounds", Pergamon Press, Oxford, 1969.

2. Langmuir, M., "A study of the absorption and fluorescence spectra of 1,10-Phenanthroline and related compounds". Ph.D. dissertation, Purdue University, 1963.

3. Jones, B., "Studies on the fluorescence of 1,10-Phenanthrolines." Ph.D. Dissertation, Kansas State University, 1965.

4. Hatchard, C.G. and Parker, C.A., Proc. Roy. Soc. (London), A235, 518 (1956).

5. Perkampus, H.H., Knop, A., and Knop, J.V., Z. Naturforsch, 23a, 840 (1968).

6. Brinen, J.S., Rosebrook, D.D., and Hirt, R.C., J. Phys. Chem., 67, 2651 (1963).

7. Birks, J.B. and Munro, I.H., in "Progress in Reaction Kinetics", Porter G. (Editor), Pergamon Press, Oxford, Vol. 4, 1967, p. 239-303.

8. Strickler, S.J., and Berg, R.Z., J. Chem. Phys., 37, 814 (1962).

9. Birks, J.B. and Dyson, D.J., Proc. Roy. Soc. (London) A275, 135 (1963).

10. Berlman, I.B., "Handbook of Fluorescence Spectra of Aromatic Molecules", Academic Press, 1965.

11. Leeman, H.G., Stich, K., and Thomas, M., in "Progress in Drug Research", Jucker, E. (Editor), Berkhauser, Basel, Vol. 6, 1963, p. 151.

12. Barrow, G.M., "Molecular Spectroscopy", McGraw Hill, New York, 1962, p. 81.

13. Parker, C.A., "Photoluminescence of Solutions", Elsevier Publishing Comp., Amsterdam, 1968. (13a) p. 27; (13b) p. 438; (13c) p. 261-268; (13d) p. 252-258.

14. Udenfriend, S. "Fluorescence Assay in Biology and Medicine", Academic Press, New York, Vol. 1, 1962, p. 99.

15. Instruction Manuals for the Coleman Hitachi Model EPS-3T Spectrophotometer with the Model G-3 Spectral Fluorescence attachment.

16. Chen, R.F., Anal. Biochem., 20, 339 (1967).

17. Fletcher, A.N., J. Phys. Chem., 72, 2742 (1968).

18. Melhuish, W.H., J. Opt. Soc. Am., 52, 1256 (1962).

19. Melhuish, W.H., J. Phys. Chem., 64, 762 (1960).

20. Argauer, R.J. and White, C.E., Anal. Chem., 36, 368 (1964).

21. Drushel, H.V., Sommers, A.L., and Cox, R.C., Anal. Chem., 35, 2166 (1963).

22. Petz, I.A., "Measurement of Fluorescence Lifetimes of Biologically Significant Compounds". Ph.D. Dissertation, University of the Pacific, 1968.

23. Bennett, R.G., Rev. Sci. Inst., 31, 1275 (1960).

24. Malmberg, J.H., Rev. Sci. Inst., 28, 1027 (1957).

25. Berlman, I.B., Steingraber, O.J., and Benson, M.J., Rev. Sci. Inst., 39, 54 (1968).

26. Macrey, R.C., Pollack, S.A., and Witte, R.S., Rev. Sci. Inst., 36, 1715 (1965).

27. Ware, W.R., and Baldwin, B.A., J. Chem. Phys., 40, 1703 (1964).

28. Chen, R.F., Vurek, G.G., and Alexander, N., Science, 156, 949 (1967).

29. Brody, S.S., Rev. Sci. Inst., 28, 1021 (1957).

30. Munro, I.H. and Ramsay, I.A., J. Sci. Inst., Series 2, Vol. 2(E) (1968); Herb, G.K., and Van Sciver, W.J., Rev. Sci. Inst., 36, 1650 (1965); Cooper, D.H., Rev. Sci. Inst., 37, 1407 (1966); Swank, R.K., Phillips, H.B., Buck, W.L., and Basile, L.J., IRE Trans. Nucl. Sci. NS-5, No. 3, 183 (1958b).

31. Crosby, G.A., and Demas, J.N., Anal. Chem., 42, 1010 (1970).

32. Birks, J.B., " The theory and practice of Scintillation Counting ", Macmillan Comp., New York, 1964. p. 175-176.

33. Tanasescu, T., I.R.E. Trans. Nucl. Sci. NS-7, No. 2-3, 39 (1960).

34. Kaplan, W., "Ordinary Differential Equations", Addison-Wesley Publ. Comp., 1958. p. 104.

35. Parker, C.A. and Rees, W.T., Analyst, 85, 587 (1960).

36. Rusakowicz, R., and Testa, A.C., J. Phys. Chem., 72, 2680 (1968).

37. Testa, A.C., American Instrument Co. Newsletter, 4, 4(1),(1969).

38. Longuet-Higgens, H.C., and Coulson, C.A., J. Chem. Soc. 1954, 1534.

39. Dawson, W.R., and Kropp, J.L., J. Phys. Chem., 73, 693 (1969).

40. Lang, "Absorption Spectra in the UV and VIS Region", Vol. 2, p. 389-390; Vol. 3, p. 391-392; Vol. 8, p. 377-386.

41. Kasha, M., Faraday Soc. Disc., 9, 14 (1950).

42. Calvert, J.G., and Pitts, J.N., "Photochemistry", Wiley, 1967. p. 260.

43. Brealey, G.J. and Kasha, M., J. Am. Chem. Soc., 77, 4462 (1955).

APPENDIX

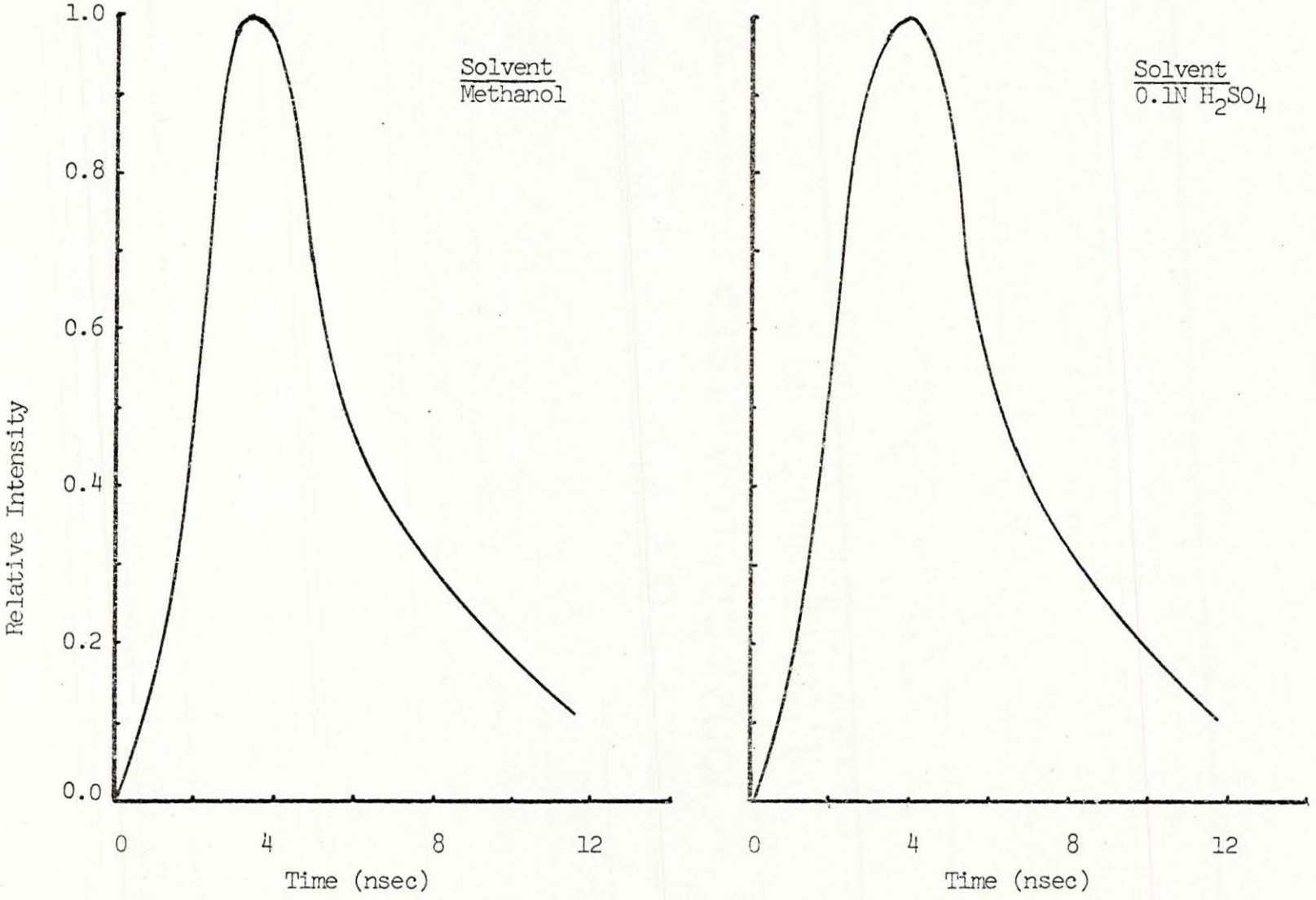

Figure 6: Fluorescence Decay Curve of 1,10-Phenanthroline
(The Lamp Decay is as in Figure 7)

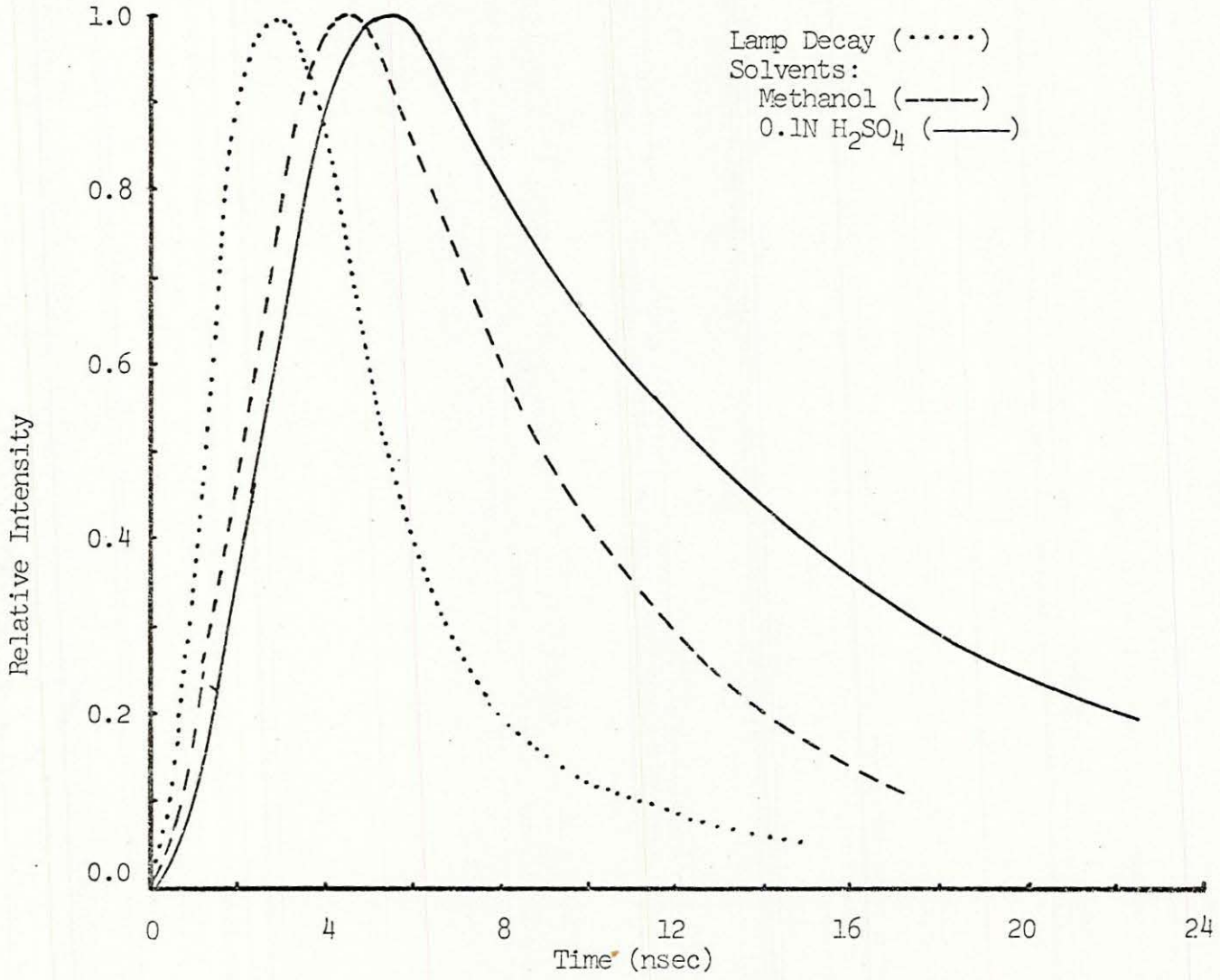

Figure 7: Fluorescence Decay Curve of 5-Methyl-1,10-Phenanthroline

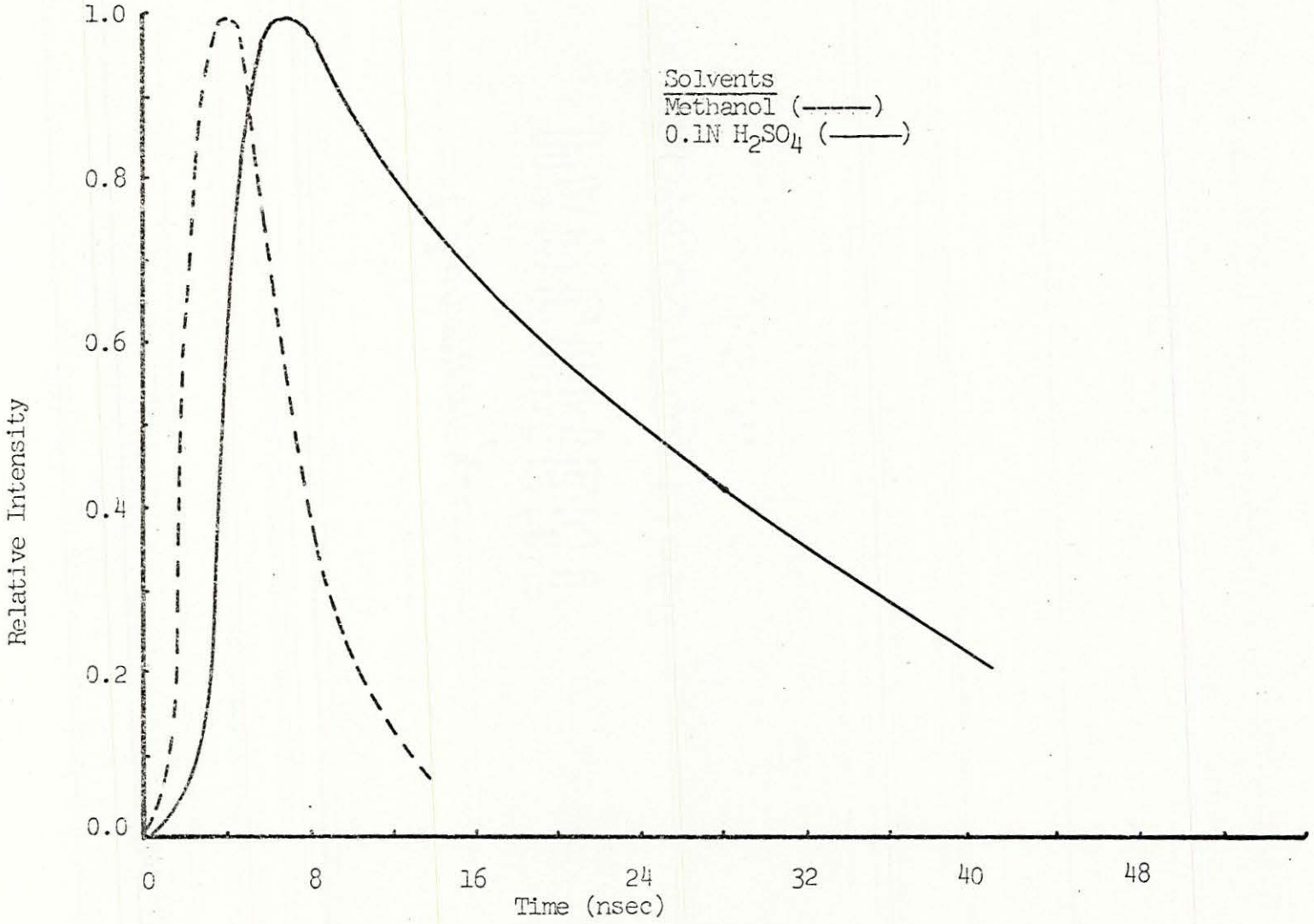

Figure 8: Fluorescence Decay Curve of 5-Phenyl-1,10-Phenanthroline
(The Lamp Decay is as shown in Figure 7)

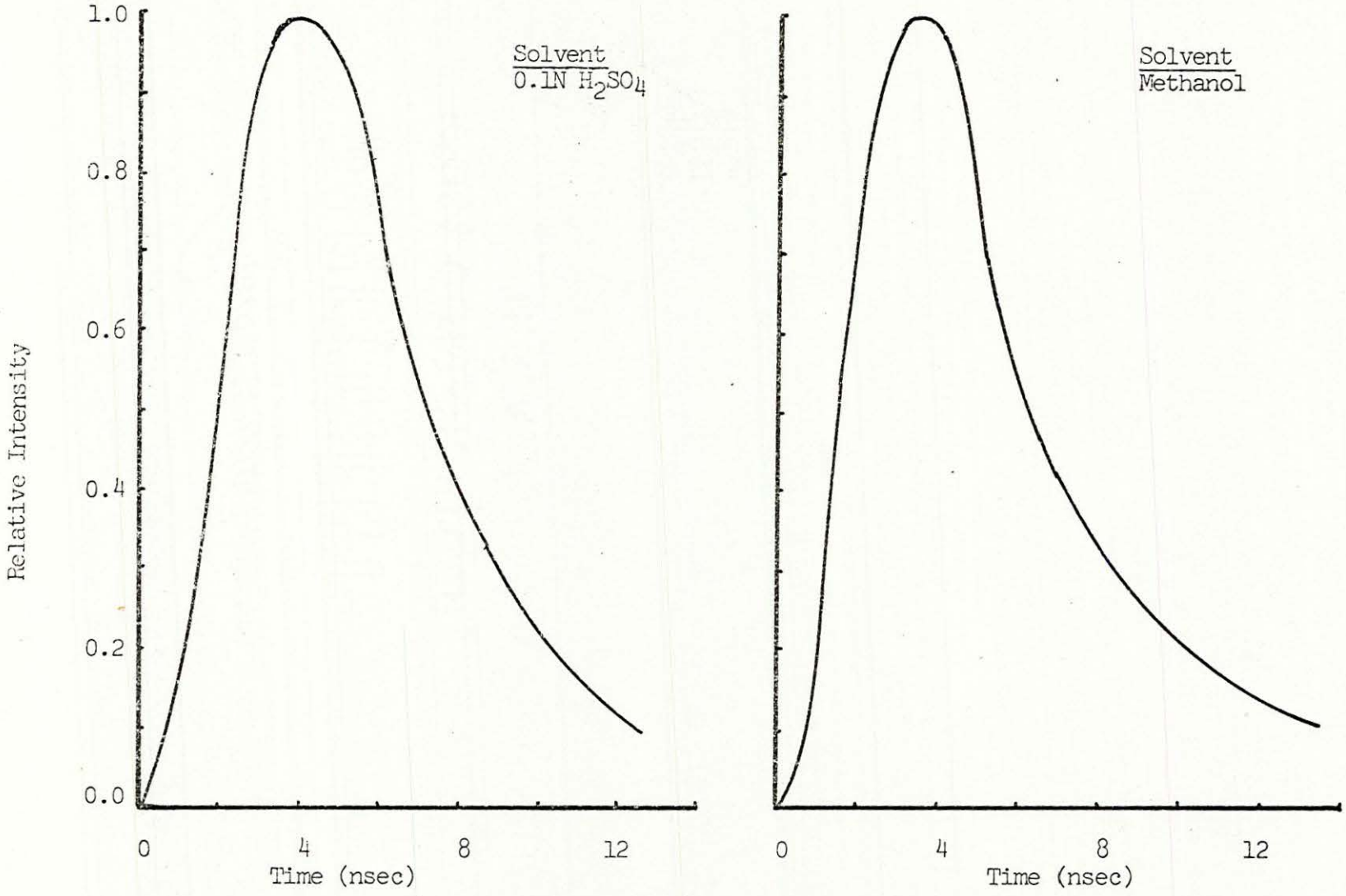

Figure 9: Fluorescence Decay Curve of 5-Chloro-1,10-Phenanthroline
(The Lamp Decay is as in Figure 7)

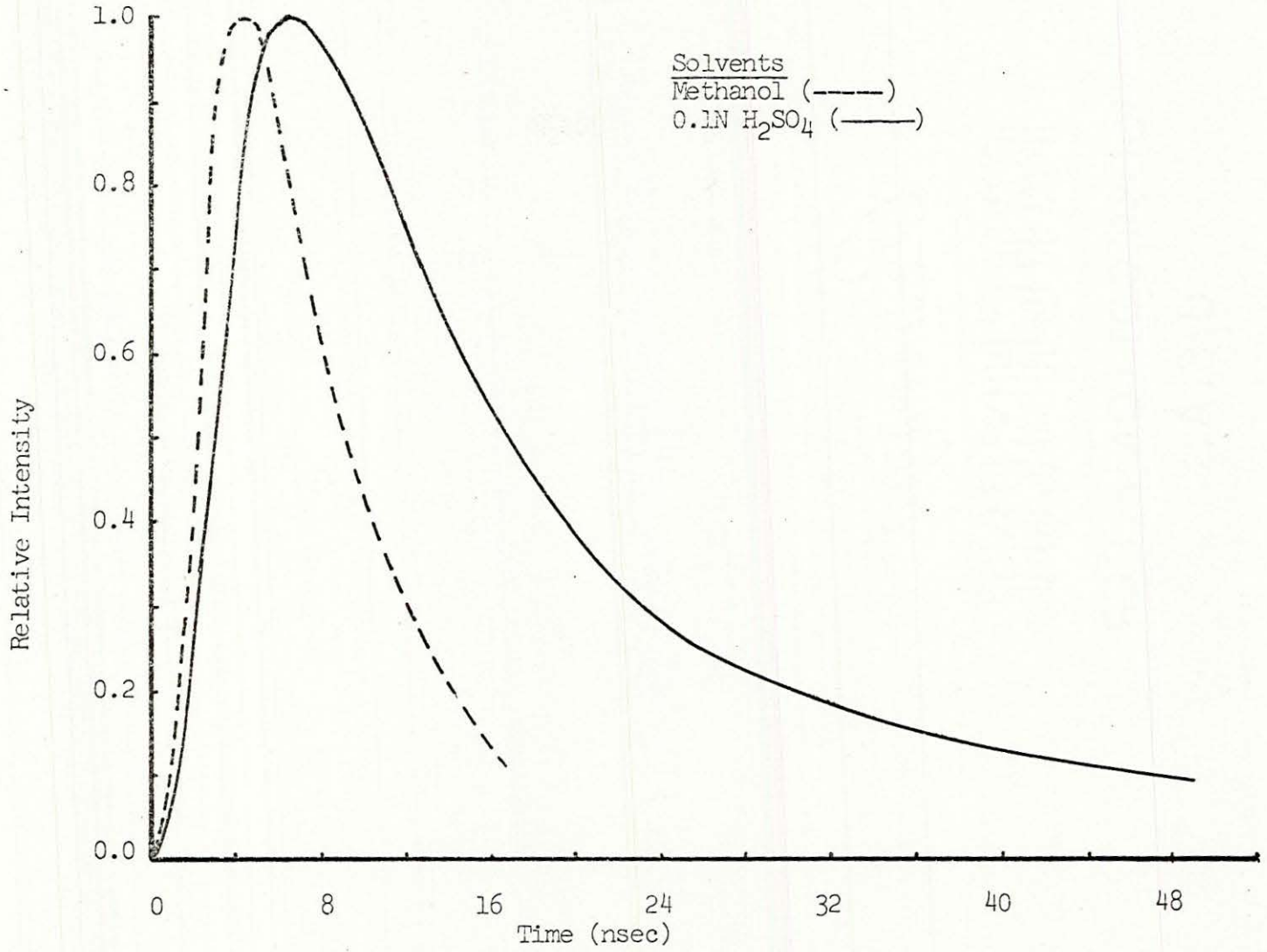

Figure 10: Fluorescence Decay Curve of 5,6-Dimethyl-1,10-Phenanthroline (The Lamp Decay is as in Figure 7)

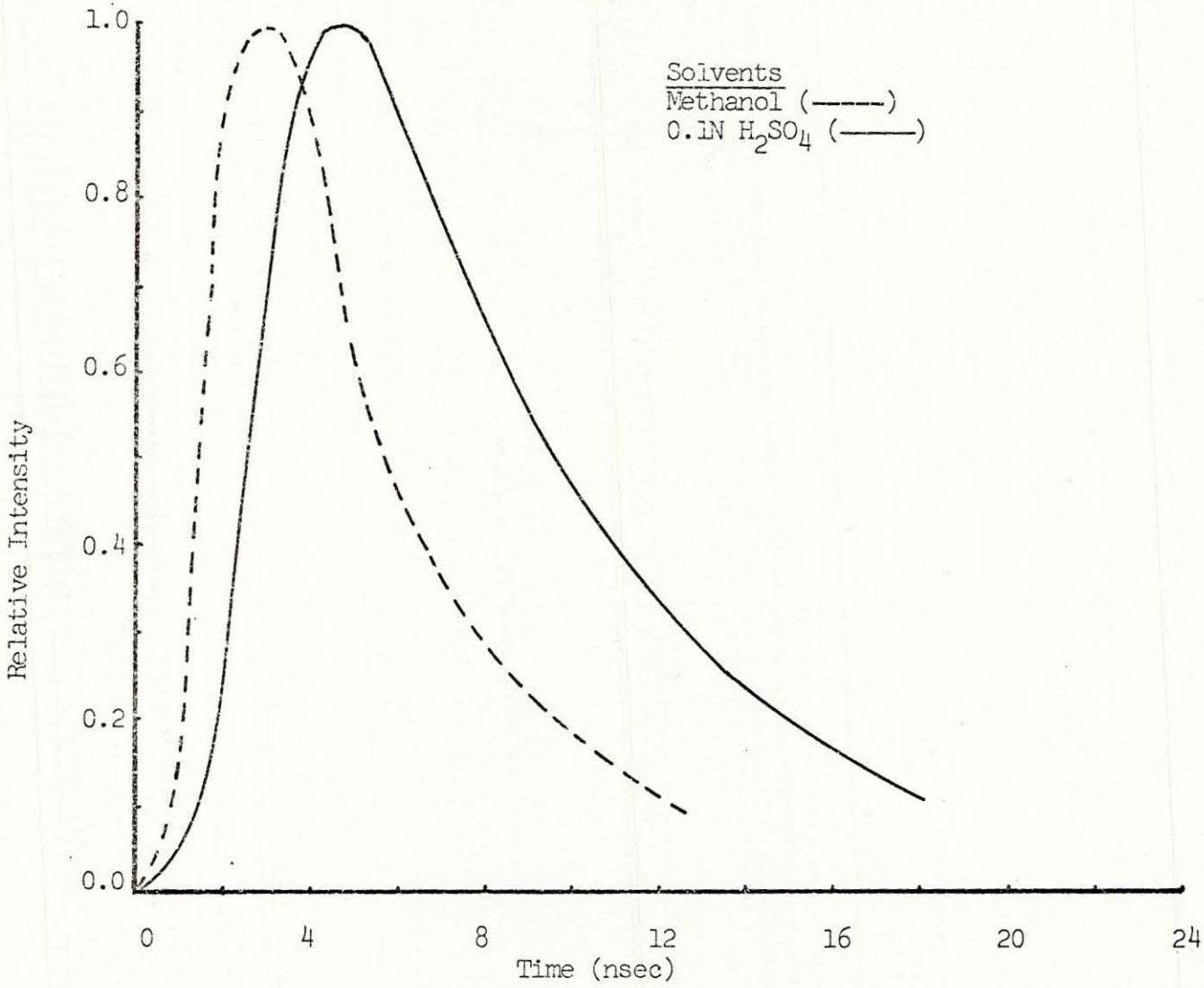

Figure 11: Fluorescence Decay Curve of 2,9-Dimethyl-1,10-Phenanthroline (The Lamp Decay is as in Figure 7)

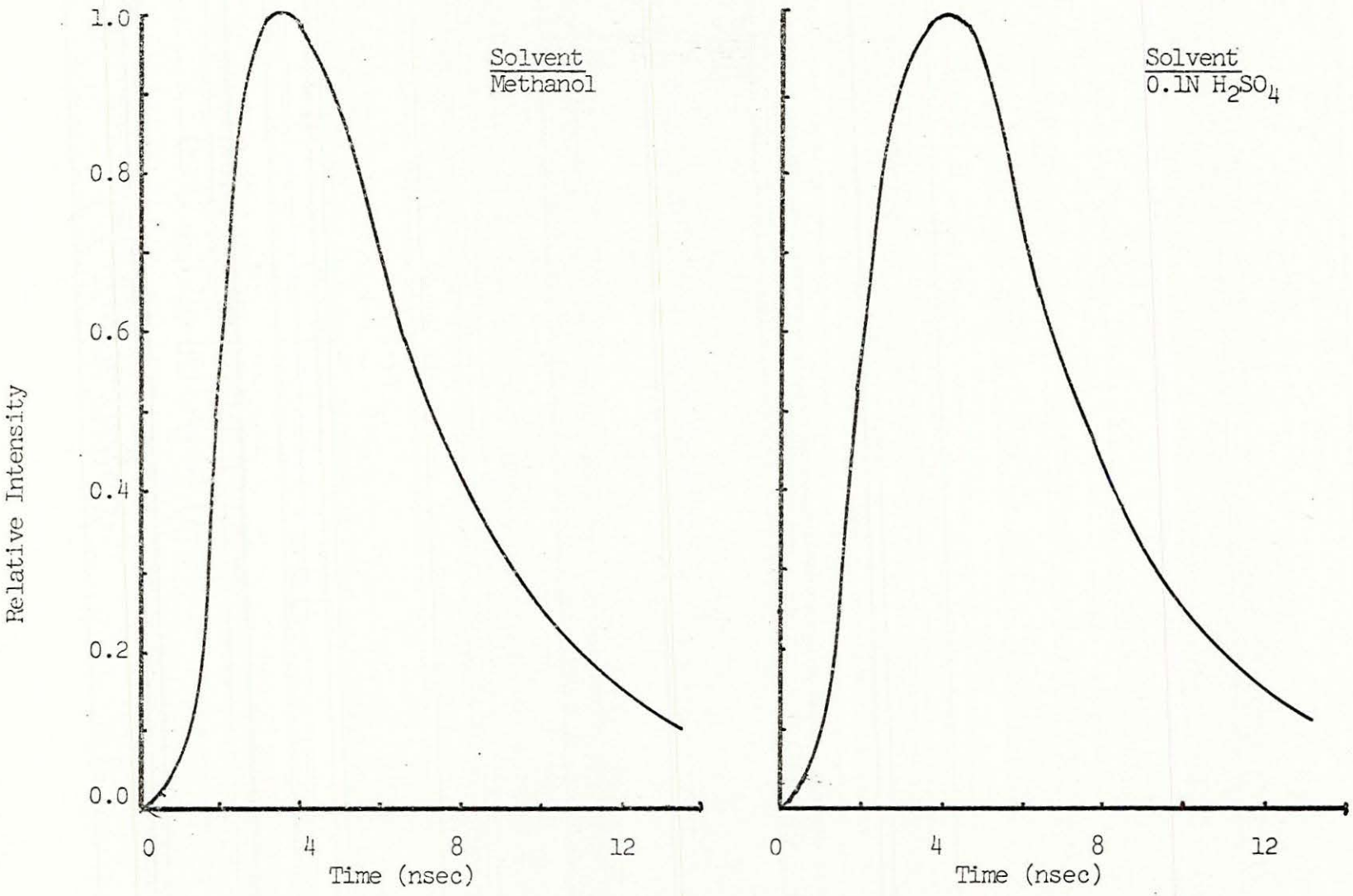

Figure 12: Fluorescence Decay Curve of 4,7-Dimethyl-1,10-Phenanthroline
(The Lamp Decay is as in Figure 7)

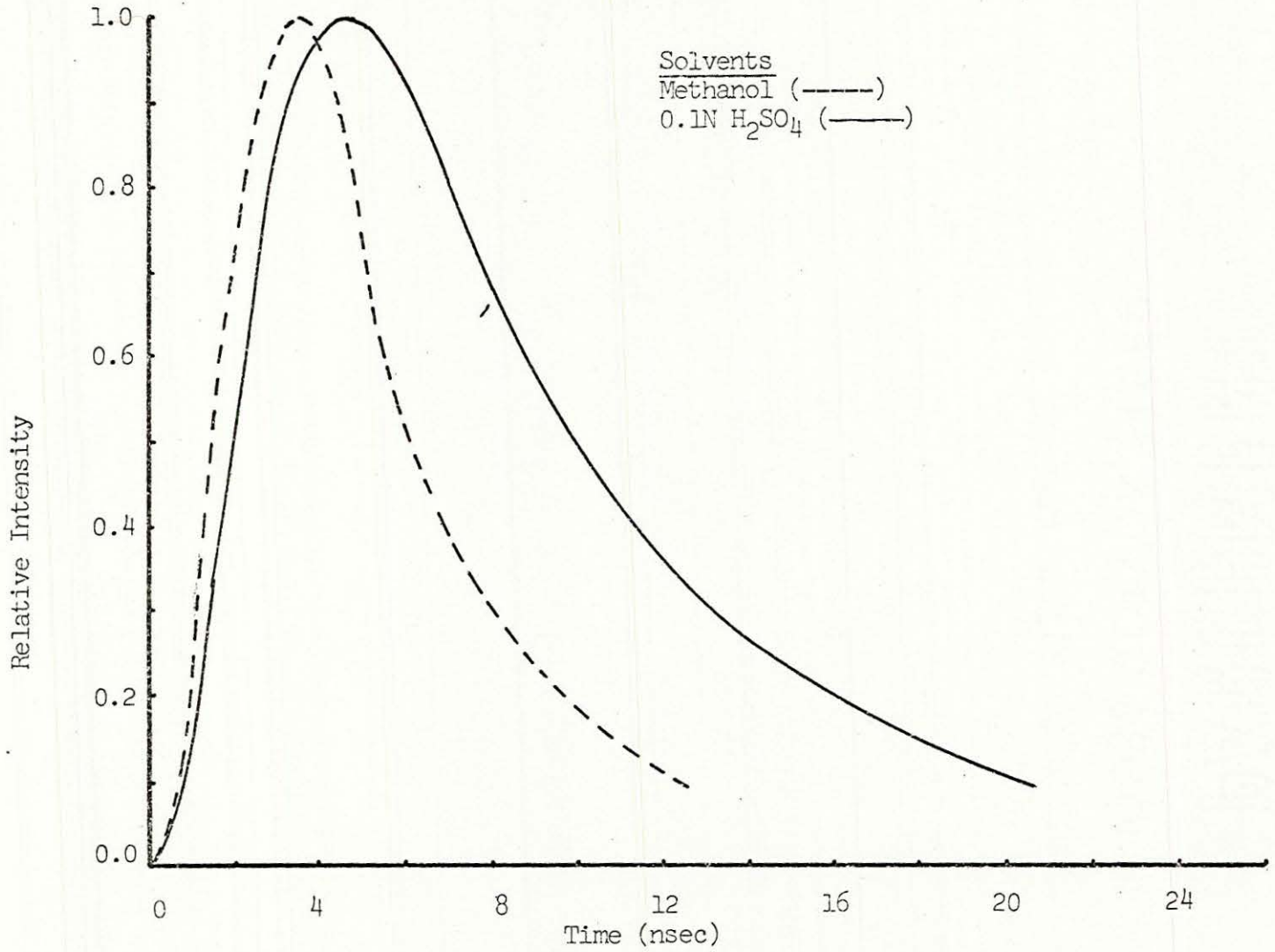

Figure 13: Fluorescence Decay Curve of 4,7-Diphenyl-1,10-Phenanthroline (The Lamp Decay is as in Figure 7)

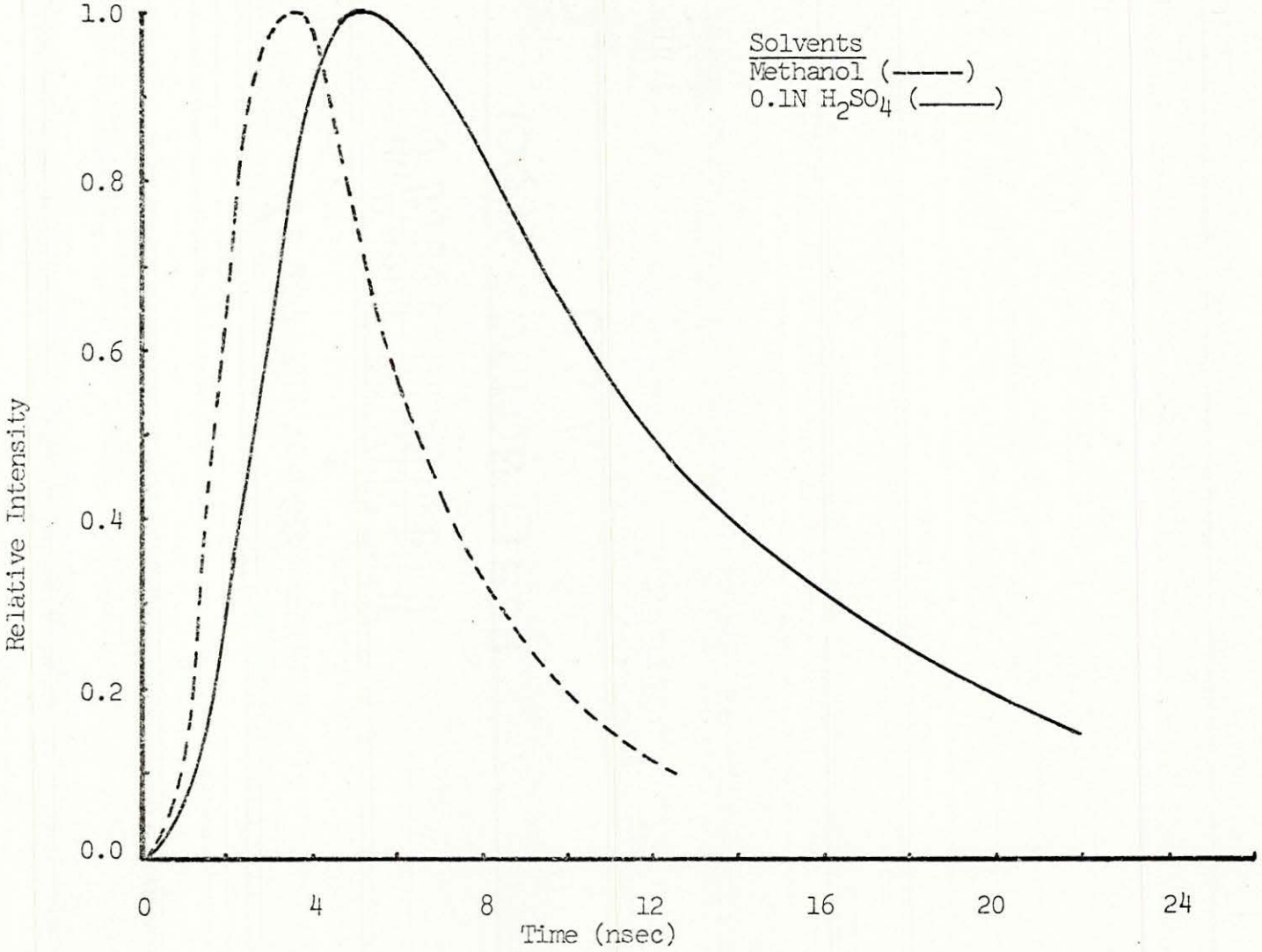

Figure 14: Fluorescence Decay Curve of 2,9-Dimethyl-4,7-Diphenyl-1,10-Phenanthroline
(The Lamp Decay is as shown in Figure 7)

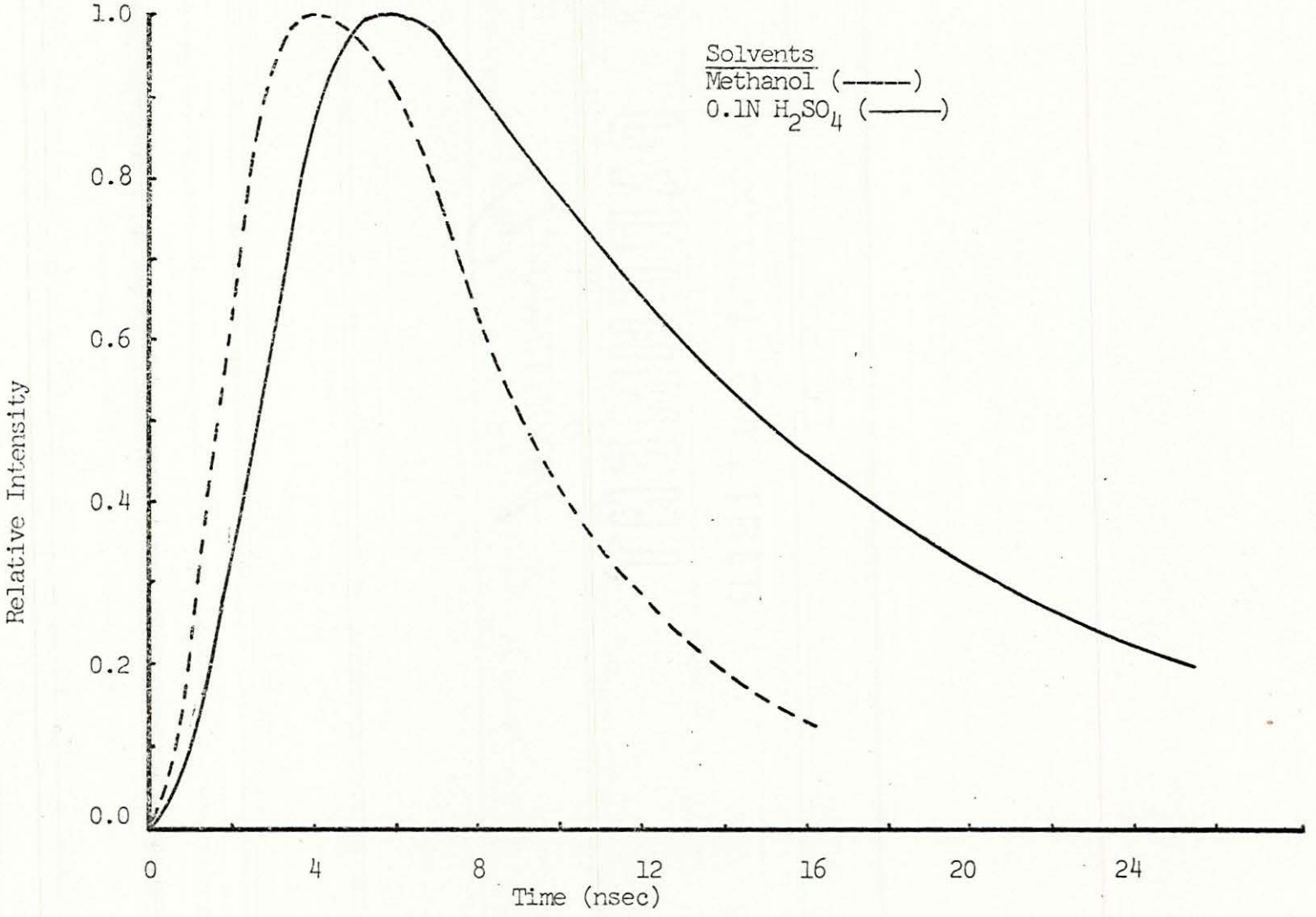

Figure 15: Fluorescence Decay Curve of 3,5,6,8-Tetramethyl-1,10-Phenanthroline
(The Lamp Decay is as in Figure 7)

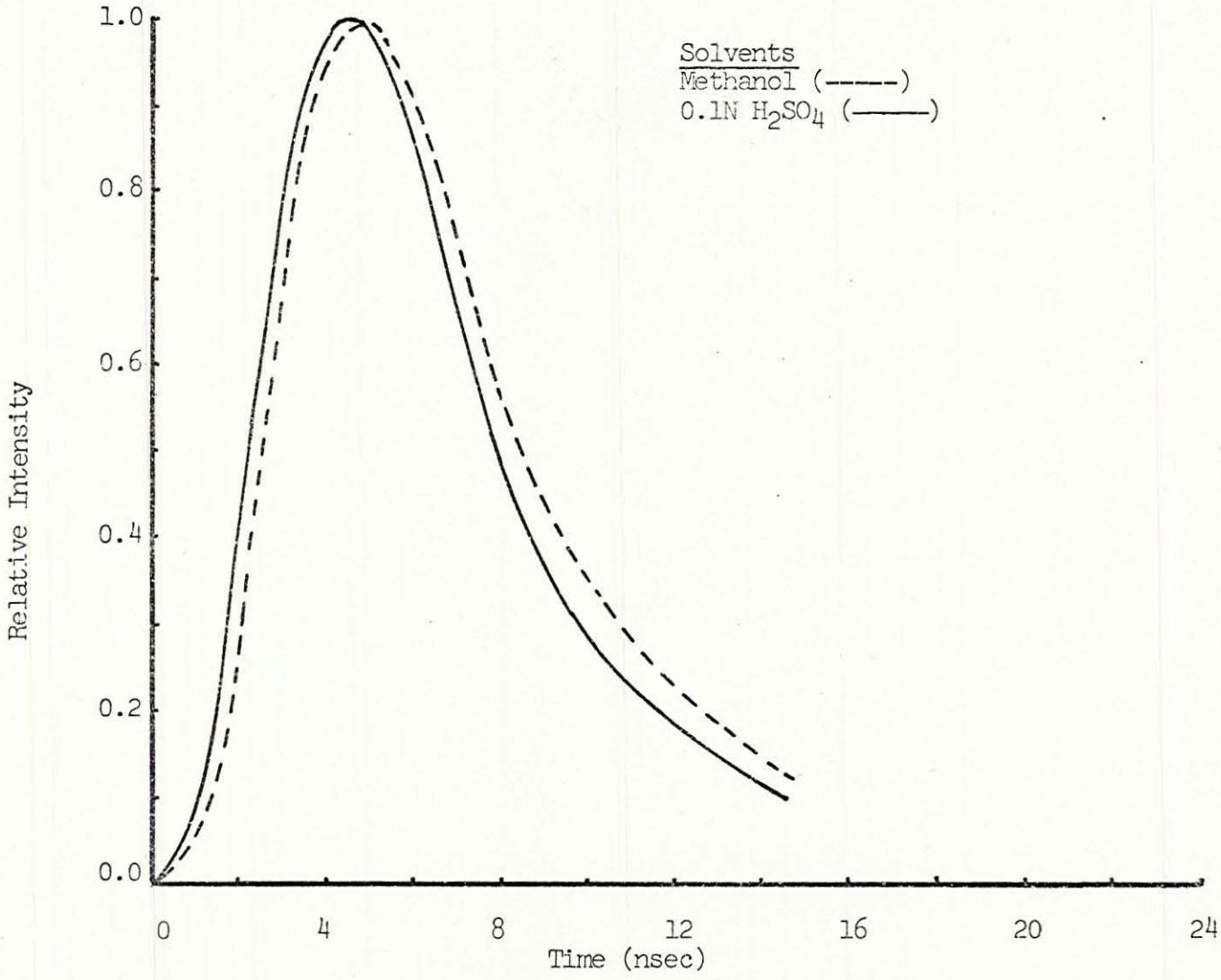

Figure 16: Fluorescence Decay Curve of 3,4,7,8-Tetraethyl-1,10-Phenanthroline (The Lamp Decay is as in Figure 7)

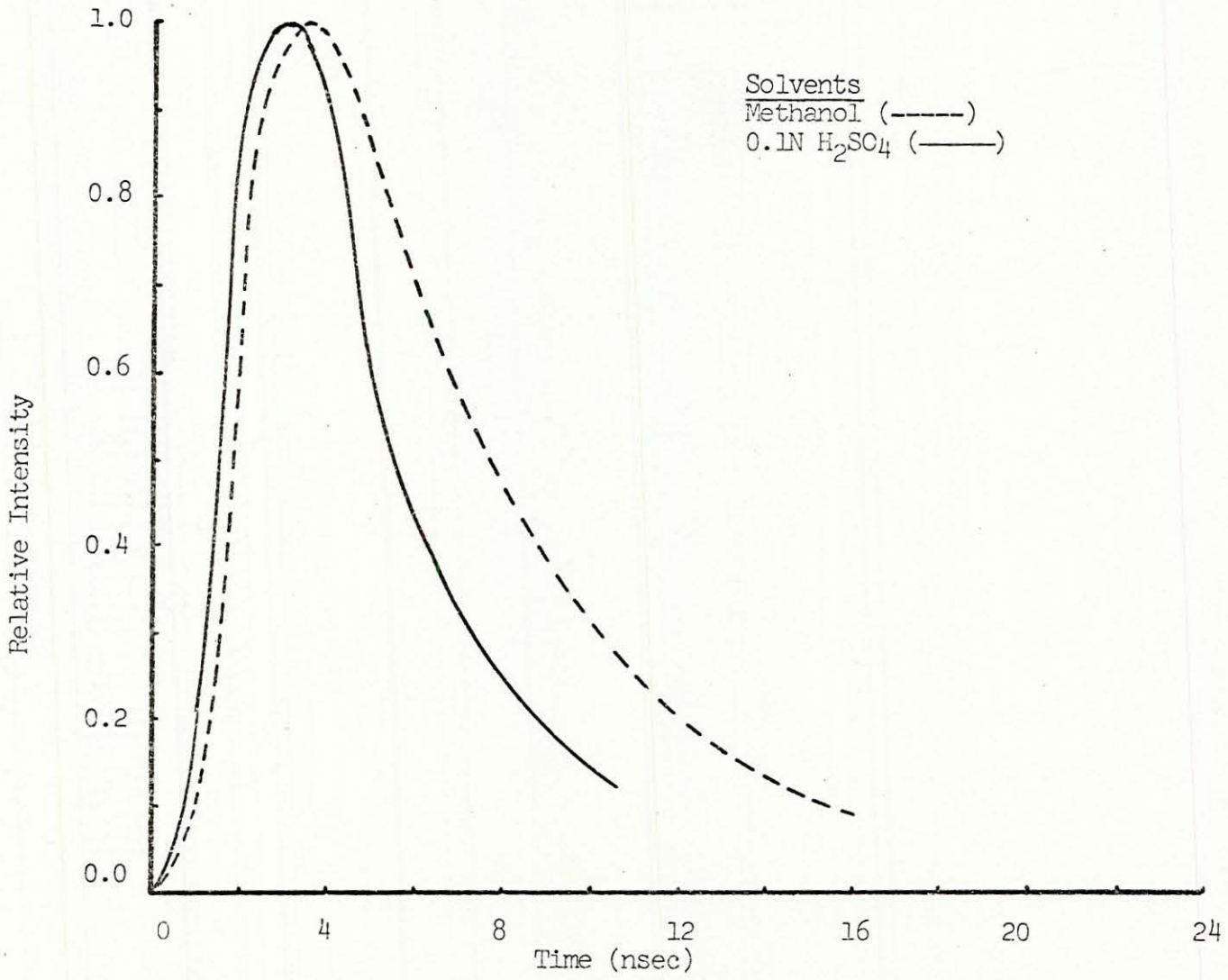

Figure 17: The Fluorescence Decay Curve of 1,10-Phenanthroline-4,7-Diol Monohydrochloride
(The Lamp Decay is as in Figure 7)

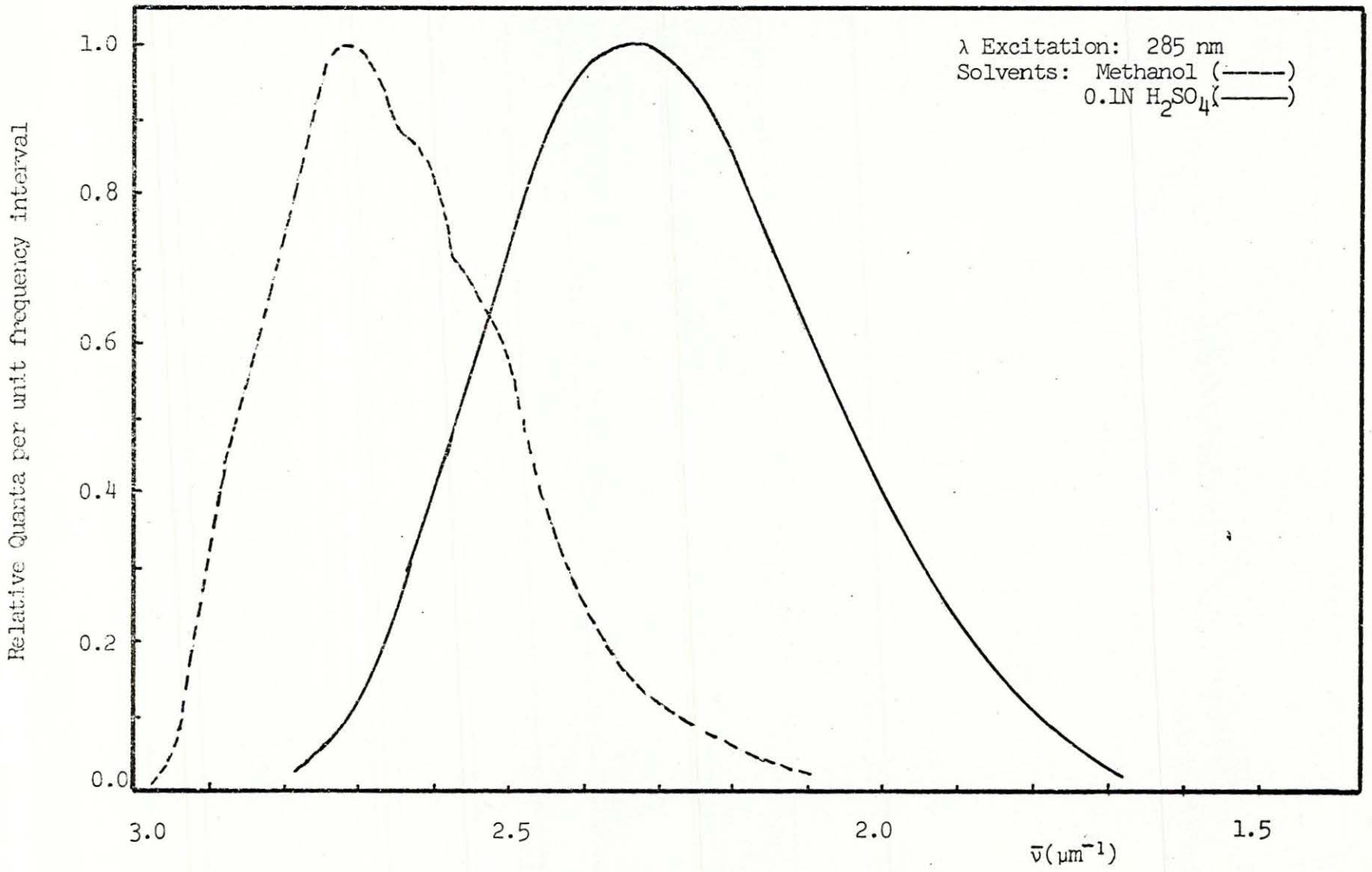

Figure 18: Fluorescence Spectrum of 1,10-Phenanthroline

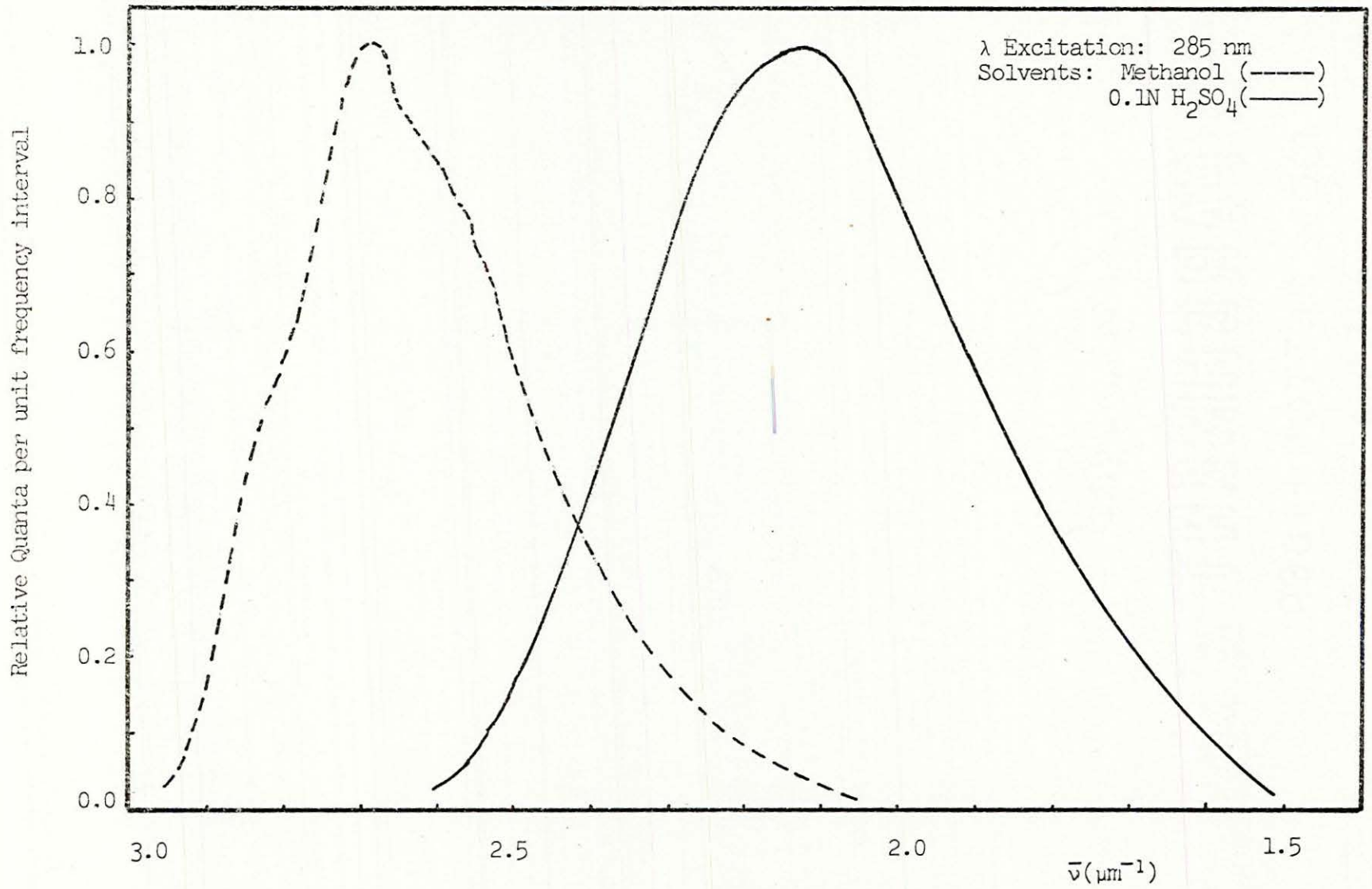

Figure 19: Fluorescence Spectrum of 5-Methyl-1,10-Phenanthroline

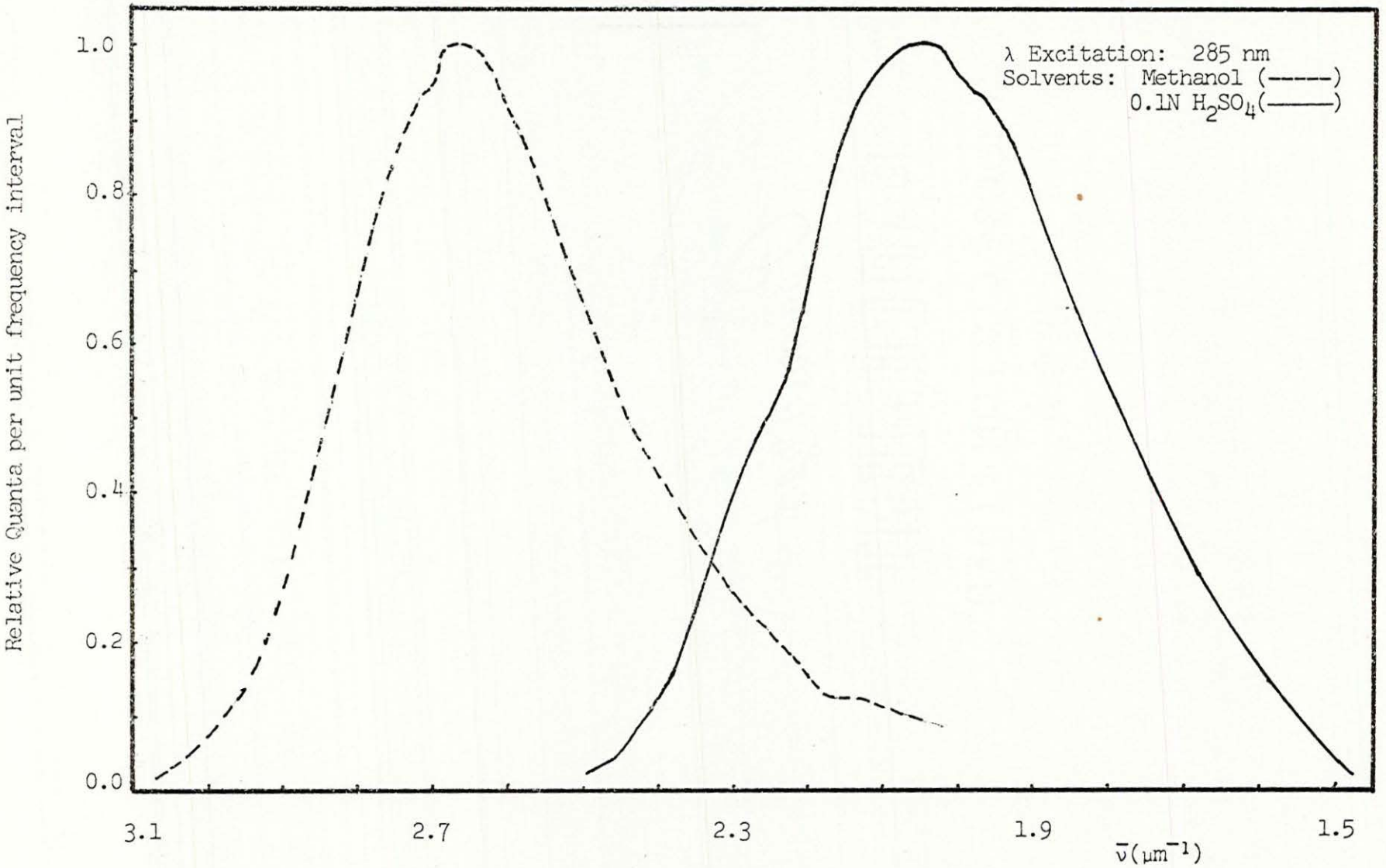

Figure 20: Fluorescence Spectrum of 5-Phenyl-1,10-Phenanthroline

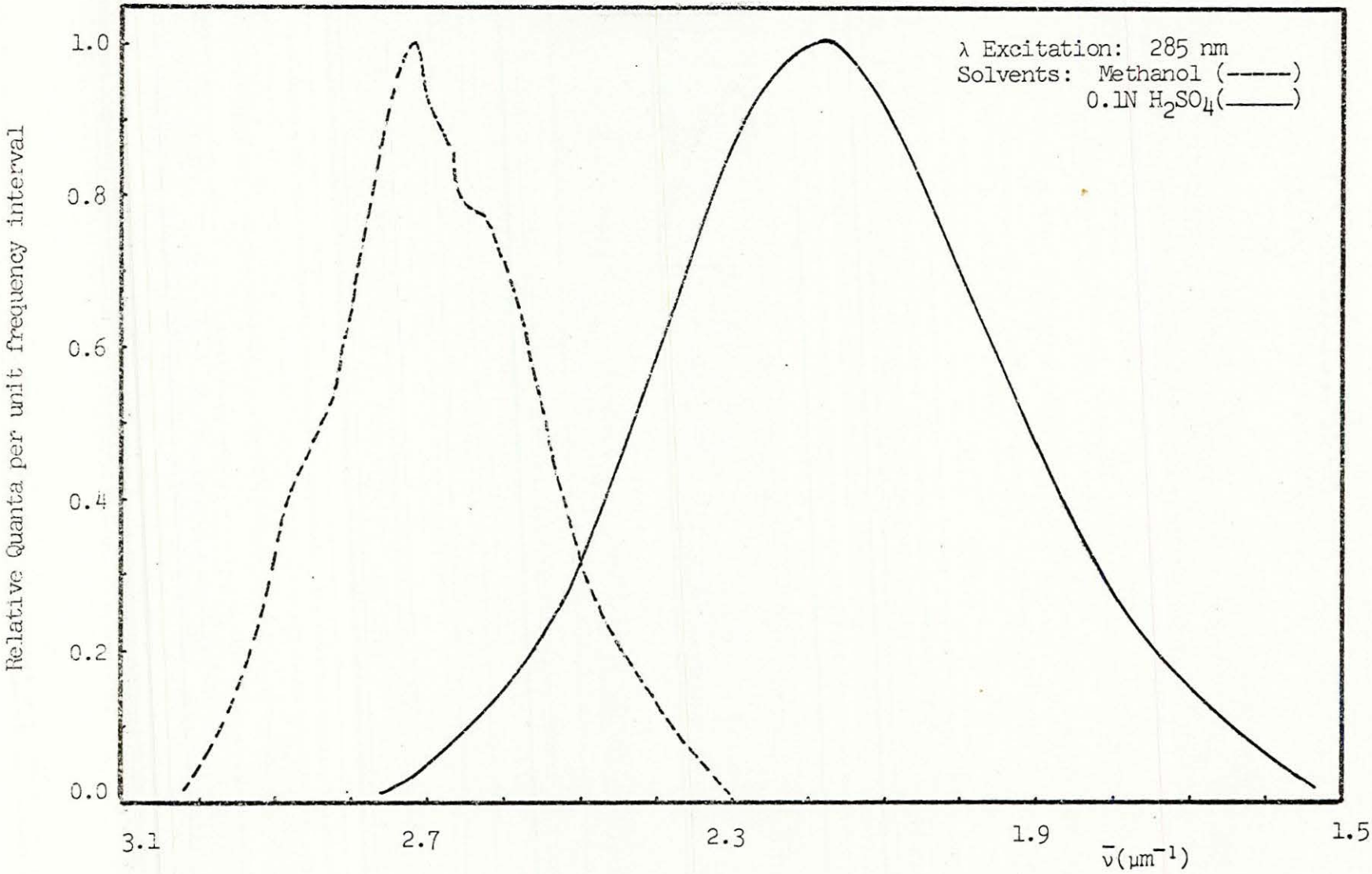

Figure 21: Fluorescence Spectrum of 5-Chloro-1,10-Phenanthroline

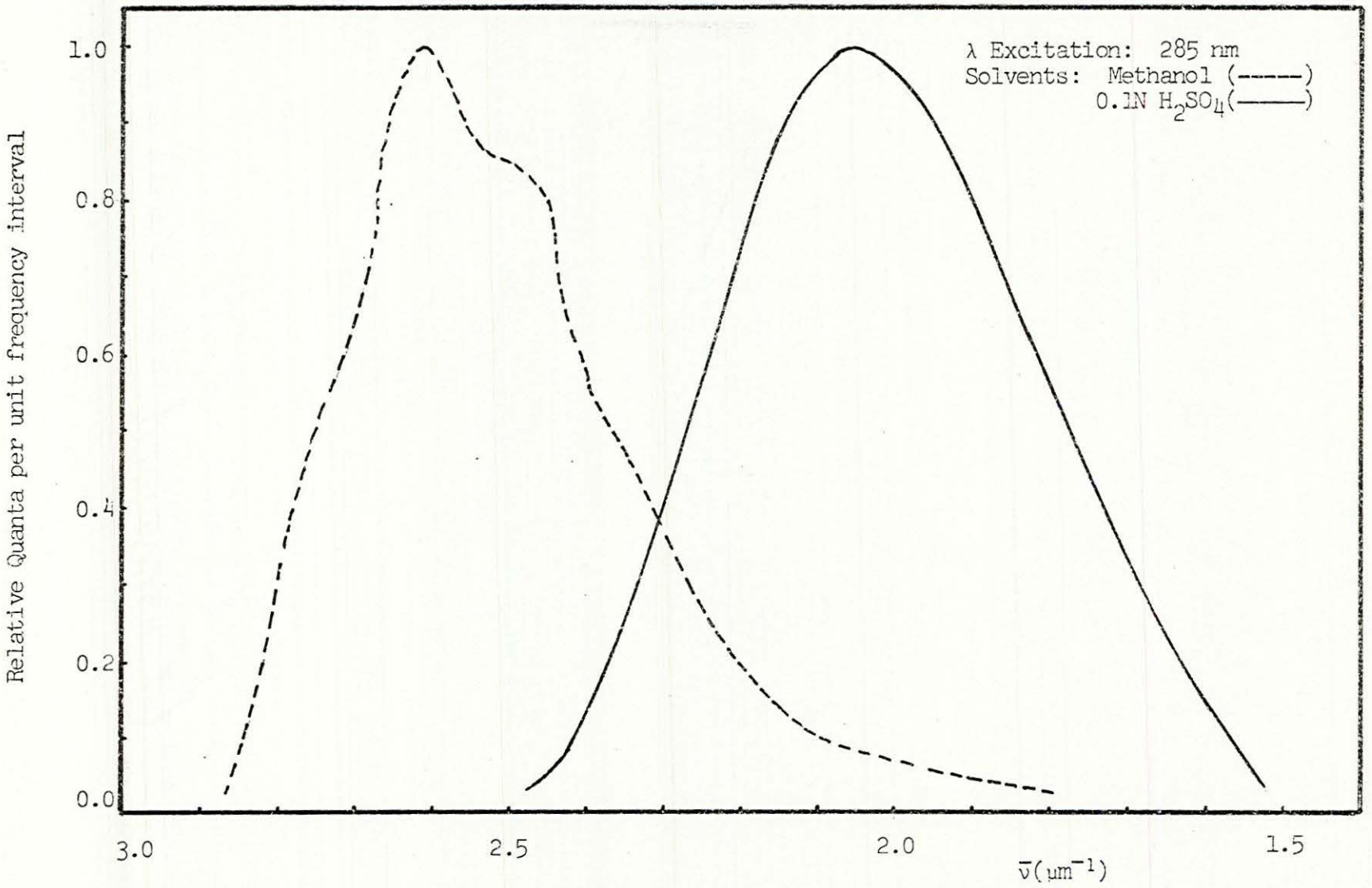

Figure 22: Fluorescence Spectrum of 5,6-Dimethyl-1,10-Phenanthroline

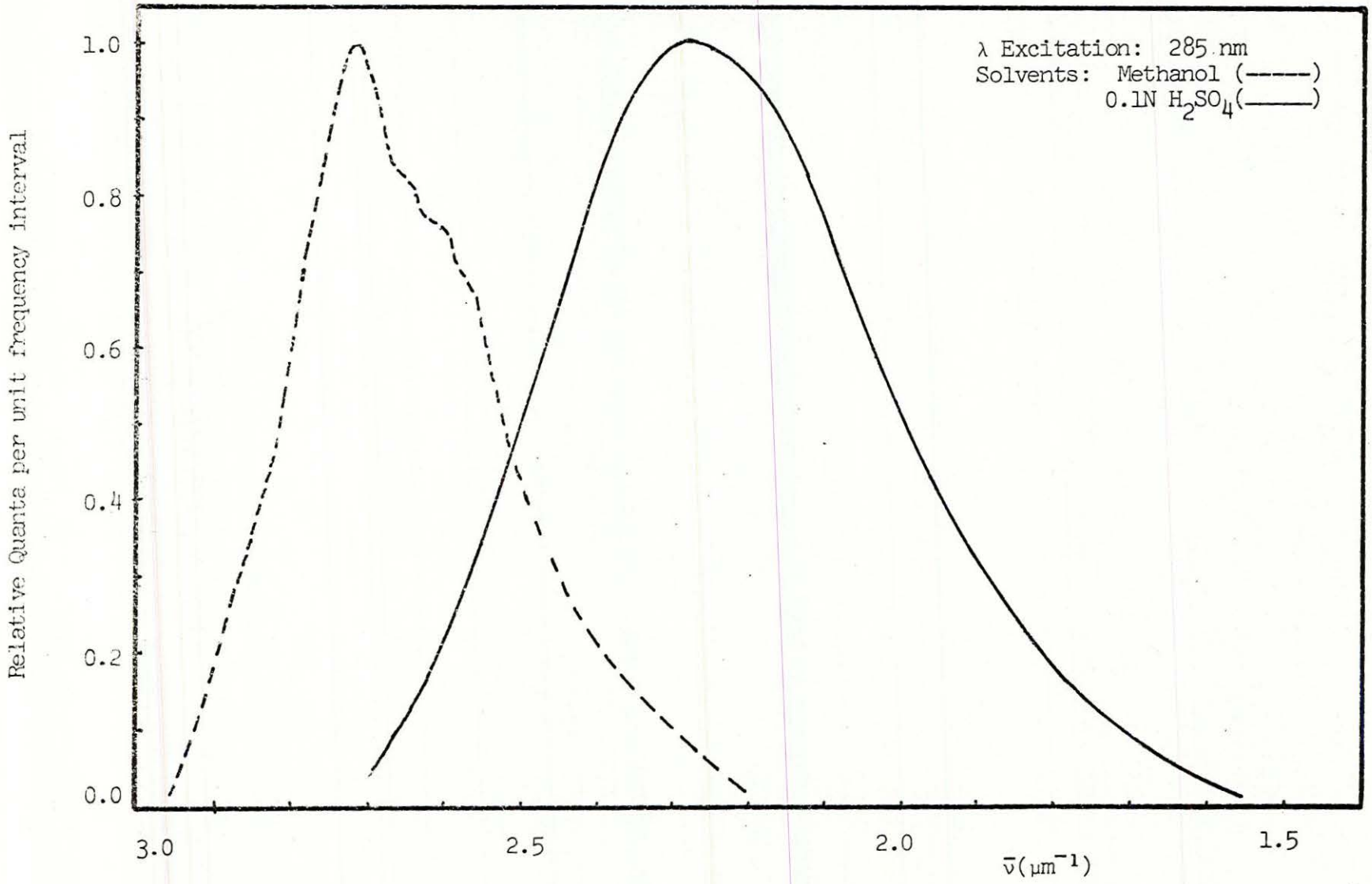

Figure 23: Fluorescence Spectrum of 2,9-Dimethyl-1,10-Phenanthroline

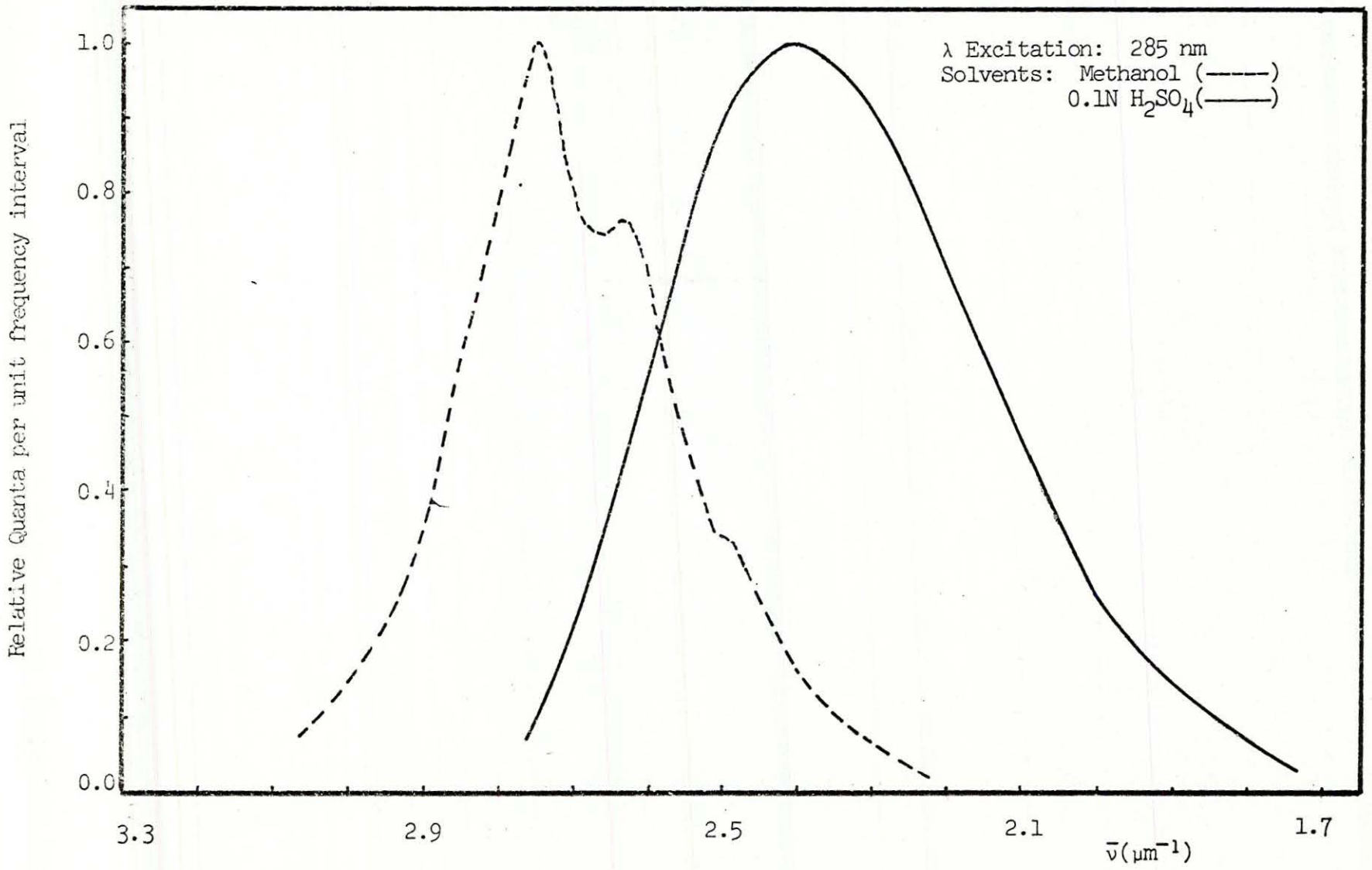

Figure 24: Fluorescence Spectrum of 4,7-Dimethyl-1,10-Phenanthroline

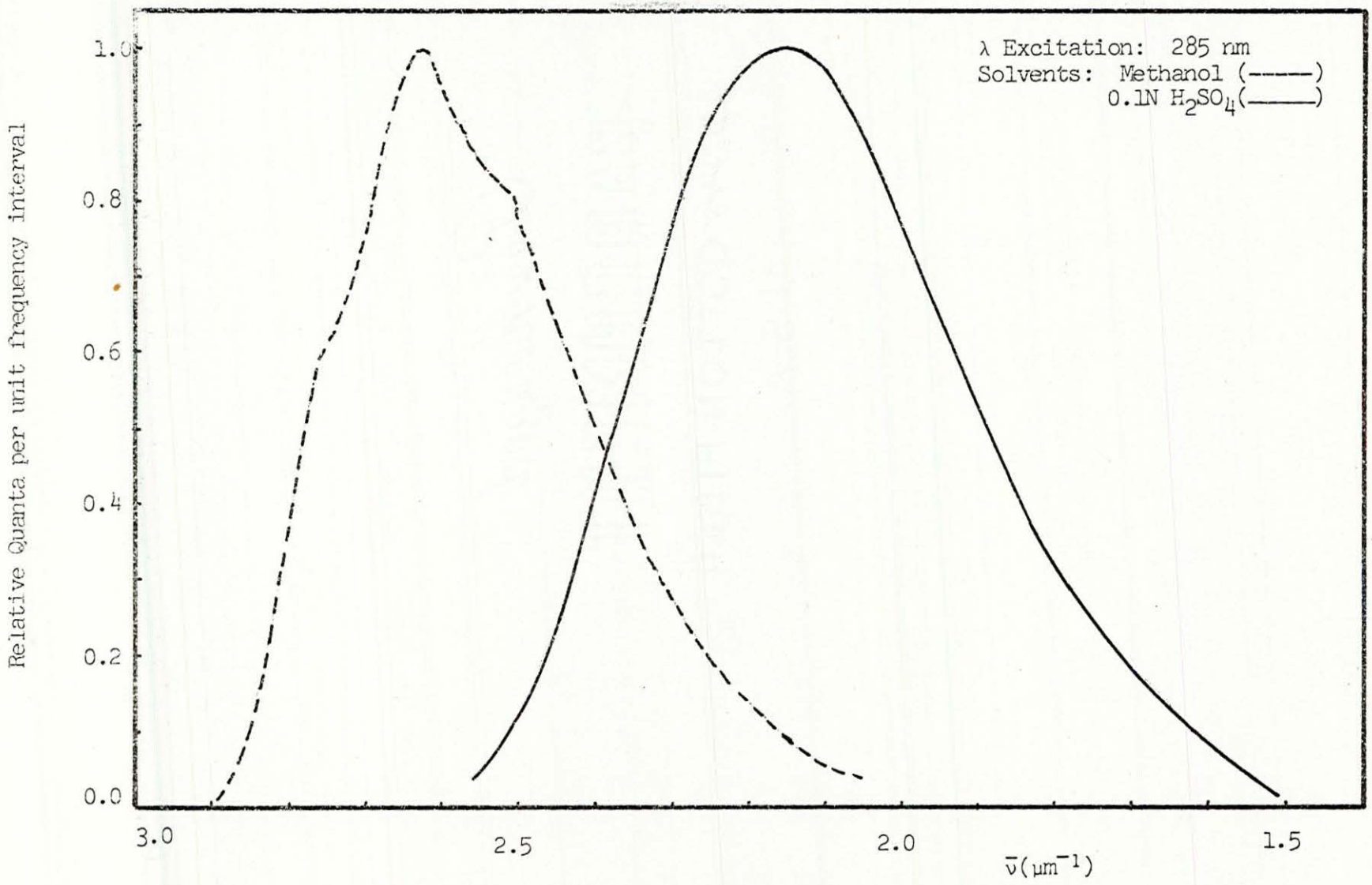

Figure 25: Fluorescence Spectrum of 4,7-Diphenyl-1,10-Phenanthroline

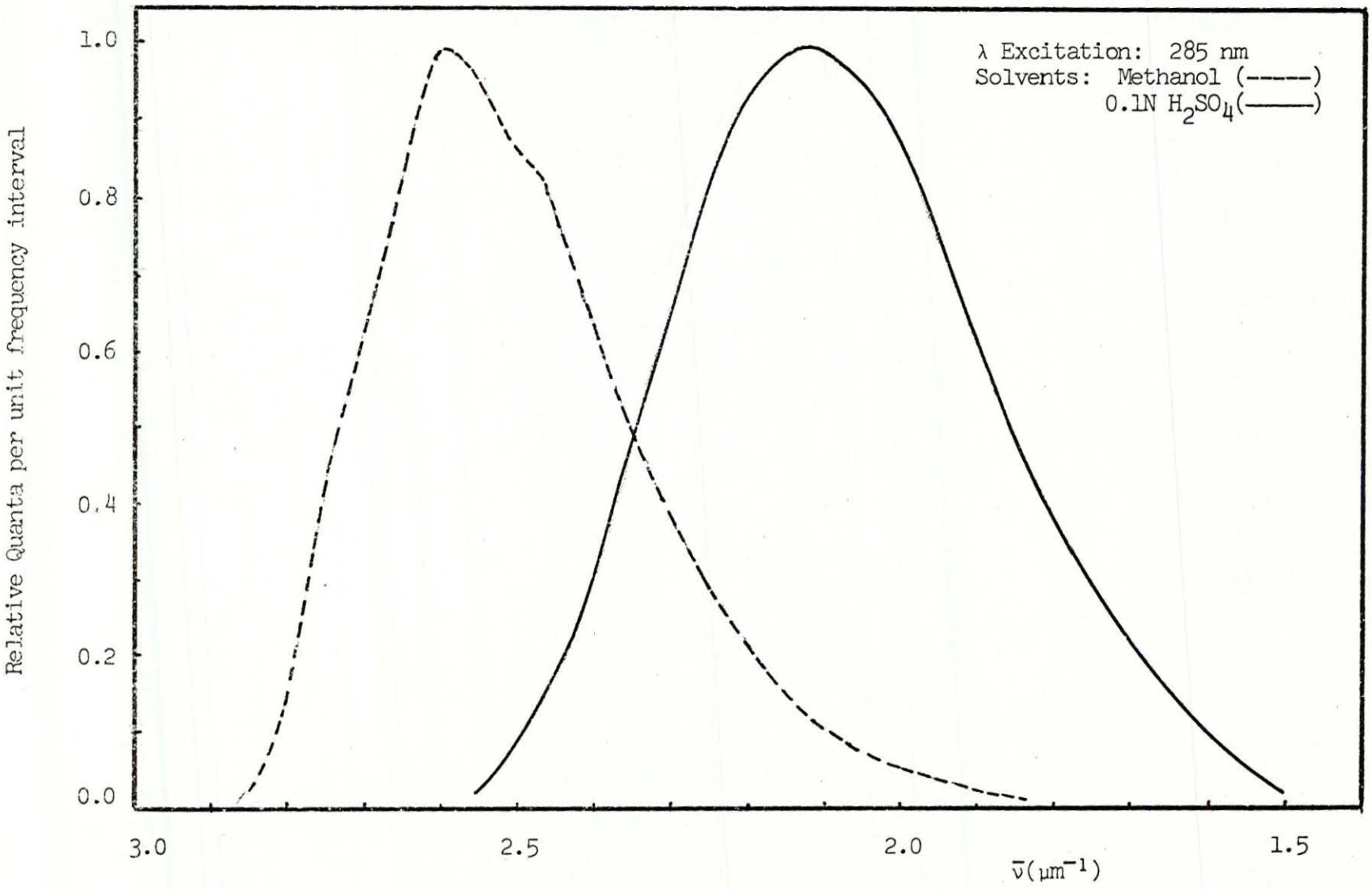

Figure 26: Fluorescence Spectrum of 2,9-Dimethyl-4,7-Diphenyl-1,10-Phenanthroline

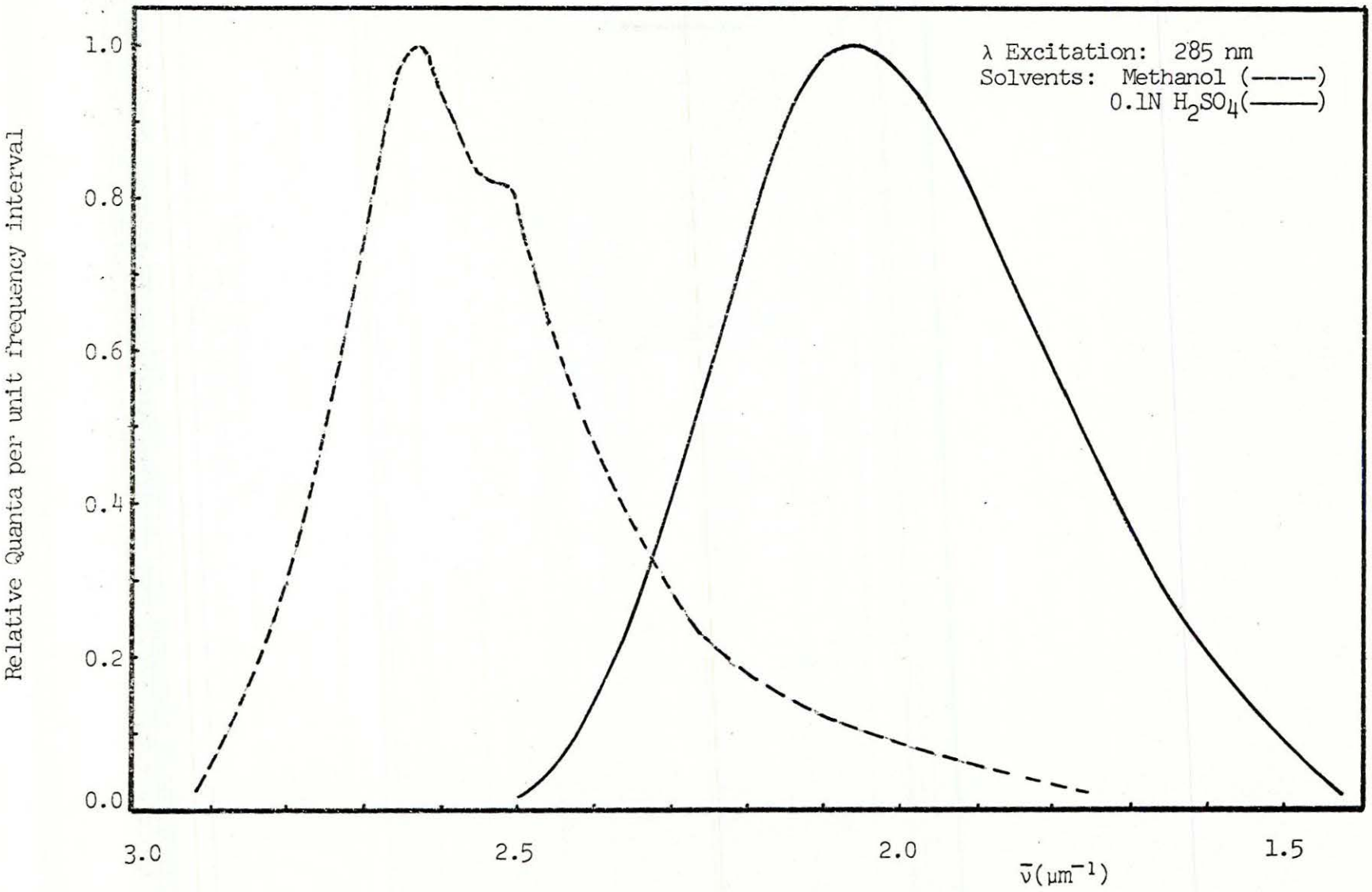

Figure 27: Fluorescence Spectrum of 3,5,6,8-Tetramethyl-1,10-Phenanthroline

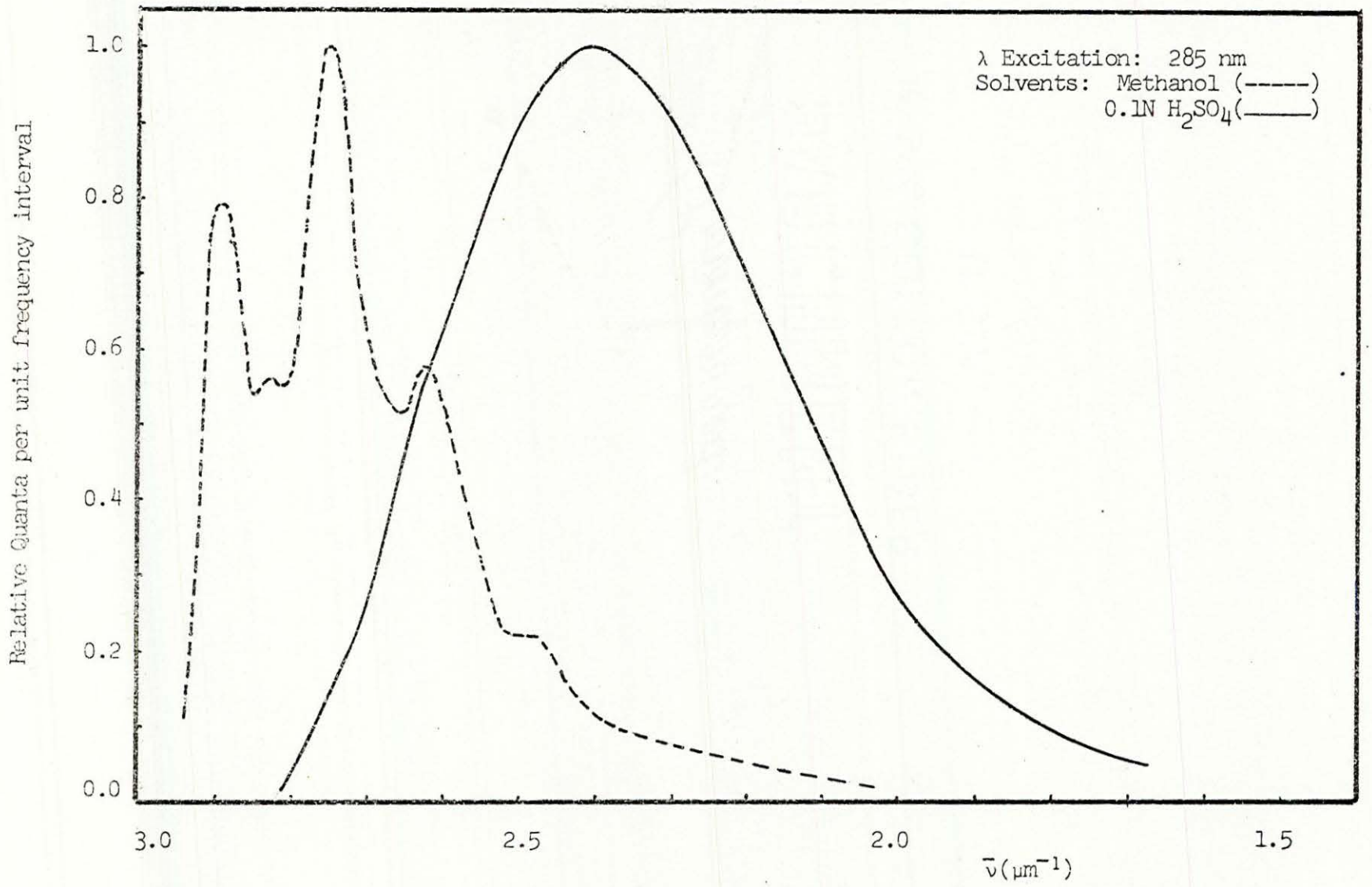

Figure 28: Fluorescence Spectrum of 3,4,7,8-Tetramethyl-1,10-Phenanthroline

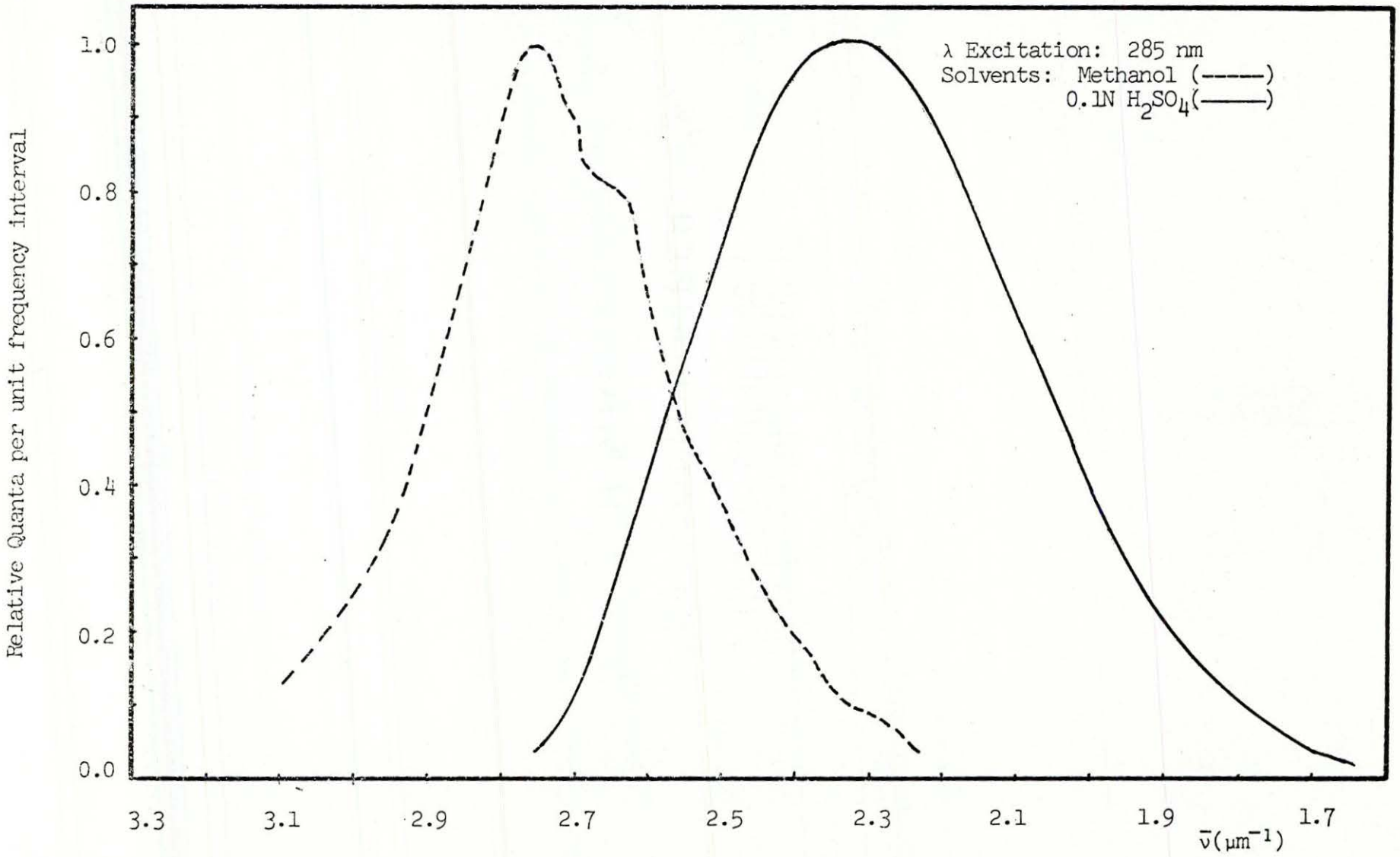

Figure 29: Fluorescence Spectrum of 1,10-Phenanthroline-4,7-Diol-Monohydrochloride

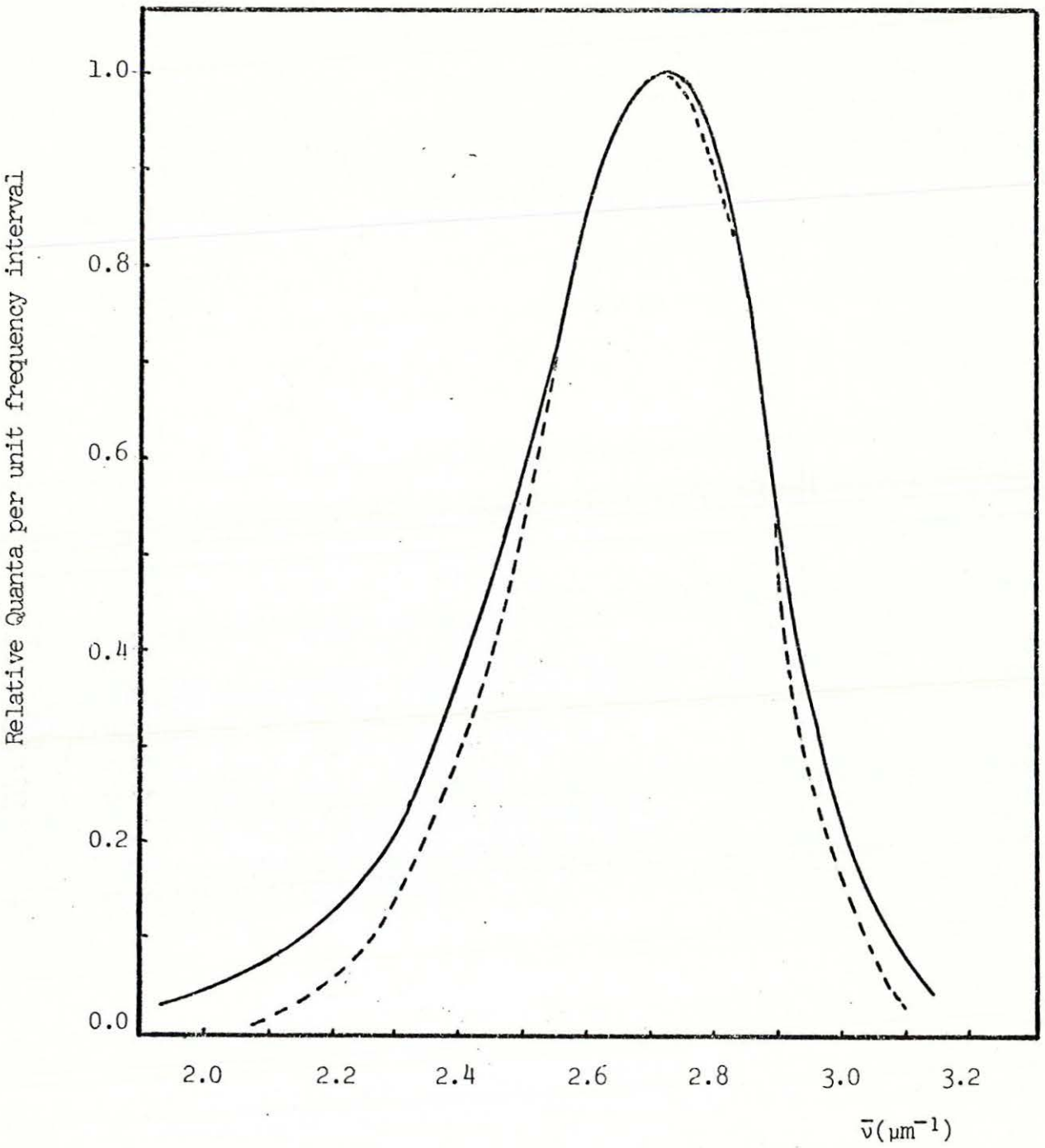

Figure 30: Fluorescence Spectrum of 2-Aminopyridine

(——) our values; (-----) from reference (36)

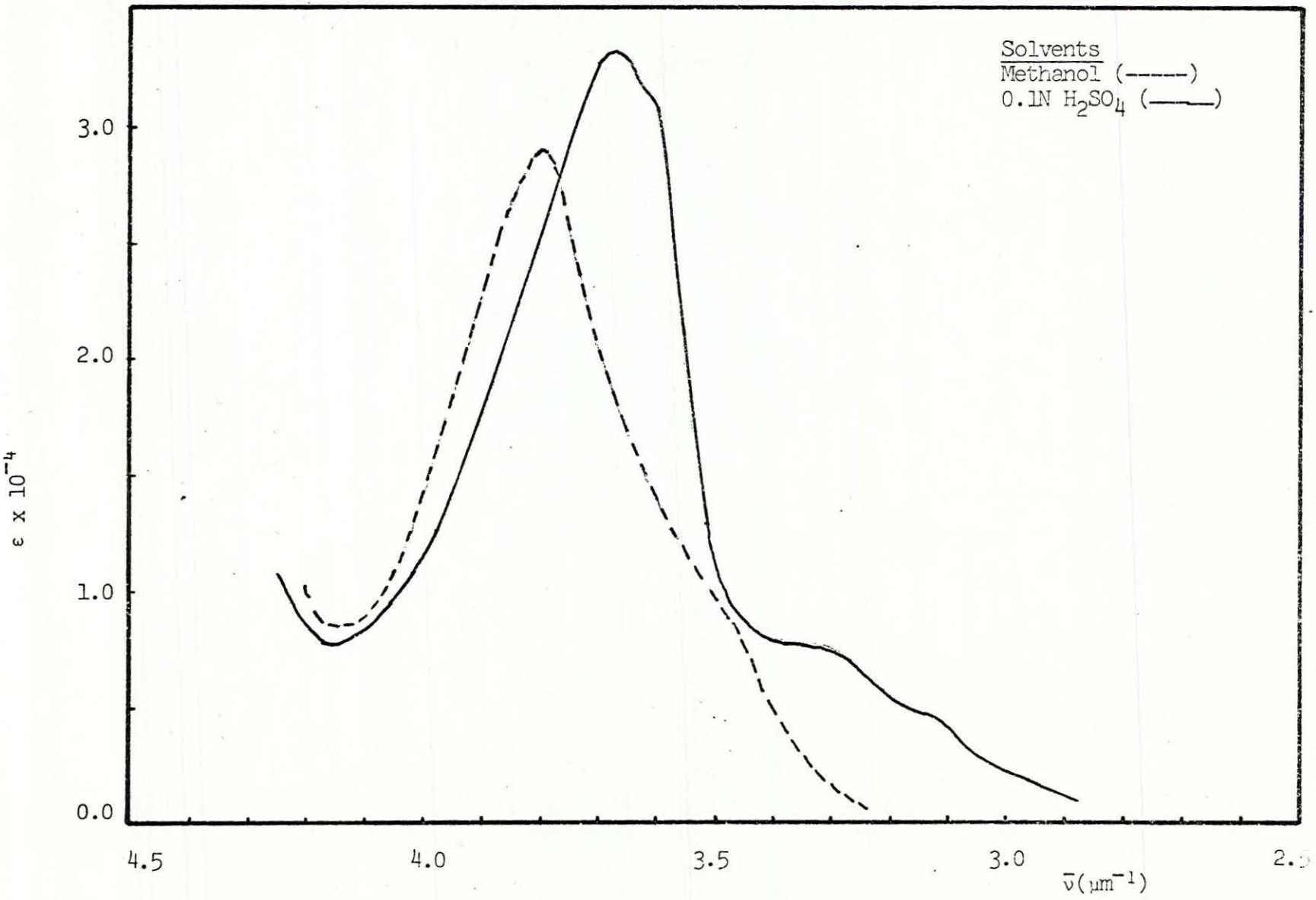

Figure 31: Absorption Spectra of 1,10-Phenanthroline

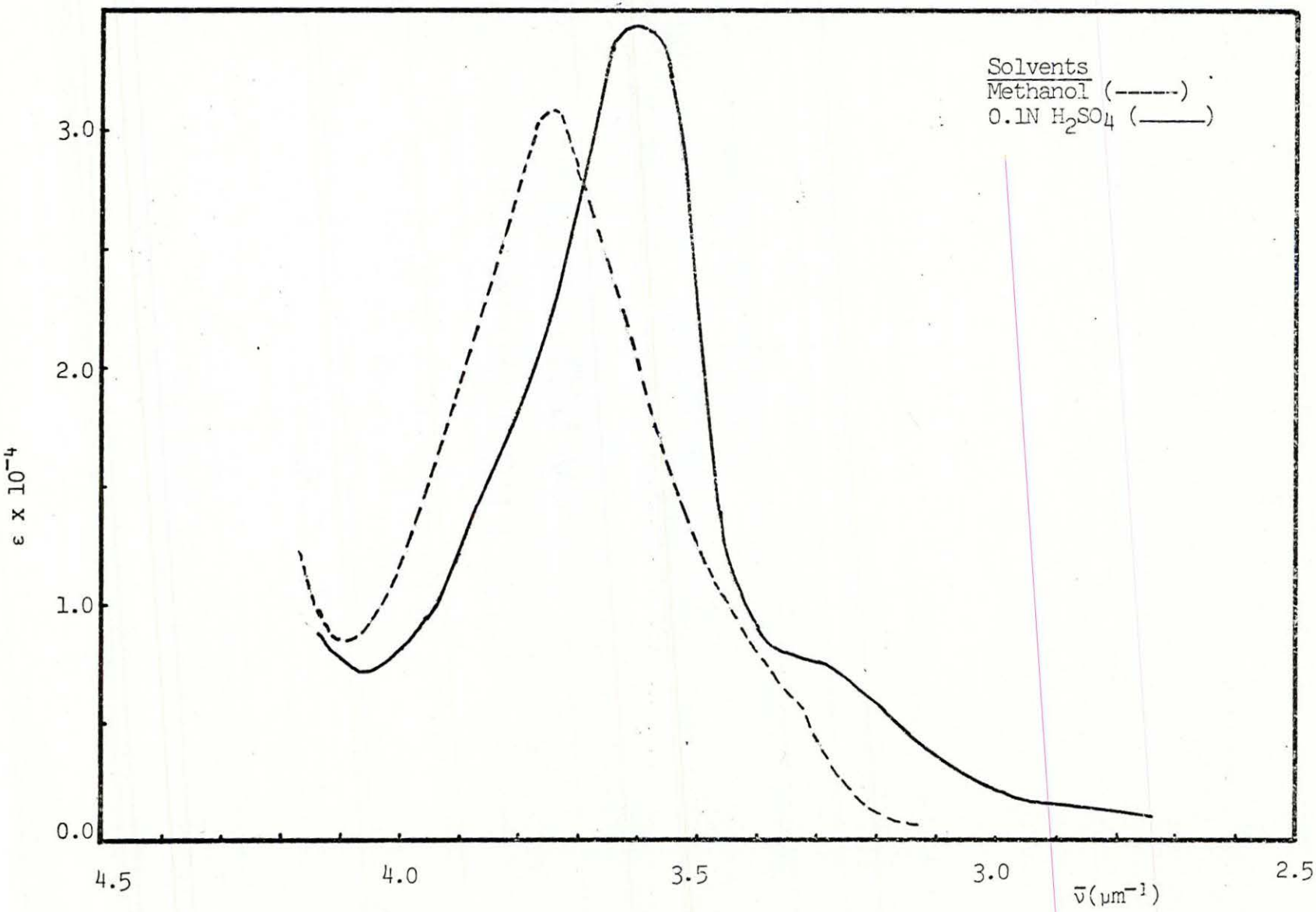

Figure 32: Absorption Spectrum of 5-Methyl-1,10-Phenanthroline

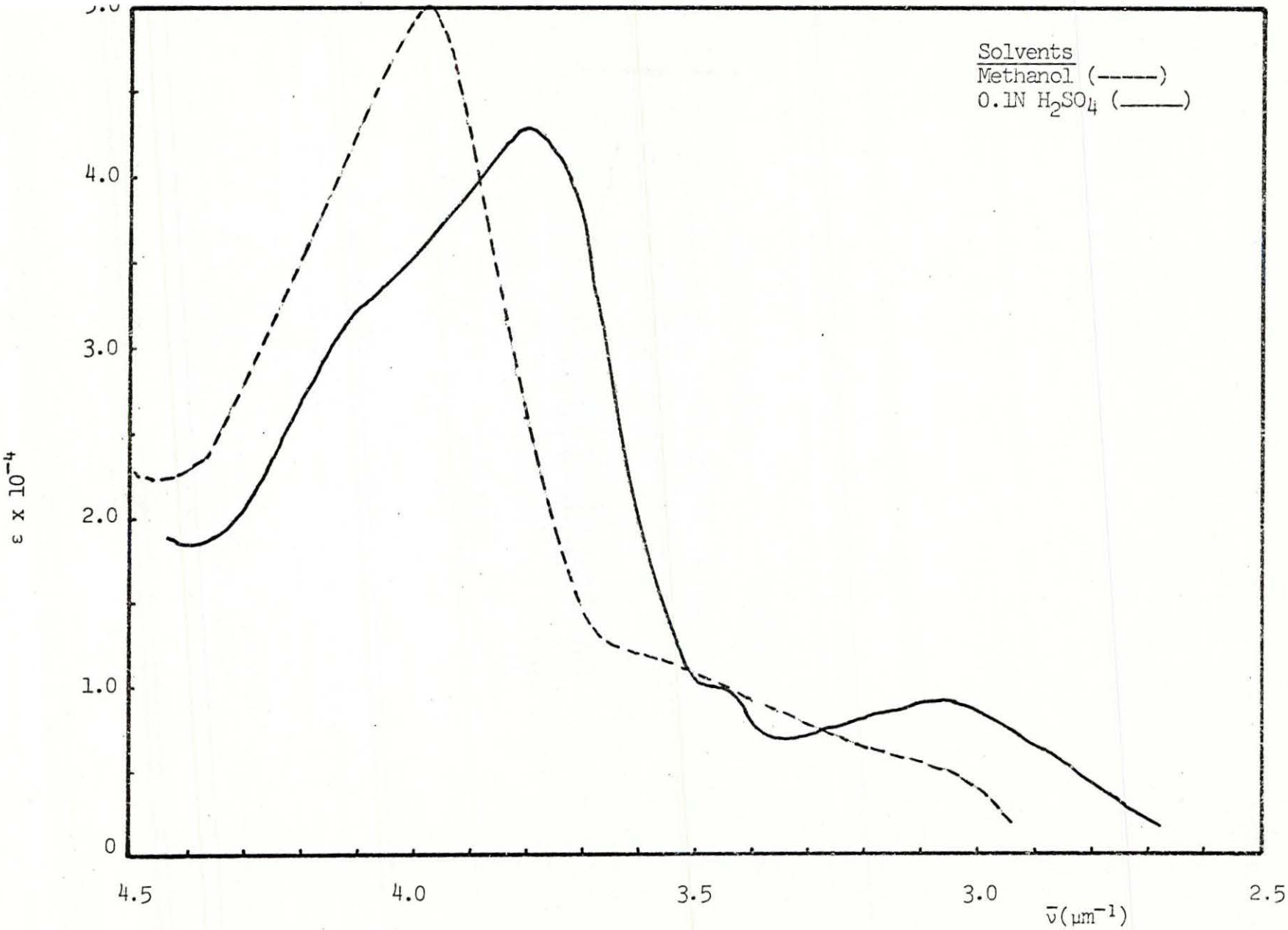

Figure 33: Absorption Spectrum of 5-Phenyl-1,10-Phenanthroline

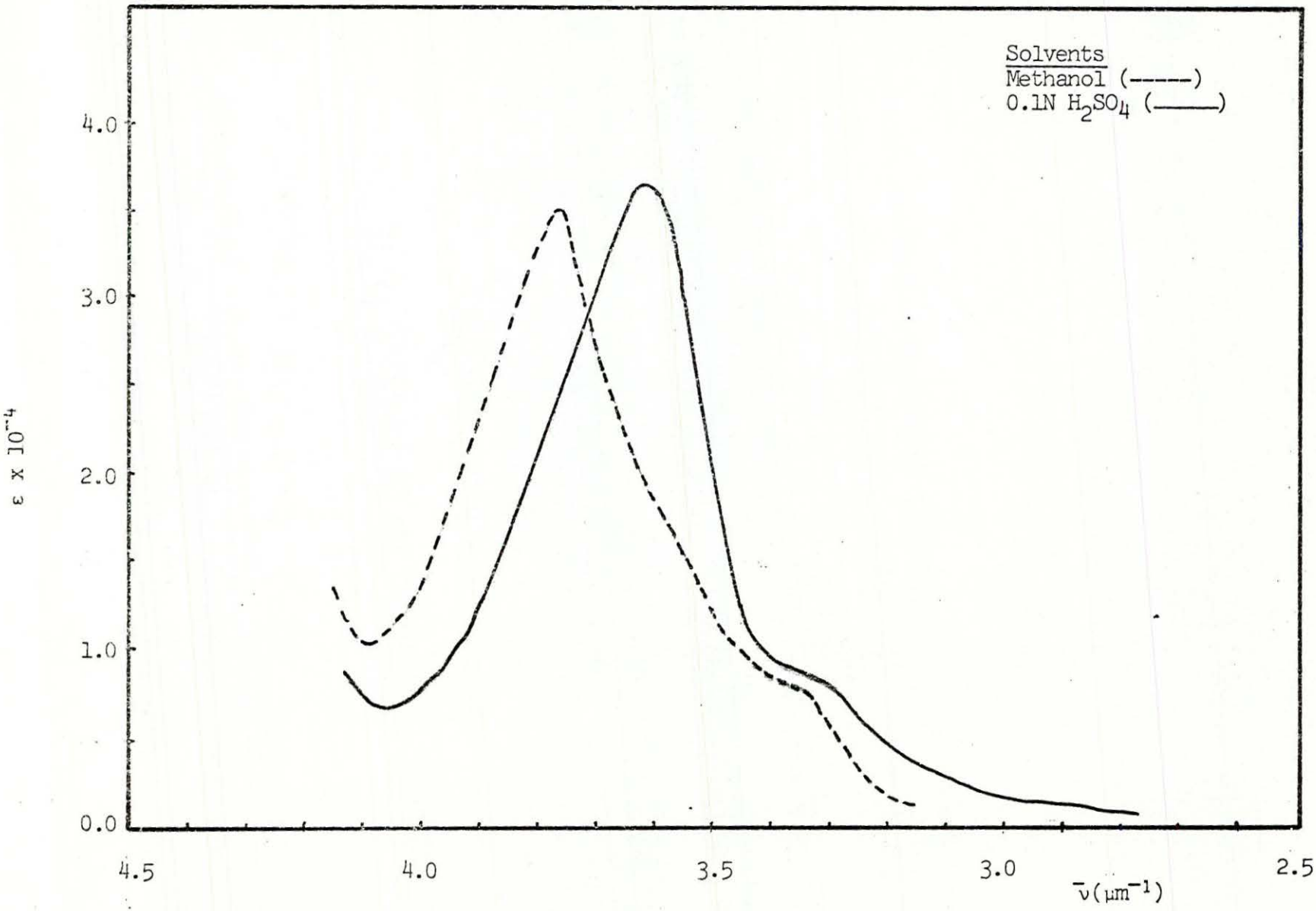

Figure 34: Absorption Spectrum of 5-Chloro-1,10-Phenanthroline

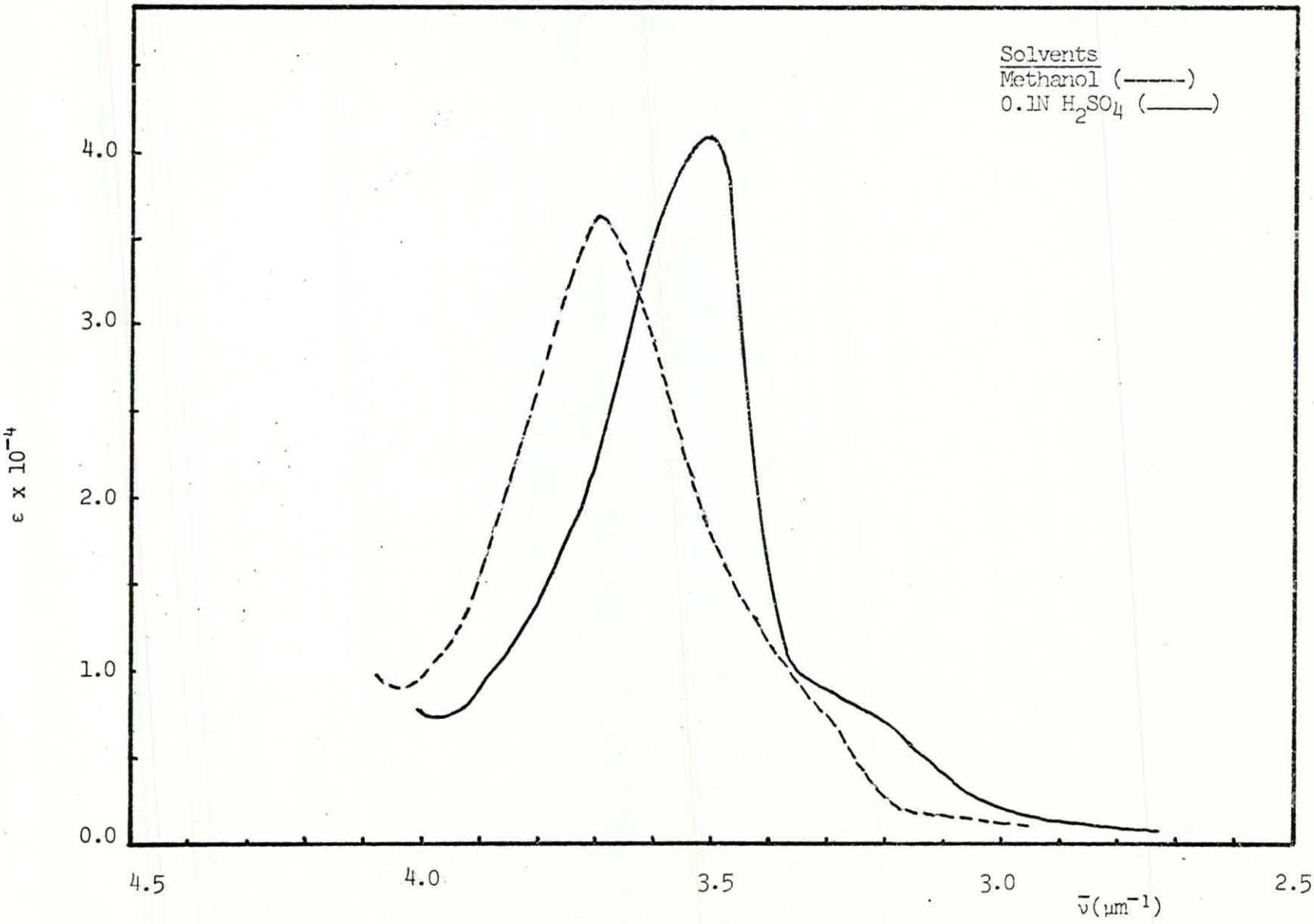

Figure 35: Absorption Spectrum of 5,6-Dimethyl-1,10-Phenanthroline

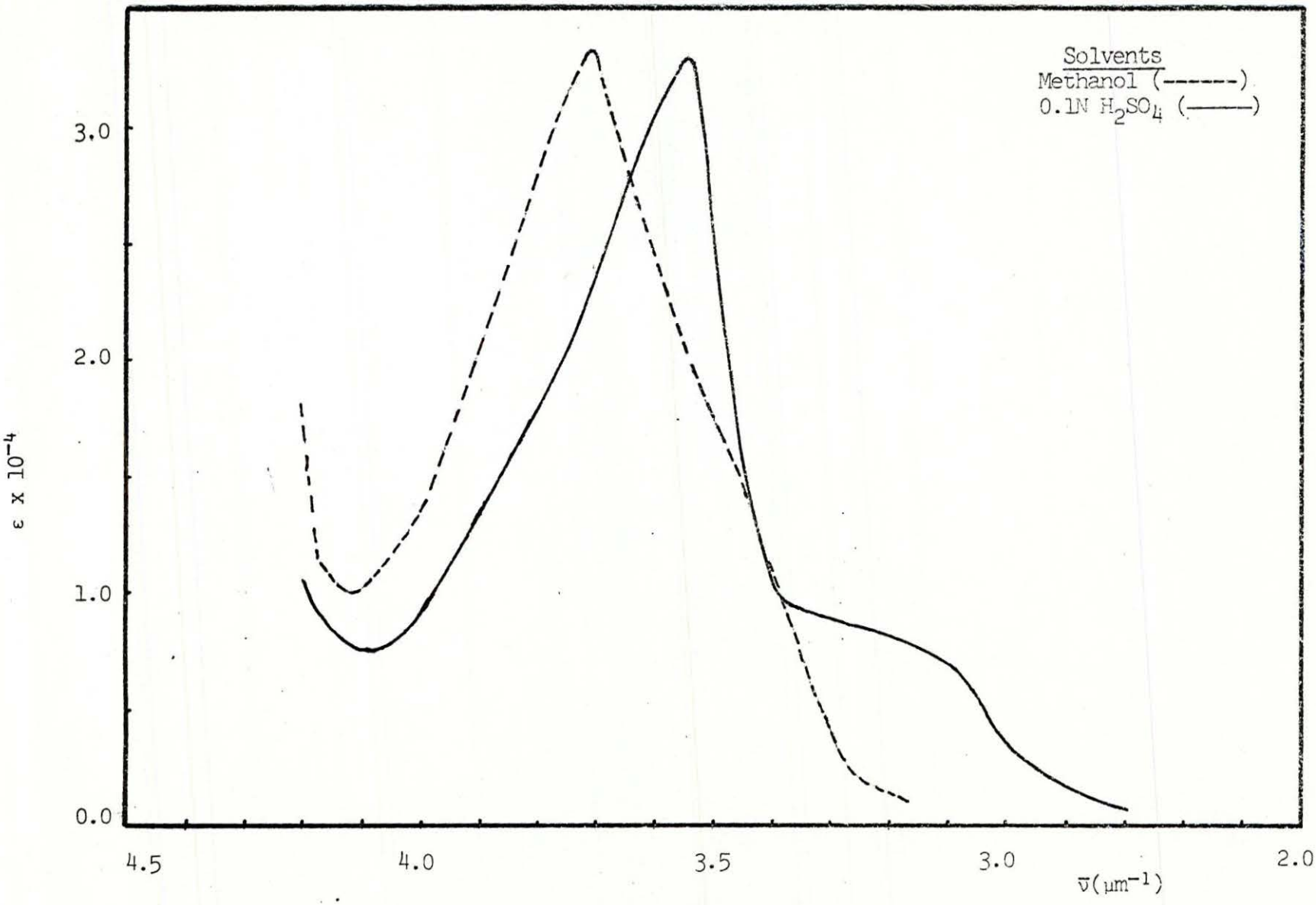

Figure 36: Absorption Spectrum of 2,9-Dimethyl-1,10-Phenanthroline

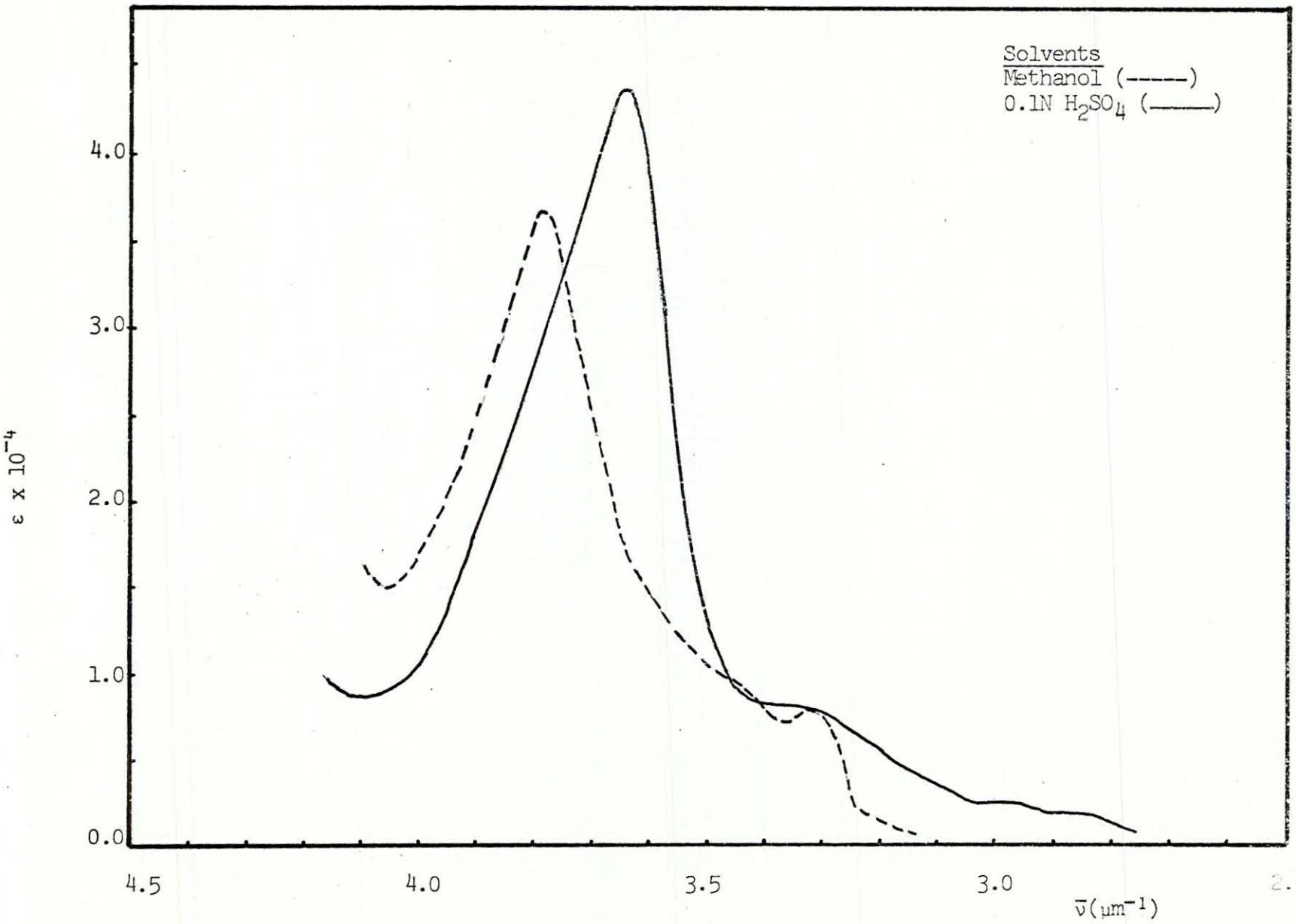

Figure 37: Absorption Spectrum of 4,7-Dimethyl-1,10-Phenanthroline

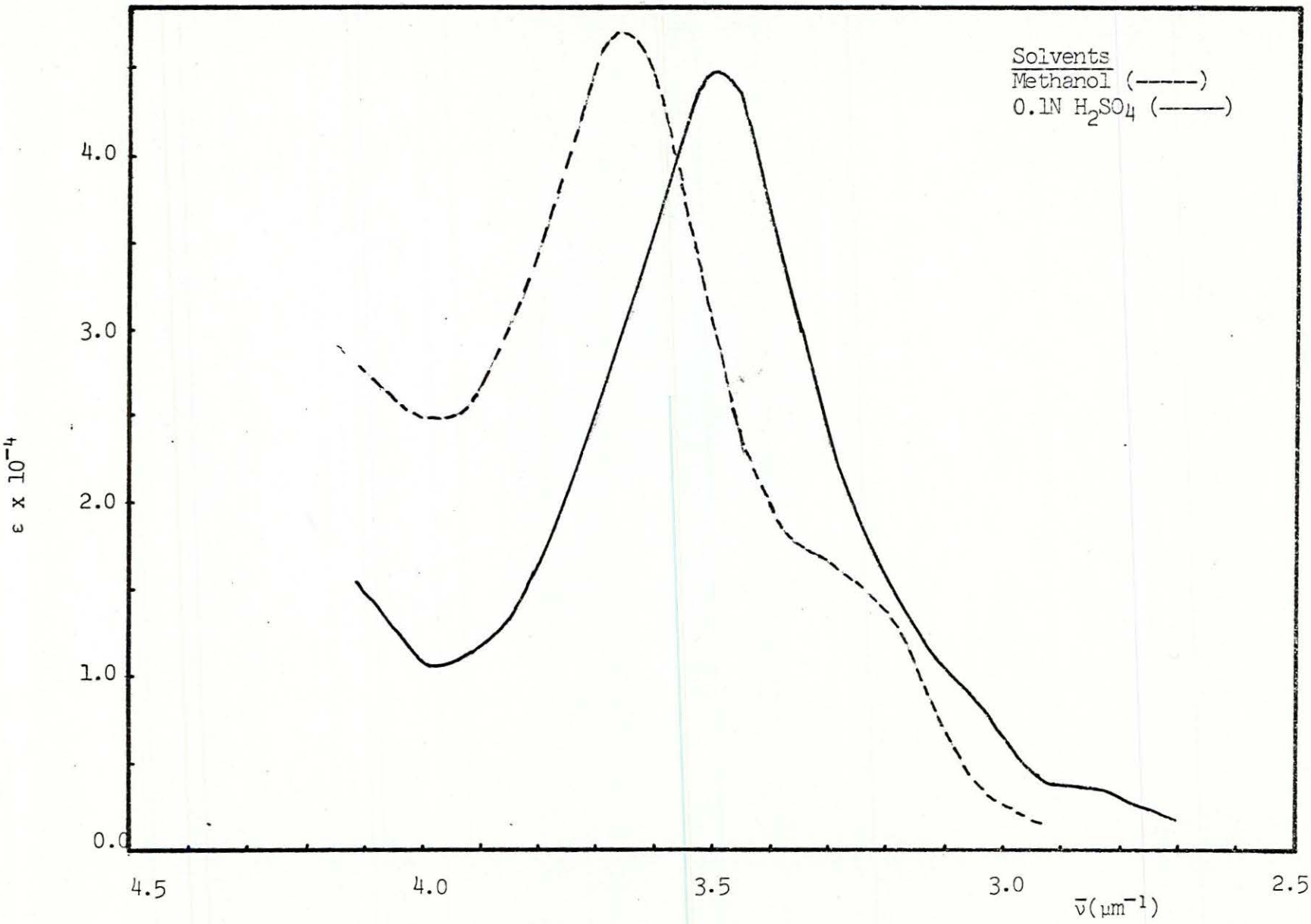

Figure 38: Absorption Spectrum of 4,7-Diphenyl-1,10-Phenanthroline

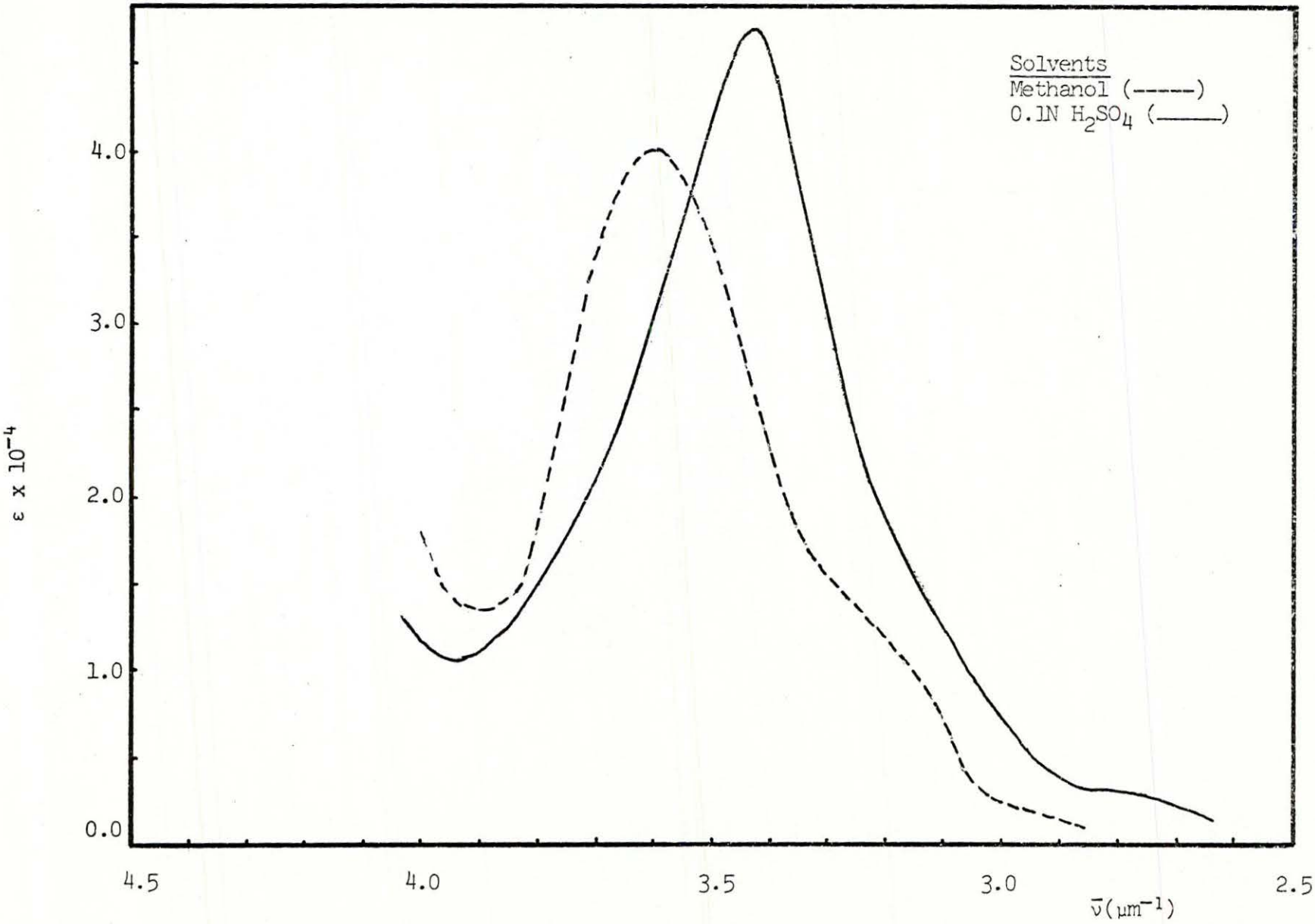

Figure 39: Absorption Spectrum of 2,9-Dimethyl-4,7-Diphenyl-1,10-Phenanthroline

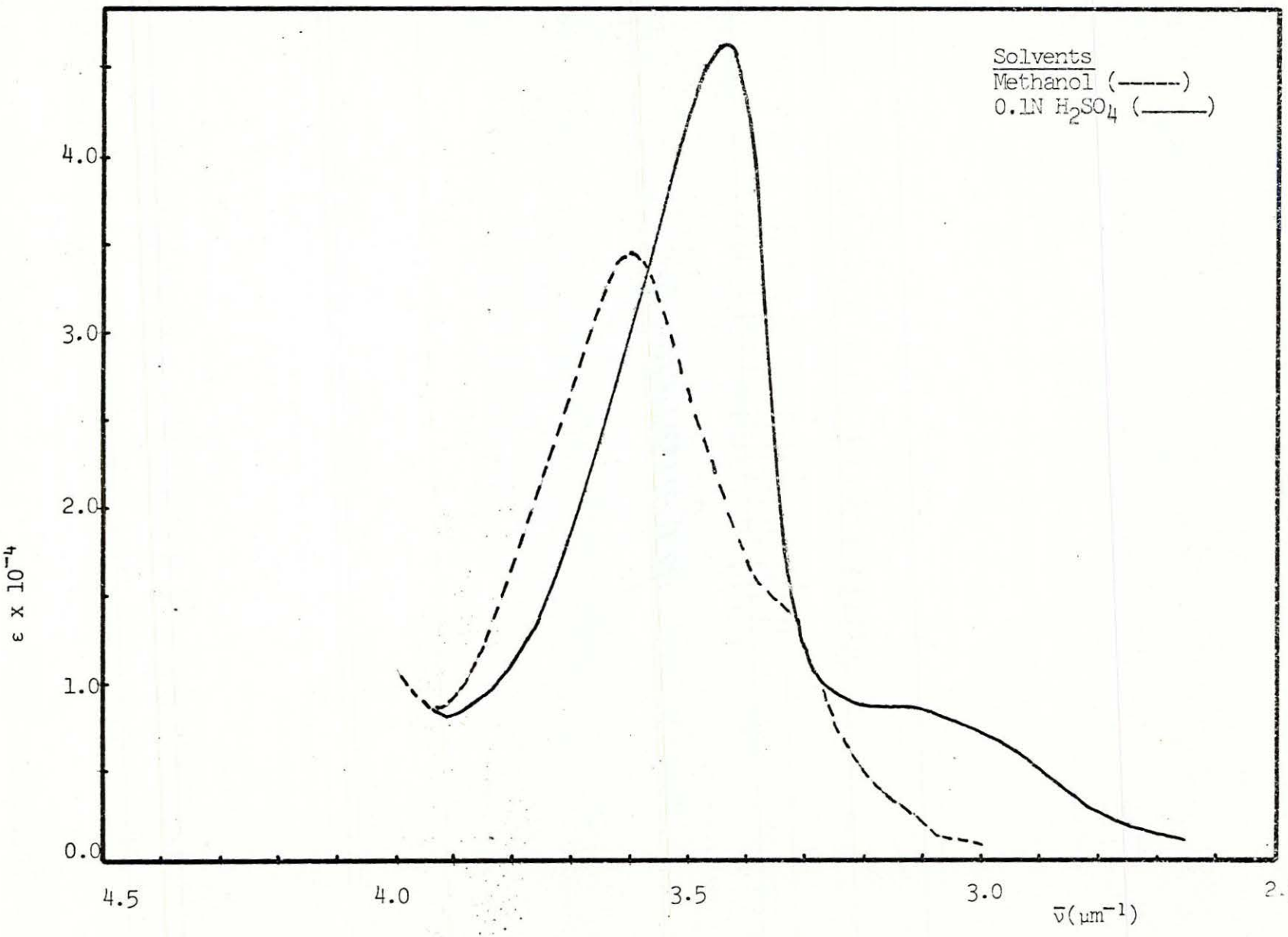

Figure 40: Absorption Spectrum of 3,5,6,8-Tetramethyl-1,10-Phenanthroline

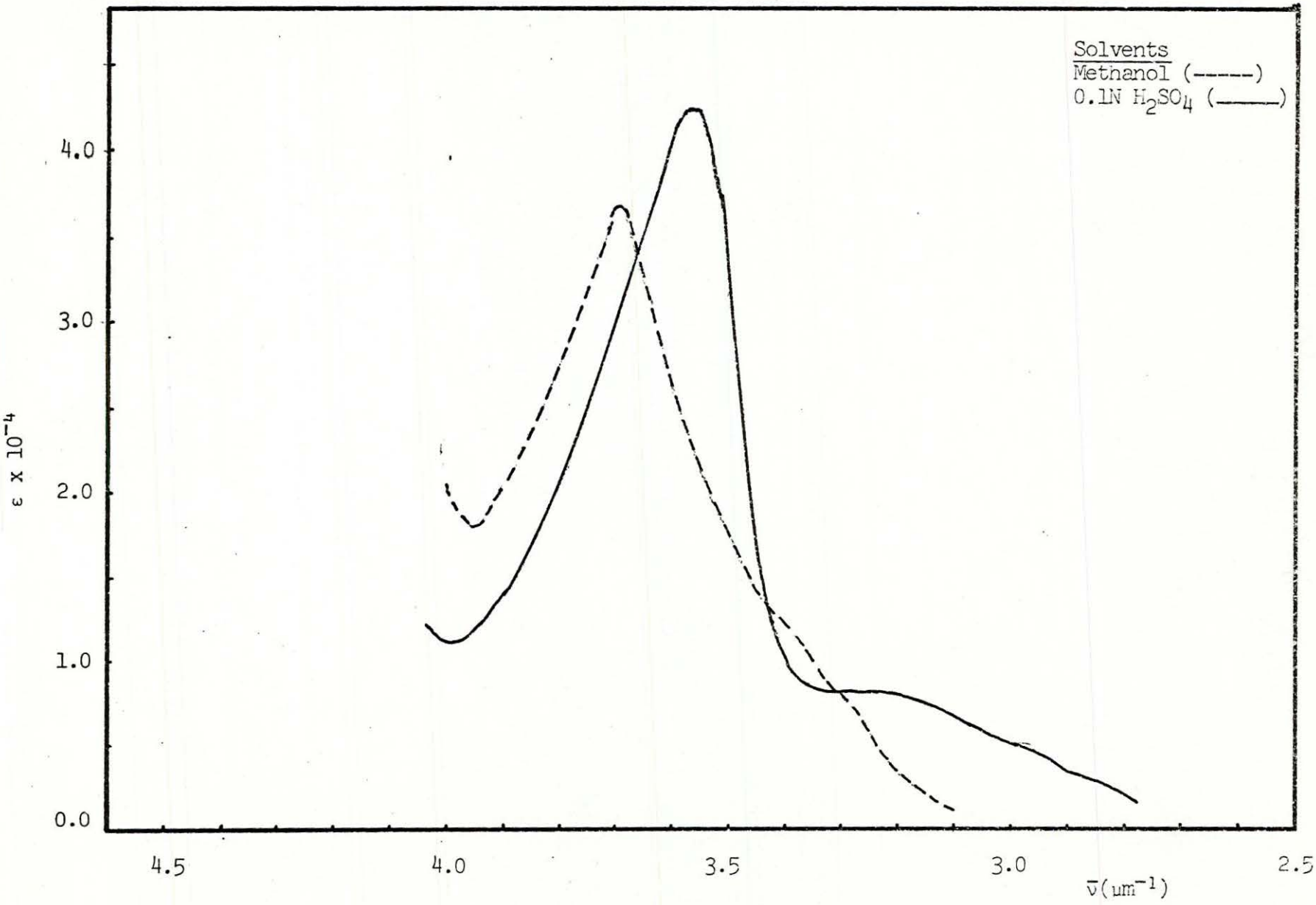

Figure 41: Absorption Spectrum of 3,4,7,8-Tetramethyl-1,10-Phenanthroline

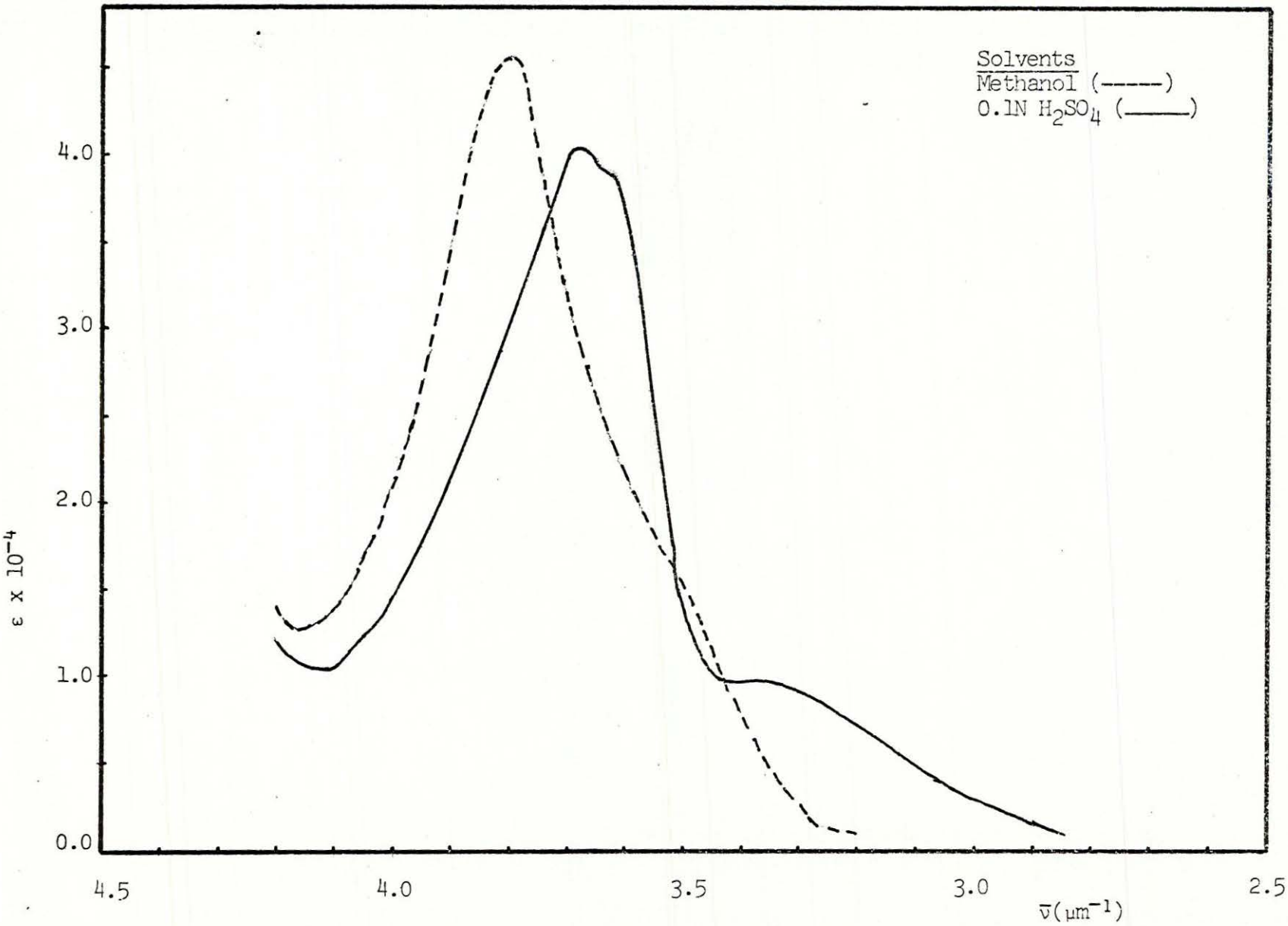

Figure 42: Absorption Spectrum of 1,10-Phenanthroline-4,7-Diol-Monohydrochloride